

**BIOSYNTHESIS AND CHARACTERIZATION OF GOLD  
NANOPARTICLES BY USING *VERNONIA AMYGDALINA*,  
*PANDANUS AMARYLLIFOLIUS*, AND *CITRUS MAXIMA* LEAVES**

**TAN MING ZHENG**

**A project report submitted in partial fulfilment of the  
requirements for the award of the degree of  
Bachelor of Engineering (Honours) Industrial Engineering**

**Faculty of Engineering and Green Technology  
Universiti Tunku Abdul Rahman**

**SEPTEMBER 2019**

## DECLARATION

I hereby declare that this project report is based on my original work except for citations and quotations which have been duly acknowledged. I also declare that it has been not previously and concurrently submitted for any other degree or award at UTAR or other institutions.

Signature : \_\_\_\_\_

Name : TAN MING ZHENG

ID No. : 15AGB07701

Date : \_\_\_\_\_

**APPROVAL FOR SUBMISSION**

I certify that this project report entitled **“BIOSYNTHESIS AND CHARACTERIZATION OF GOLD NANOPARTICLES BY USING *VERNONIA AMYGDALINA*, *PANDANUS AMARYLLIFOLIUS*, AND *CITRUS MAXIMA LEAVES*”** was prepared by **TAN MING ZHENG** has met the required standard for submission in partial fulfilment of the requirements for the award of Bachelor of Engineering (Honours) Industrial Engineering at Universiti Tunku Abdul Rahman.

Approved by,

Signature : \_\_\_\_\_

Supervisor : Dr. Ng Soo Ai

Date : \_\_\_\_\_

Signature : \_\_\_\_\_

Co-Supervisor : Ms. Tan Zi Yi

Date : \_\_\_\_\_

The copyright of this report belongs to the author under the terms of the copyright Act 1987 as qualified by Intellectual Property Policy of Universiti Tunku Abdul Rahman. Due acknowledgement shall always be made of the use of any material contained in, or derived from, this report.

© 2019, Tan Ming Zheng. All right reserved.

Specially dedicated to  
my beloved parent, brother and friends.

## ACKNOWLEDGEMENTS

I would like to take this opportunity to express my deepest gratitude to my helpful supervisor, Dr. Ng Soo Ai for her advice, guidance, inspiration and patience throughout the research studies. Besides that, I would like to thank my co-supervisor, Ms. Tan Zi Yi for her supervision, valuable comments and constructive advice truly help the progression and smoothness of the project.

In addition, I am thankful to several close friends who helped me directly and indirectly during my study, Lian Wan Yee, Lee Zi Xin and Terry Kong Kah Tshun. The research would not be success without their enthusiasm and assistance from them.

Lastly, I would like to specially thank my beloved parent for their everlasting love, patience and care provided me all the necessary strength for the completion of study.

**BIOSYNTHESIS AND CHARACTERIZATION OF GOLD  
NANOPARTICLES BY USING *VERNONIA AMYGDALINA*, *PANDANUS  
AMARYLLIFOLIUS*, AND *CITRUS MAXIMA* LEAVES**

**ABSTRACT**

As the demand of gold nanoparticles is increasing rapidly due to widespread use of gold nanoparticles in biology, pharmaceuticals and medicines, green methods with the use of plant extracts has gained great importance because most of the plants are readily available, inexpensive and toxic free. Besides, plant extracts are rich in different types of reducing, capping and stabilizing agents. In this study, the method used was simple, cost effective and eco-friendly. Biosynthesis of gold nanoparticles by using *Vernonia Amygdalina*, *Pandanus Amaryllifolius* and *Citrus Maxima* leaves extract has been reported. The synthesised gold nanoparticles were characterized with UV-visible spectrophotometry, X-ray diffraction (XRD), field emission scanning electron microscopy (FESEM), Energy Dispersive X-Ray Spectra (EDX), Fourier transform infrared spectroscopy (FTIR), and particle size analysis. The UV-Vis spectra confirmed the presence of biosynthesised gold nanoparticles. The FESEM images revealed spherical, hexagonal and hollow shape of gold nanoparticles. The size of gold nanoparticles was determined to be 22.22-148.37 nm. Crystalline nature of the nanoparticles in the face-centred cubic (FCC) structure was confirmed by the peaks in the XRD pattern. Elemental composition analysis by using EDX confirmed the presence of gold. FTIR results showed the functional groups involved in leaves extract for reduction of gold ions to nanoparticles.

**TABLE OF CONTENTS**

<b>DECLARATION</b>	<b>ii</b>
<b>APPROVAL FOR SUBMISSION</b>	<b>iii</b>
<b>ACKNOWLEDGEMENTS</b>	<b>vi</b>
<b>ABSTRACT</b>	<b>vii</b>
<b>TABLE OF CONTENTS</b>	<b>viii</b>
<b>LIST OF TABLES</b>	<b>xii</b>
<b>LIST OF FIGURES</b>	<b>xiv</b>
<b>LIST OF SYMBOLS / ABBREVIATIONS</b>	<b>xviii</b>

**CHAPTER**

<b>1</b>	<b>INTRODUCTION</b>	<b>1</b>
	1.1 Problem Statement	3
	1.2 Aims and Objectives	4
<b>2</b>	<b>LITERATURE REVIEW</b>	<b>5</b>
	2.1 Introduction of nanoscience, nanotechnology and nanoparticles	5
	2.2 Classification of nanoparticles	6
	2.3 Types of nanoparticles	7

2.3.1	Ceramic nanoparticles	7
2.3.2	Carbon-based nanoparticles	7
2.3.3	Semiconductor nanoparticles	8
2.3.4	Polymeric nanoparticles	8
2.3.5	Lipid-based nanoparticles	8
2.3.6	Metallic nanoparticles	9
2.4	Methods of synthesising nanoparticles	9
2.5	Plant in nanoparticles synthesis	14
2.5.1	<i>Vernonia Amygdalina</i>	17
2.5.1.1	Medicinal properties	18
2.5.1.2	Phytochemical compositions	19
2.5.1.3	Nutritional compositions	20
2.5.2	<i>Pandanus Amaryllifolius</i>	21
2.5.2.1	Medicinal properties	22
2.5.2.2	Phytochemical compositions	23
2.5.3	<i>Citrus Maxima</i> leaf	24
2.5.3.1	Medicinal properties	24
2.5.3.2	Phytochemical compositions	25
2.6	Applications of biosynthesised gold nanoparticles	26
2.6.1	Biosensors	27
2.6.2	Water purification	27
2.6.3	Catalysis	27
2.6.4	Antimicrobial	28
2.6.5	Drug delivery	28

	2.6.6	Memory device	28
	2.6.7	Cosmeceutical	29
<b>3</b>		<b>METHODOLOGY</b>	<b>30</b>
	3.1	Preparation of leaves extract	30
	3.2	Biosynthesis of gold nanoparticles	30
	3.3	Characterization of gold nanoparticles	31
	3.3.1	UV-Vis Spectrophotometer analysis	32
	3.3.2	X-ray Diffraction (XRD) measurement	32
	3.3.3	Energy Dispersive X-Ray Spectra (EDX)	33
	3.3.4	Field Emission Scanning Electron Microscopy (FESEM)	33
	3.3.5	Fourier Transform Infrared Spectrometer (FTIR)	34
	3.3.6	Particle Size Analysis	35
<b>4</b>		<b>RESULTS AND DISCUSSIONS</b>	<b>38</b>
	4.1	Introduction	38
	4.2	Effect of <i>Citrus Maxima</i> leaf extract volume on formation of gold nanoparticles.	39
	4.3	Effect of chloroauric acid (HAuCl <sub>4</sub> ) concentration on formation of gold nanoparticles using <i>Citrus Maxima</i> leaf broth.	45
	4.4	Effect of <i>Pandanus Amaryllifolius</i> leaf extract volume on formation of gold nanoparticles.	53

4.5	Effect of chloroauric acid (HAuCl <sub>4</sub> ) concentration on formation of gold nanoparticles using <i>Pandanus Amaryllifolius</i> leaf broth.	63
4.6	Effect of <i>Vernonia Amygdalina</i> leaf extract volume on formation of gold nanoparticles.	71
4.7	Effect of chloroauric acid (HAuCl <sub>4</sub> ) concentration on formation of gold nanoparticles using <i>Vernonia Amygdalina</i> leaf broth.	80
<b>5</b>	<b>CONCLUSION AND RECOMMENDATIONS</b>	<b>89</b>
	<b>REFERENCES</b>	<b>91</b>

## LIST OF TABLES

TABLE	TITLE	PAGE
Table 2.1:	Different methods for synthesising nanoparticles.	11
Table 2.2:	Differences between chemically and biologically synthesised nanoparticles.	13
Table 2.3:	The tabular data on gold nanoparticles synthesis using plant extracts.	16
Table 2.4:	Phytochemical components of ethanolic extracts of <i>V.amygdalina</i> and <i>O.gratissimum</i> .	19
Table 2.5:	Nutritional analysis of <i>Vernonia Amygdalina</i> .	21
Table 2.6:	Result from phytochemical test of <i>Pandan</i> leaves extracts.	23
Table 2.7:	Phytochemical test of Pomelo leaves extracts.	25
Table 4.1:	Functional groups of <i>Citrus Maxima</i> leaf.	40
Table 4.2:	The average particle size synthesised by different volume of <i>Citrus Maxima</i> leaf extract with constant H <sub>Au</sub> Cl <sub>4</sub> concentrations.	44
Table 4.3:	The average particle size synthesised by different concentration of H <sub>Au</sub> Cl <sub>4</sub> with constant volume of <i>Citrus Maxima</i> leaf extracts.	51
Table 4.4:	Functional groups of <i>Pandanus Amaryllifolius</i> leaf.	55
Table 4.5:	The average particle size synthesised by different volume of <i>Pandanus Amaryllifolius</i> leaf extract with constant H <sub>Au</sub> Cl <sub>4</sub> concentrations.	62
Table 4.6:	The average particle size synthesised by different concentration of H <sub>Au</sub> Cl <sub>4</sub> with constant volume of <i>Pandanus Amaryllifolius</i> leaf extracts.	69

Table 4.7:	Functional groups of <i>Vernonia Amygdalina</i> leaf.	73
Table 4.8:	The average particle size synthesised by different volume of <i>Vernonia Amygdalina</i> leaf extract with constant H <sub>AuCl</sub> <sub>4</sub> concentrations.	79
Table 4.9:	The average particle size synthesised by different concentration of H <sub>AuCl</sub> <sub>4</sub> with constant volume of <i>Vernonia Amygdalina</i> leaf extracts.	86

## LIST OF FIGURES

<b>FIGURE</b>	<b>TITLE</b>	<b>PAGE</b>
Figure 2.1:	The top-down and bottom-up approaches.	10
Figure 2.2:	Schematic representation of mechanism of biological synthesis of nanoparticles using plant extracts.	12
Figure 2.3:	<i>Vernonia amygdalina</i> (Bitter Leaf).	17
Figure 2.4:	Traditional uses of <i>Vernonia amygdalina</i> .	18
Figure 2.5:	<i>Pandanus amaryllifolius</i> (Pandanus Leaf).	22
Figure 2.6:	<i>Citrus maxima</i> leaf (Pomelo Leaf).	24
Figure 2.7:	Different applications of biosynthesised gold nanoparticles.	26
Figure 3.1:	Flow chart of research work optimization.	31
Figure 3.2:	Jasco V-730 UV-vis spectrophotometer.	32
Figure 3.3:	JEOL JSM-6701F FESEM.	34
Figure 3.4:	Perkin Elmer Spectrum RX1 FTIR spectrometer.	35
Figure 3.5:	Malvern Mastersizer 2000 Particle Size Analyser.	36
Figure 3.6:	Flowchart of the project.	37
Figure 4.1:	FTIR spectra of the <i>Citrus Maxima</i> leaf.	39
Figure 4.2:	UV-vis spectra of gold nanoparticles at different volume of <i>Citrus Maxima</i> leaf extract from 4 to 6 mL and constant concentration of H <sub>Au</sub> Cl <sub>4</sub> (0.0025 M).	41
Figure 4.3:	FESEM image of gold nanoparticles formed by exposing 4 mL of <i>Citrus Maxima</i> leaf extract to 0.0025 M of H <sub>Au</sub> Cl <sub>4</sub> .	42

Figure 4.4:	FESEM image of gold nanoparticles formed by exposing 5 mL of <i>Citrus Maxima</i> leaf extract to 0.0025 M of H <sub>AuCl</sub> <sub>4</sub> .	43
Figure 4.5:	FESEM image of gold nanoparticles formed by exposing 6 mL of <i>Citrus Maxima</i> leaf extract to 0.0025 M of H <sub>AuCl</sub> <sub>4</sub> .	44
Figure 4.6:	Size distribution of gold nanoparticles formed by different volume of <i>Citrus Maxima</i> leaf extract and constant concentrations of H <sub>AuCl</sub> <sub>4</sub> (0.0025 M).	45
Figure 4.7:	UV-vis spectra of gold nanoparticles at different concentrations of H <sub>AuCl</sub> <sub>4</sub> from 0.0025 to 0.0100 M and constant volume of <i>Citrus Maxima</i> leaf extract (5 mL).	46
Figure 4.8:	FESEM image of gold nanoparticles formed by exposing 5 mL <i>Citrus Maxima</i> leaf extract to 0.0025 M of H <sub>AuCl</sub> <sub>4</sub> .	48
Figure 4.9:	FESEM image of gold nanoparticles formed by exposing 5 mL <i>Citrus Maxima</i> leaf extract to 0.0050 M of H <sub>AuCl</sub> <sub>4</sub> .	49
Figure 4.10:	FESEM image of gold nanoparticles formed by exposing 5 mL <i>Citrus Maxima</i> leaf extract to 0.0100 M of H <sub>AuCl</sub> <sub>4</sub> .	50
Figure 4.11:	EDX spectrum of gold nanoparticles resulting from experiment using <i>Citrus Maxima</i> leaf.	51
Figure 4.12:	XRD patterns for gold nanoparticles synthesised using <i>Citrus Maxima</i> leaves on silicon substrates.	52
Figure 4.13:	Size distribution of gold nanoparticles formed by different concentrations of H <sub>AuCl</sub> <sub>4</sub> and constant volume of <i>Citrus Maxima</i> leaf extract (5 mL)	53
Figure 4.14:	FTIR spectra of the <i>Pandanus Amaryllifolius</i> leaf	54
Figure 4.15:	UV-vis spectra of gold nanoparticles at different volume of <i>Pandanus Amaryllifolius</i> leaf extract from 4 to 6 mL and constant concentration of H <sub>AuCl</sub> <sub>4</sub> (0.0025 M).	57
Figure 4.16:	FESEM image of gold nanoparticles formed by exposing 4 mL of <i>Pandanus Amaryllifolius</i> leaf extract to 0.0025 M of H <sub>AuCl</sub> <sub>4</sub> .	59
Figure 4.17:	FESEM image of gold nanoparticles formed by exposing 5 mL of <i>Pandanus Amaryllifolius</i> leaf extract to 0.0025 M of H <sub>AuCl</sub> <sub>4</sub> .	60
Figure 4.18:	FESEM image of gold nanoparticles formed by exposing 6 mL of <i>Pandanus Amaryllifolius</i> leaf extract to 0.0025 M of H <sub>AuCl</sub> <sub>4</sub> .	61

Figure 4.19:	Size distribution of gold nanoparticles formed by different volume of <i>Pandanus Amaryllifolius</i> leaf extract and constant concentrations of H <sub>Au</sub> Cl <sub>4</sub> (0.0025 M).	62
Figure 4.20:	UV-vis spectra of gold nanoparticles at different concentrations of H <sub>Au</sub> Cl <sub>4</sub> from 0.0025 to 0.0100 M and constant volume of <i>Pandanus Amaryllifolius</i> leaf extract (5 mL).	64
Figure 4.21:	FESEM image of gold nanoparticles formed by exposing 5 mL <i>Pandanus Amaryllifolius</i> leaf extract to 0.0025 M of H <sub>Au</sub> Cl <sub>4</sub> .	66
Figure 4.22:	FESEM image of gold nanoparticles formed by exposing 5 mL <i>Pandanus Amaryllifolius</i> leaf extract to 0.0050 M of H <sub>Au</sub> Cl <sub>4</sub> .	67
Figure 4.23:	FESEM image of gold nanoparticles formed by exposing 5 mL <i>Pandanus Amaryllifolius</i> leaf extract to 0.0100 M of H <sub>Au</sub> Cl <sub>4</sub> .	68
Figure 4.24:	EDX spectrum of gold nanoparticles resulting from experiment using <i>Pandanus Amaryllifolius</i> leaf.	69
Figure 4.25:	XRD patterns for gold nanoparticles synthesised using <i>Pandanus Amaryllifolius</i> leaves on silicon substrates.	70
Figure 4.26:	Size distribution of gold nanoparticles formed by different concentrations of H <sub>Au</sub> Cl <sub>4</sub> and constant volume of <i>Pandanus Amaryllifolius</i> leaf extract (5 mL).	71
Figure 4.27:	FTIR spectra of the <i>Vernonia Amygdalina</i> leaf	72
Figure 4.28:	UV-vis spectra of gold nanoparticles at different volume of <i>Vernonia Amygdalina</i> leaf extract from 4 to 6 mL and constant concentration of H <sub>Au</sub> Cl <sub>4</sub> (0.0025 M).	74
Figure 4.29:	FESEM image of gold nanoparticles formed by exposing 4 mL of <i>Vernonia Amygdalina</i> leaf extract to 0.0025 M of H <sub>Au</sub> Cl <sub>4</sub> .	76
Figure 4.30:	FESEM image of gold nanoparticles formed by exposing 5 mL of <i>Vernonia Amygdalina</i> leaf extract to 0.0025 M of H <sub>Au</sub> Cl <sub>4</sub> .	77
Figure 4.31:	FESEM image of gold nanoparticles formed by exposing 6 mL of <i>Vernonia Amygdalina</i> leaf extract to 0.0025 M of H <sub>Au</sub> Cl <sub>4</sub> .	78

Figure 4.32:	Size distribution of gold nanoparticles formed by different volume of <i>Vernonia Amygdalina</i> leaf extract and constant concentrations of H <sub>AuCl</sub> <sub>4</sub> (0.0025 M).	79
Figure 4.33:	UV-vis spectra of gold nanoparticles at different concentrations of H <sub>AuCl</sub> <sub>4</sub> from 0.0025 to 0.0100 M and constant volume of <i>Vernonia Amygdalina</i> leaf extract (5 mL).	81
Figure 4.34:	FESEM image of gold nanoparticles formed by exposing 5 mL <i>Vernonia Amygdalina</i> leaf extract to 0.0025 M of H <sub>AuCl</sub> <sub>4</sub> .	83
Figure 4.35:	FESEM image of gold nanoparticles formed by exposing 5 mL <i>Vernonia Amygdalina</i> leaf extract to 0.0050 M of H <sub>AuCl</sub> <sub>4</sub> .	84
Figure 4.36:	FESEM image of gold nanoparticles formed by exposing 5 mL <i>Vernonia Amygdalina</i> leaf extract to 0.0100 M of H <sub>AuCl</sub> <sub>4</sub> .	85
Figure 4.37:	EDX spectrum of gold nanoparticles resulting from experiment using <i>Vernonia Amygdalina</i> leaf .	86
Figure 4.38:	XRD patterns for gold nanoparticles synthesised using <i>Vernonia Amygdalina</i> leaves on silicon substrates.	87
Figure 4.39:	Size distribution of gold nanoparticles formed by different concentrations of H <sub>AuCl</sub> <sub>4</sub> and constant volume of <i>Vernonia Amygdalina</i> leaf extract (5 mL).	88

**LIST OF SYMBOLS / ABBREVIATIONS**

%	Percentage
$\theta$	Angle
°	Degree
DNA	Deoxyribonucleic acid
EDX	Energy Dispersive X-Ray
FESEM	Field Emission Scanning Electron Microscopy
FTIR	Fourier Transform Infrared
UV-VIS	Ultraviolet Visible
XRD	X-ray Diffraction

## **CHAPTER 1**

### **INTRODUCTION**

Nanobiotechnology is the term that refers to the application of nanotechnologies in biological fields. It is specifically dealing with the biogenic development and environmentally friendly technology to synthesise nanoparticles. A nanoparticle is a microscopic particle with at least one dimension less than 100 nanometres and one of the most basic component in the fabrication of a nanostructure. Generally, the properties of particles larger than nanometre size do not have significant varies to their bulk counterparts. However, the physical and chemical properties such as melting point, fluorescence, electrical conductivity, magnetic permeability and chemical reactivity can be drastically changed when particles are in nanometre size. Therefore, researchers have great interest on nanoparticles due to its unique properties and potential applications in different fields like optical, electronics, medicine, catalysis, biomaterials and energy storage production (Shah, 2014).

Nanoparticles especially gold gained high significance interest because it is noble metal and one of the most stable metallic nanoparticles. Colloidal gold is very attractive because it possesses distinctive properties like surface plasmon resonance, novel optical, thermal, catalytic, toxic-free and high biocompatibility. Gold nanoparticles have been extensively and particularly exploited in a range of applications including biosensors, bio-imaging, therapeutic agents, chronic disease diagnostics, coatings, packaging, water treatment, catalysis, electron microscopy marker and DNA sequencing. Moreover, gold nanoparticles are broadly used in the areas which involve physical contact with human such as cosmetic products, shampoos, toothpaste, detergents, soaps, shoes as well as medicinal and pharmaceutical applications (Singh *et al.*, 2018).

Due to the widespread use of gold nanoparticle, various methods have been successfully developed to synthesise gold nanoparticles such as physical, chemical and biological techniques. The most popular approach to synthesise gold nanoparticles are chemical reduction method which involves the use of traditional reducing and capping agents like sodium borohydride, sodium citrate, and sodium dodecyl sulphate. Although conventional chemical and physical methods such as photochemical reduction of gold, ultraviolet irradiation, ultrasonic fields, aerosol technologies, lithography and laser ablation can be used to produce gold nanoparticles in large quantities with desired sizes and shapes in a very short period of time, but these techniques are expensive, large amount of energy required, complex, low efficiency, outdated, non-environmentally friendly and involve the use of hazardous chemicals. Therefore, gold nanoparticles produced by these conventional methods cannot be used in medicine because of health-related issues, especially in clinical fields (Patra and Baek, 2014).

In response to these concerns, green methods to generate gold nanoparticles with non-toxic raw materials have gained more importance being actively developed because they are lower cost, clean, reliable, simple, easily produced in large scale, benign and environmentally friendly, when in comparison with the conventional physical and chemical methods. The development of green methods have embraced the principles of green chemistry, such as limiting waste products, synthesis at ambient temperature and pressure, the use of biodegradable reagents and low toxicity of chemical products. Recently, biological approaches become more popular alternative as it exploits the natural resources which act as reducing and capping agent in synthesising gold nanoparticles, for example plants, microorganisms and viruses or their by-products (carbohydrates, lipids, nucleic acids and proteins) (Kane, Mishra and Dutta, 2016).

In recent years, plant-based gold nanoparticles synthesis is proven to be more advantageous over other biological system methods because plants are generally inexpensive, simple, readily available, high reaction rate and toxic free. Almost every parts of plants have been used for synthesising gold nanoparticles including leaves, root, stem, latex, flowers and seeds. Biosynthesis using plant products need not complicated techniques to prepare the extract like purification steps, long incubation

time, intracellular synthesis and preservation of microbial cell culture. There are numerous articles have reported the biosynthesis of gold nanoparticles by using different plants or plant extracts. Various bio-components naturally present in plants possess functional groups which responsible for reducing and capping gold nanoparticles such as flavonoids, phytosterols and quinones. The procedures needed to obtain specific shapes and sizes of gold nanoparticles involve mixing the gold salt with extracts of plant for certain amount of time under varied reaction conditions like temperature, pH and incubation time (Shah, 2014).

Subsequently, several studies have been done to synthesise silver nanoparticles using *Vernonia Amygdalina* (Adesuji *et al.*, 2014) and *Pandanus Amaryllifolius* (Akhir, Fairuzi and Ismail, 2015) extract. So far, no study has reported on the synthesis of gold nanoparticles using *Vernonia Amygdalina*, *Pandanus Amaryllifolius*, and *Citrus Maxima* leaf extracts. In this study, a simple, eco-friendly and reproducible technique was used to synthesis gold nanoparticles by using leaf extract of *Vernonia Amygdalina*, *Pandanus Amaryllifolius*, and *Citrus Maxima*. These plants extract have been well studied and discussed with their phytochemical, nutritional and medicinal properties.

## 1.1 Problem Statement

The gold nanoparticles in a colloid are attracted to one another by van der Waals interactions, so in the absence of a counteracting force, aggregation and destabilization of the colloidal system are possible to take place. Therefore, aggregation will affect the morphology, size distribution and surface area of gold nanoparticles. There is a growing need for the development of new methods for synthesising gold nanoparticles. The conventional physical and chemical methods to synthesis gold nanoparticles involve the use of hazardous chemicals, expensive, complex and non-environmentally friendly. Hence, there is a need to develop a cleaner and greener method to produce gold nanoparticles that can be used in medical applications.

## 1.2 Aims and Objectives

- i) To develop an environmentally friendly method for synthesising gold nanoparticles by using the leaves extraction of *Vernonia Amygdalina*, *Pandanus Amaryllifolius*, and *Citrus Maxima* as solvent.
- ii) To determine the morphology of the biosynthesised gold nanoparticles by tuning concentration of chloroauric acid ( $\text{HAuCl}_4$ ) and volume of leaves extract.
- iii) To determine optimum the shape and size of biosynthesised gold nanoparticles for each of the extracted solvents (*Vernonia Amygdalina*, *Pandanus Amaryllifolius*, and *Citrus Maxima* leaves).

## CHAPTER 2

### LITERATURE REVIEW

#### 2.1 Introduction of nanoscience, nanotechnology and nanoparticles

The study of structures and materials on the scale of nanometres (one billionth of a metre,  $10^{-9}$  m = 1 nm) is so called Nanoscience (Singh, 2016). The field of Nanoscience is multidisciplinary and its study is related to different sciences such as physics, chemistry, material science, biochemistry or biotechnology (Sutherland, 2010). Nanoscience is said to be the science of the future since it involves a “horizontal-integrating interdisciplinary science that includes all vertical sciences and engineering disciplines” (Nouailhat, 2008).

Nanotechnology is known as any technology in the real world with the applied knowledge of nanoscience. It forms the materials, structures, components, devices and systems in nanoscale by manipulating, controlling and integrating the atoms and molecules (Sutherland, 2010). Research in Nanotechnology has commitment to breakthrough in areas such as nanoelectronics, medicine and healthcare, information technology, and national security. Nanotechnology is one of the fastest growing markets in the world and interrelated with Fourth Industrial (Nanotechnology, 2004).

Generally, a nanoparticle is a microscopic particle spans the range between 1 and 100 nm. Nanoparticles have been empirically synthesised and drawn irresistibly the attention and interest of scientist for over a century because of its high potential in nanotechnology (Mody *et al.*, 2010). Nanoparticle manufacturing is a crucial element in nanotechnology because of its specific physical and chemical properties such as mechanical strengths, optical properties, magnetizations and higher surface areas

which are attractive in industrial applications (Khan, Saeed and Khan, 2017). The most common way to generate nanostructured materials is the assembly of precursor particles and related structures (Singh, 2016).

## 2.2 Classification of nanoparticles

Nanomaterials can be divided more precisely into four different types (Tiwari, Tiwari and Kim, 2012):

- Zero dimensional → All three dimensions are in between 1 to 100 nm.  
(eg. Quantum dots)
- One dimensional → Two dimensions below 100 nm.  
(eg. Nanowires, Nanorods, Nanotubes)
- Two dimensional → Two dimensions larger than 100 nm.  
(eg. Nanofilms, Nanoplates, Nanoprisms)
- Three dimensional → Three dimensions larger than 100 nm, but components of their microstructures are at nanoscale.  
(eg. Nanocrystalline, Nanocones, Nanopillers)

Based on these structures, nanoparticles are generally classified into three classifications (Swiss Reinsurance Company, 2004):

- One dimensional (eg. Thin film)
- Two dimensional (eg. Carbon nanotubes)
- Three dimensional (eg. Dendrimers, Quantum Dots, Fullerenes)

## **2.3 Types of nanoparticles**

According to the shape, size, physical and chemical properties, nanoparticles can be classified into different types such as ceramic nanoparticles, carbon-based nanoparticles, semiconductor nanoparticles, polymeric nanoparticles, lipid-based nanoparticles and metallic nanoparticles.

### **2.3.1 Ceramic nanoparticles**

Ceramic nanoparticles are inorganic solids mainly formed by oxides, carbides, carbonates and phosphates of metals. These nanoparticles have high heat resistance and chemical inertness which are preferable in many applications such as imaging, photocatalysis, photodegradation of dyes and drug delivery. They have been widely used as drug delivery systems against a number of diseases by monitoring size, surface area, porosity and surface to volume ratio (Sajti *et al.*, 2010; Hong, Reis and Mano, 2009; Thomas *et al.*, 2015).

### **2.3.2 Carbon-based nanoparticles**

Carbon nanotubes and fullerenes are two main materials for carbon-based nanoparticles. Chemical and physical properties of carbon-based nanoparticles such as high mechanical strength, thermal and electrical conductivity and electron affinity are broadly applied for high-strength materials and electronics applications. These unique properties also being explored in the field of biomedical engineering (Dizaj *et al.*, 2015; Yuan *et al.*, 2011; Cha *et al.*, 2013).

### **2.3.3 Semiconductor nanoparticles**

Semiconductor nanoparticles have wide bandgaps and properties like those of metals and non-metals especially size dependent properties which can be applied to increase the efficiency of fluorescence or the internal magnetic field strength in doped semiconductors. They have been useful in electronics devices, photo-optics and water splitting applications. Some examples of semiconductor nanoparticles are ZnS, CdS and ZnO (Galoppini, 2004; Correa-Duarte, Giersig and Liz-Marzán, 1998; Bangal *et al.*, 2005).

### **2.3.4 Polymeric nanoparticles**

Polymeric nanoparticles are particulate dispersions or solid particles with size between 10-1000 nm and have structures shaped like nanocapsules or nanospheres. The field of polymer nanoparticles is rapidly expanding for medicine as they can effectively carry drugs, proteins, and DNA to target cells and organs with their controlled and sustained release properties, subcellular size, biocompatibility with tissue and cells (Caruso *et al.*, 2012; Kumari, Yadav and Yadav, 2010; Nagavarma *et al.*, 2012).

### **2.3.5 Lipid-based nanoparticles**

Lipid-based nanoparticles are particles with the dimension of approximately 100 nm that formed by the combination of various lipids and other chemical components in order to deal with biological barriers. The nanoscale allows their capabilities to be changeable depending on functional requirements. Consequently, these nanoparticles have applications in the biomedical field to carry therapeutic agents and cancer diagnosis (Smith *et al.*, 2012; Gobbi *et al.*, 2010; Miller, 2013).

### 2.3.6 Metallic nanoparticles

Metallic nanoparticles are made of metals precursors and have the characteristics such as large surface energies, quantum confinement, plasmon excitation, and large surface area to volume ratio compared to bulk. The localized surface plasmon resonance (LSPR) characteristics allow these nanoparticles to have distinctive optoelectronic properties. These nanoparticles are applied in detection and imaging of biomolecules, environmental, bioanalytical and research areas (Mody *et al.*, 2010; Hasan, 2014; Venkatesh, 2018). Gold nanoparticles are tiny gold particles with nanometre-sized. They are noble metal and known as the most stable metallic nanoparticles. Once they dispersed in water, are also known as colloidal gold. They have advantageous characteristics like low toxicity, good biocompatibility and optoelectronic properties. Their unique optoelectronic properties can be altered by changing the size, shape, surface chemistry, or aggregation state and have been explored and exploited in advance technology applications including biological and medical applications, electronic conductors and materials science (Yeh, Creran and Rotello, 2012; Coulie *et al.*, 2006; Hall *et al.*, 2008).

## 2.4 Methods of synthesising nanoparticles

There are two approaches for the synthesis of nanoparticles (Figure 2.1) which are summarized as below:

### A. Top-Down Approach

The principle of top-down approach is about the successive cutting of a bulk material with the purpose of getting nanometre scale particles. Top-down clearly indicates means from larger to smaller, it is analogous to the production process from stone to statue. The giant stone experiences the process of carving and cutting until the desired shape is formed. Similarly for nanoparticles, the energy applied can be mechanical,

chemical or thermal. Milling is a typical top-down method and offers the cheapest way in the production of nanoparticles (Arole and Munde, 2014; Habiba *et al.*, 2014).

## B. Bottom-Up Approach

Bottom-up approach starts with atoms or molecules to form nanoparticles. This refers to the combination of a structure between atom by atom, molecule by molecule or cluster by-cluster or are allowed to produce through self-assembly. The colloidal dispersion is one of the best method for bottom-up approach since it can produce nanoparticles with less contamination, more homogenous chemical composition and less defects (Pandey, Rawtani and Agrawal, 2016; Arole and Munde, 2014).

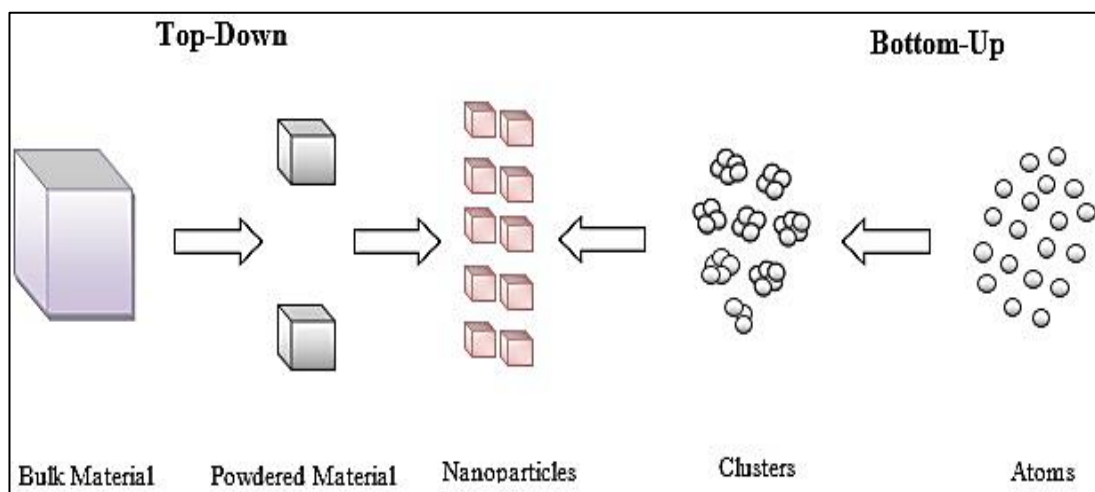


**Figure 2.1: The top-down and bottom-up approaches** (Pandey, Rawtani and Agrawal, 2016).

These two approaches consist of three sub-methods to synthesis nanoparticles which are summarized in Table 2.1.

**Table 2.1: Different methods for synthesising nanoparticles** (Patra and Baek, 2014).

<b>Physical Method</b>	<b>Chemical Method</b>	<b>Biological Method</b>
<ul style="list-style-type: none"> <li>• Arc discharge method</li> <li>• Electron beam lithography</li> <li>• Ion implantation</li> <li>• Inert gas condensation</li> <li>• Mechanical grinding</li> <li>• Milling</li> <li>• Spray pyrolysis</li> <li>• Vapour-phase synthesis</li> </ul>	<ul style="list-style-type: none"> <li>• Coprecipitation method</li> <li>• Chemical reduction of metal salts</li> <li>• Electrochemical method (electrolysis)</li> <li>• Microemulsion method</li> <li>• Pyrolysis</li> <li>• Phytochemical (irradiation) method</li> <li>• Sonochemical method</li> <li>• Sol-gel process</li> <li>• Solvothermal synthesis</li> </ul>	<ul style="list-style-type: none"> <li>• Using plant and their extracts</li> <li>• Using microorganisms (bacteria, fungi and actinomycetes)</li> <li>• Using algae (micro-seaweeds)</li> <li>• Using enzymes and biomolecules</li> <li>• Using industrial and agricultural wastes</li> </ul>

The biological procedure used in synthesising metallic nanoparticles using plant extracts (Figure 2.2) involves capping and stabilizing mediators that contribute higher stability.

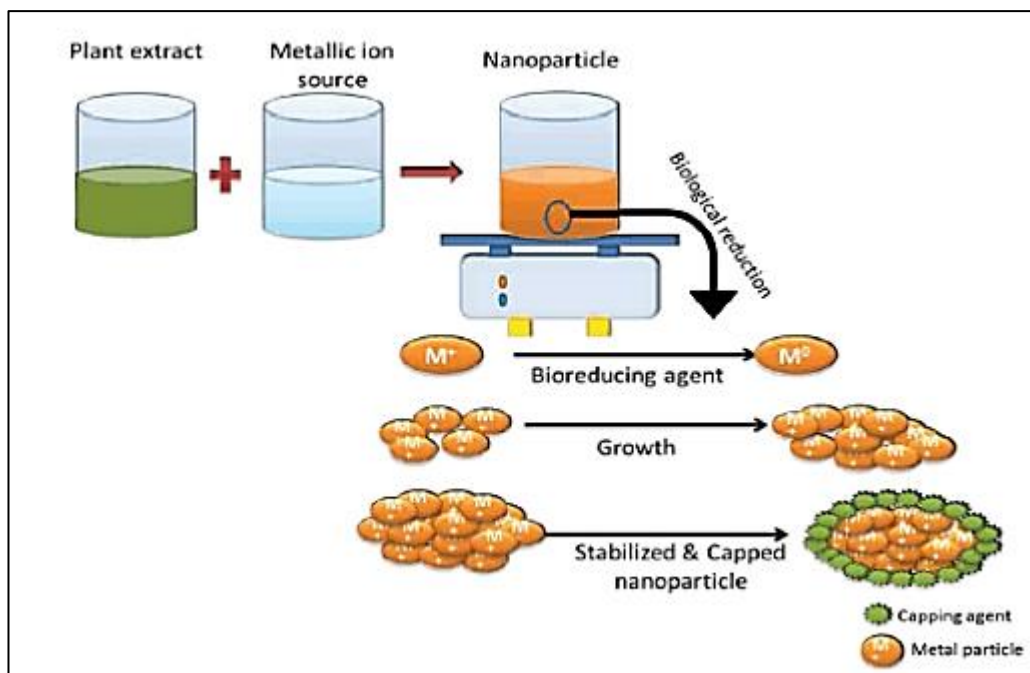


**Figure 2.2: Schematic representation of mechanism of biological synthesis of nanoparticles using plant extracts (Dikshit *et al.*, 2018).**

Among all the listed methods for synthesising nanoparticles, the chemical reduction method and biological synthesis method were broadly applied because of its advantage to control the size of particle and morphology very praiseworthy. The comparison between chemically and biologically synthesised nanoparticles is shown in Table 2.2.

**Table 2.2: Differences between chemically and biologically synthesised nanoparticles (Dikshit *et al.*, 2018).**

<b>Properties</b>	<b>Chemical</b>	<b>Biological</b>
<b>Nature</b>	Expensive, High Toxicity.	Cost effective, Non-toxic.
<b>Reducing Agent</b>	Dimethylformamide, ethylene glycol, hydrazine hydrate, sodium borohydride, polyol, sodium citrate and N,N-dimethylformamide.	Biomolecules include phenolics, polysaccharides, flavones, terpenoids, alkaloids, proteins, amino acids, enzymes, predominantly, nitrate reductase.
<b>Method</b>	Stabiliser (surfactant) is added to the first solution to prevent the agglomeration of nanoparticles.	There is no need to add a stabilising agent.
<b>Environmental Impact</b>	Environment pollution, Energy-intensive.	Synthesis carried out in environmental conditions and they are safe enough, and consume less energy.
<b>Antibacterial Activity</b>	The chemically synthesised nanoparticles showing comparatively lower antimicrobial activity against pathogenic bacteria.	The nanoparticles synthesised from biological means are showing better antimicrobial activity against the pathogenic bacteria.

## 2.5 Plant in nanoparticles synthesis

The widespread use of metallic nanoparticles are emerging significantly in different fields like pharmaceutical, biosensor, bioimaging and antimicrobial because of their totally new or developed properties. Among the metallic nanoparticles, gold nanoparticle is the most essential and useful nanoparticle because of its biocompatibility which can be applied to deal with cancer and arthritis. Although there are many physical and chemical methods have been used effectively to produce pure and well-defined gold nanoparticles, but the chemicals needed are very hazardous, high toxicity, costly, high energy consumption and not suitable for biological applications (Noruzi, 2015).

Green chemistry emphasizes on the environmental impact of chemistry, including technologies to prevent pollution and minimize the use of non-renewable energy sources. Eco-friendly methods to synthesis nanoparticles has received an increasing attention when the people are getting worried about the environmental issues. The development of biologically-inspired experimental processes is treated as one of the milestone achievement in nanotechnology. For instance, the biosynthesis of nanoparticles is getting more important by reason of its uncomplicatedness, eco-friendliness and rapid formation of nanoparticles, especially using microorganisms and plants (Ahmed *et al.*, 2016).

Generally, the use of plants for synthesising nanoparticles is better due to most of the plants are inexpensive, available, and non-hazardous. Additionally, different types of natural capping and reducing agents are readily supplied by plants such as phenols, polysaccharides, flavones, terpenoids, alkaloids, proteins, amino acids, enzymes and alcoholic compounds. It has been reported that gold nanoparticles were synthesised using plant extracts or parts of the plants such as *Coriander* leaf (Narayanan and Sakthivel, 2008), *Cinnamomum Camphora* leaf (He *et al.*, 2007), *Terminalia Catappa* (Ankamwar, 2010), *Psidium Guajava* leaf (Taha and Shamsuddin, 2013), *Ziziphus Zizyphus* (Al-Batayneh *et al.*, 2018), *Tinospora Crispa* (Kane, Mishra and Dutta, 2016), *Magnolia Kobus* and *Diopyros Kaki* leaf (Song, Jang and Kim, 2009), *Vitis Vinifera* leaves and seeds (Ismail *et al.*, 2014), *Olive* leaf (Khalil, Ismail and El-

Magdoub, 2010) and *Euphrasia Officinalis* leaf (Singh *et al.*, 2018). The research studies have been done in this field to compare nanoparticles in terms of particle size and shape in Table 2.3.

**Table 2.3: The tabular data on gold nanoparticles synthesis using plant extracts.**

<b>Plant Type</b>	<b>Size (nm)</b>	<b>Shape</b>	<b>References</b>
<i>Coriander</i>	6.75 - 57.91	Spherical	(Narayanan and Sakthivel, 2008)
<i>Cinnamomum Camphora</i>	10 - 40	Spherical	(He <i>et al.</i> , 2007)
<i>Terminalia Catappa</i>	10 - 35	Spherical	(Ankamwar, 2010)
<i>Psidium Guajava</i>	4 - 24	Spherical	(Taha and Shamsuddin, 2013)
<i>Ziziphus Zizyphus</i>	40 - 50	Spherical	(Al-Batayneh <i>et al.</i> , 2018)
<i>Tinospora Crispa</i>	20 - 30	Spherical	(Kane, Mishra and Dutta, 2016)
<i>Magnolia Kobus</i> and <i>Diopyros Kaki</i>	5 - 300	Triangular, Pentagonal, Hexagonal and Spherical	(Song, Jang and Kim, 2009)
<i>Vitis Vinifera</i>	18 – 25	Hexagonal, Triangular and Quasi-spherical	(Ismail <i>et al.</i> , 2014)
<i>Olive</i>	50 – 100	Triangular	(Khalil, Ismail and El-Magdoub, 2010)
<i>Euphrasia Officinalis</i>	49.72 ± 1.2	Quasi-spherical	(Singh <i>et al.</i> , 2018)

### 2.5.1 *Vernonia Amygdalina*

*Vernonia amygdalina* (Figure 2.3) is a tropical shrub or small tree with dark green coloured leaves and a bitter taste that usually found in Asia and Africa. It is kind of medicinal plant that belongs to the Asteraceae family and generally so-called bitter leaf (English), olubu (Igbo), shikawa(Hausa), ewuro (Yoruba), etidot (Ibibio), ilo (Igala), grawa (Amharic) and oriwo (Edo) (Kadiri and Olawoye, 2017). The presence of anti-nutritional phytochemicals such as glycosides, tannins, saponins and alkaloids act as bittering agent in *Vernonia amygdalina*. It is treated as multipurpose edible plants by farmers due to its great adaptability and compatibility with other crops. Therefore, it helps to improve the fertility of soil and growth of perennial crops instead of competing for soil nutrients (Habtamu and Melaku, 2018).



**Figure 2.3:** *Vernonia amygdalina* (bitter leaf).

### 2.5.1.1 Medicinal properties

*Vernonia amygdalina* is commonly used in traditional medicine as its leaves can be eaten either as vegetable or aqueous extracts for the prevention and treatment of various diseases. Chimpanzees were observed to consume the leaves suffering parasitic infections in the wild. Hence, health workers in Africa recommend their patients to ingest the aqueous extracts of bitter leaf for treatment of different illnesses such as diabetes, dysentery, emesis, nausea, loss of appetite and other gastrointestinal tract issues to sexually transmitted diseases and diabetes mellitus among others. Some of these claims have been experimentally proved and documented while others are yet to be validated. Figure 2.4 shows the traditional uses of *Vernonia amygdalina* (Farombi and Owoeye, 2011).



**Figure 2.4:** Traditional uses of *Vernonia amygdalina* (Farombi and Owoeye, 2011).

### 2.5.1.2 Phytochemical compositions

Phytochemicals are natural occurring, biological active chemical compounds produced by plants. They are mainly in charge for the colour, flavour and aroma of fruits and particularly vegetables. The beginning of several chronic illnesses such as diabetes, cancers, heart and Alzheimer's disease can be prevented by all these bioactive compounds. In *Vernonia amygdalina*, phytochemicals consist of bioactive compounds that are anti-viral in nature and have a prophylactic and therapeutic effect on cancer cells. According to (Udochukwu *et al.*, 2015), *Vernonia amygdalina* contained more bioactive compounds than *Ocimum gratissimum* except for phytate and cyanogenic glycosides (Table 2.4). The listed phytochemicals have the ability of reducing, stabilizing, capping and preventing accumulation of nanoparticles.

**Table 2.4: Phytochemical components of ethanolic extracts of *V. amygdalina* and *O. gratissimum* (mg/100g) (Udochukwu *et al.*, 2015).**

Phytochemical	<i>V. amygdalina</i>	<i>O. gratissimum</i>
Oxalate	3.48	0.75
Phytate	3.95	5.56
Tannins	9.62	2.48
Saponins	5.97	3.52
Flavonoid	4.89	1.74
Cyanogenic glycoside	1.11	2.38
Alkaloids	2.16	1.07
Anthraquinone	0.14	0.31
Steroid	0.38	0.30
Phenol	3.24	0.73

### **2.5.1.3 Nutritional compositions**

Many studies have established the nutritional content of *Vernonia amygdalina* and shown that it is enriched with proteins, fats, fibres, amino acids, minerals vitamins, and carbohydrates. However, the nutritional compositions of *Vernonia amygdalina* leaf, root and stems differed from one study to another, possibly because of geographical position, genetic, biological, harvest situations, and ecology of the plant. Table 2.5 illustrates the nutritional composition of dried *Vernonia amygdalina* which reported by (Kadiri and Olawoye, 2017). The nutritional compositions present in *Vernonia amygdalina* act as both reducing agents as well as capping agents that can be used to stabilize and govern the morphology of nanoparticles.

**Table 2.5: Nutritional analysis of *Vernonia amygdalina*** (Kadiri and Olawoye, 2017).

<b>Nutrient</b>	<b>Value (g/mg)</b>
Crude protein	23.10 g
Ash	17.13 g
Cellulose	12.31 g
Edible portion	100 g
Fats	0.4 g
Protein	5.2 g
Water	82.0 g
Energy	218 g
Carbohydrates	10.0 g
Dietary Fibre	1.5 g
Calcium	145 mg
Phosphorus	6.7 mg
Iron	5.0 mg
Zinc	85.0 mg
Manganese	710.0 mg
Ascorbic acid	5.1 mg

### 2.5.2 *Pandanus Amaryllifolius*

*Pandan* leaf (Figure 2.5) with the scientific name so-called *Pandanus amaryllifolius* which belongs to the Pandanaceae family. It cultivates abundantly in tropical areas such as the pacific islands, Australia, Africa, South Asia and South East Asia. Its long, narrow, blade-like monocotyledon leaves often used to give a refreshing and sweet-scented taste and act as natural colorant to both sweet and flavoursome South East Asian dishes. The presence of vital compounds, 2-Acetyl-1-Pyrroline (ACPY) in

*pandan* leaves emit a pleasant aroma which is identified in some expensive aromatic Basmati and Jasmine rice. The main compounds that responsible for the natural colorants inside *pandan* leaves are chlorophylls and carotenoids (Food *et al.*, 2016).



**Figure 2.5:** *Pandanus amaryllifolius* (*pandan leaf*) (Wakte *et al.*, 2009).

#### 2.5.2.1 Medicinal properties

*Pandan* leaves have been widely used in Indonesia as traditional medicine for anti-inflammation because of its antioxidant compounds like vitamin E, flavonoids, phenolic compounds and ascorbic acid. The leaf contains essential oils, carotenoids, tocopherols, tocotrienols, quercetin, alkaloids, fatty acids, esters and non-specific lipid transfer proteins. The oil of the leaf is extracted and used as stimulant and antispasmodic because it is effective against headaches, rheumatism, and epilepsy and as a cure for sore throats (Nor *et al.*, 2008).

### 2.5.2.2 Phytochemical compositions

According to (Aini and Mardiyarningsih, 2016), a phytochemical test was done to determine bioactive compounds in *pandan* leaves extract and the analysis results confirmed the presence of tannin, alkaloids, flavonoids, saponin, and polyphenol (Table 2.6).

**Table 2.6: Result from phytochemical test of *pandan* leaves extract (Aini and Mardiyarningsih, 2016).**

Phytochemical	Reactant	Result	Conclusion
Alkaloids	Wagner	Sediment Formation	Positive
		Brown	
	Dragendorf	Sediment Formation	Positive
		Red	
Tannin	FeCl <sub>3</sub> 1%	Color Changing	Positive
		Bluish Green	
Saponin		Stable	Positive
		Foam Formation	
Flavonoids	Mg+HCl+Ethanol	Color Changing	Positive
		Red	
Polyphenol	FeCl <sub>3</sub> 1%	Color Changing	Positive
		Bluish Green	

### 2.5.3 *Citrus Maxima* leaf

*Citrus maxima* leaf (Figure 2.6) commonly known as pomelo or shaddock leaf which belongs to the Rutaceae family is broadly distributed indigenous plant to tropical parts of Asia. It is scientifically named as *Citrus maxima* because it is the biggest citrus fruit. The fruits consist of vitamin C, B1, B2, B12, protein and calcium. Therefore, it is cultivated for use of its medicinal properties in many countries like Japan, Vietnam, Malaysia, Indonesia and Thailand. The leaves are appearing simple, having one leaflet, ovate to elliptical, with the length of 5-20 cm and width of 2-12 cm (Agroforestry Database, 2009).



**Figure 2.6:** *Citrus maxima* leaf (pomelo leaf) (El-kholy, Aboushousha and Ageez, 2017).

#### 2.5.3.1 Medicinal properties

*Citrus maxima* have been used as traditional medicine for thousands of years since they can be easily found in rural and tribal areas. The leaves of plant are popularly used for the treatment of epilepsy, chorea, seizures, ulcer, hemorrhages and convulsive cough. Several studies have been proved potential antioxidants, hypoglycemic,

antitumor, analgesic, anti-inflammatory, antibacterial, anti-depressive, anxiolytic, anticonvulsant, hypnotic, muscle relaxant and hepatoprotective of the leaves of this plant in different extracts. The oil extracted from fresh leaves possess anti-dermatophytic activity and fungicidal activity. Flower are utilized as sedative in nervous affection. Fruits acts as cardi tonic and are used in leprosy, asthma, cough, hiccough, mental aberration, epilepsy. Rind are suitable in use for anti-asthmatic, sedative in nervous affection, brain tonic and useful in vomiting, griping of abdomen, diarrhea, headache and eye troubles (Kharjul et al., 2012).

### 2.5.3.2 Phytochemical compositions

As reported by (Vijaylakshmi and Radha, 2015), a phytochemical analysis was done to determine phytoconstituents in pomelo leaves extract and the analysis results confirmed the presence of amino acids, flavonoids and carbohydrates (Table 2.7).

**Table 2.7: Phytochemical test of pomelo leaves extracts** (Vijaylakshmi and Radha, 2015).

Amino Acids	Alanine, Asparagine, Aspartic acid, Coline, Glutamic acid, Glycine and proline
Flavonoids	Acacetin, Rutin, Tangeretin, Cosmosiin, Diosmetin, Diosmin, Eriocitrin, Hesperidin, Naringin
Carbohydrates	Phytol, Synephrine, Methyl antralinatate, Fructose, Glucose and Pectin

## 2.6 Applications of biosynthesised gold nanoparticles

Biosynthesised gold nanoparticles are widely used in numerous applications due to their properties such as low toxicity, high stability and unique electronic, optical, and spectroscopic properties. They have been used in biosensors, bioimaging, catalysis, antimicrobial, drug delivery, memory device, cosmetic, wastewater treatment, etc. (Figure 2.7).

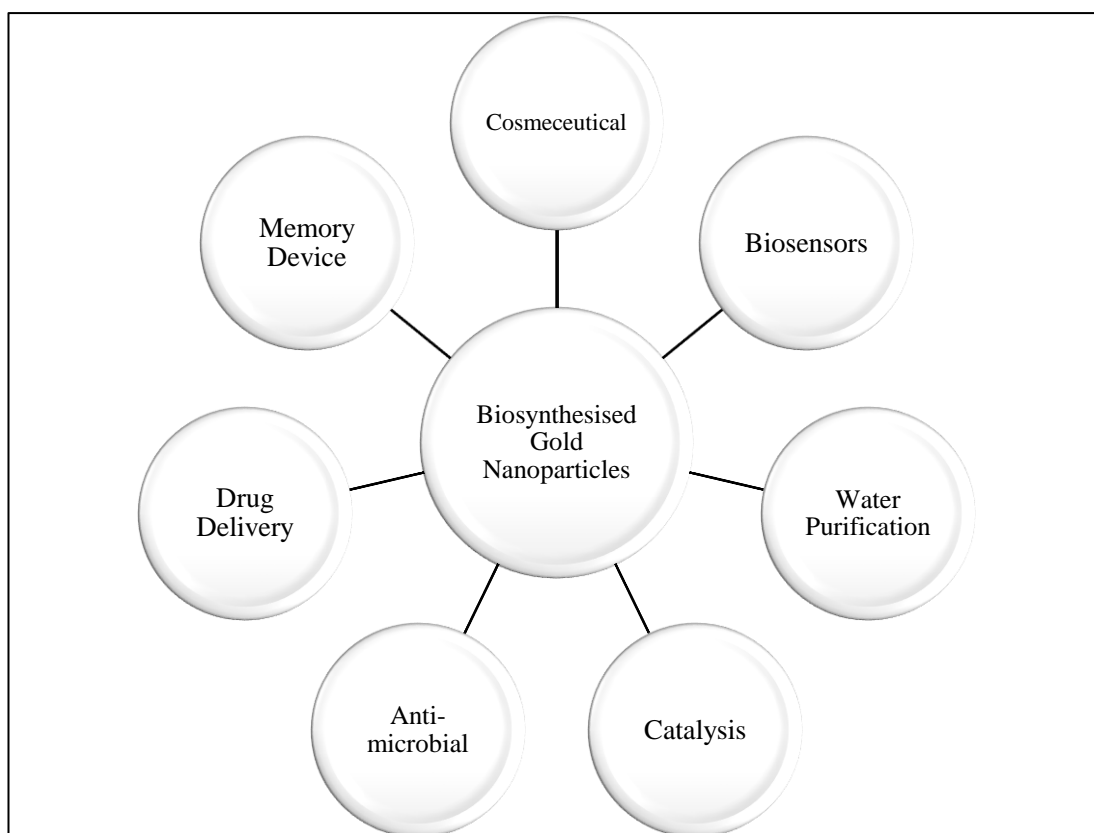


**Figure 2.7: Different applications of biosynthesised gold nanoparticles.**

### **2.6.1 Biosensors**

Gold nanoparticles have been essentially used for labelling and bioimaging applications for biosensors due to their properties of electric conductivity and optic absorption fluorescence. Their function in biosensor is to precisely identify the presence of analyte molecules and to provide a display of output that shows the concentration of the analyte. Besides, gold nanoparticles are very suitable to act as contrast agent as they can provide contrast for visualization and observation with their characteristic of high absorption and scattering visible light (Tikariha *et al.*, 2012).

### **2.6.2 Water purification**

The research has been done for obtaining pure water free from pollutants such as pesticides and pathogenic organisms as they will pose potential hazards to human health. As stated by (Das, Das and Guha, 2009), gold nanoparticles were biologically synthesised on the surface of *Rhizopus oryzae*. The nanogold-bioconjugate (NGBC) exhibited antimicrobial activity against different bacteria and yeasts and strong absorption capacity toward different organophosphorous pesticides. The use of NGBC to eliminate pesticides and pathogenic organisms is an advanced development of nanotechnology-based green approach for water purification.

### **2.6.3 Catalysis**

The use of gold nanoparticles as a catalytic agent has played a significant role in green chemistry. Nano-particulate Au catalysts are cost-effective in reducing the operating costs of chemical plants and increasing the selectivity of the reactions involved. They can be applied in pollution control such as low light-off auto catalysts, air cleaning, and purification of hydrogen streams used for fuel cells as their durability and poison resistance are shown to be better than expected (Thompson, 2007).

#### **2.6.4 Antimicrobial**

Gold nanoparticles have good antibacterial activities and bactericidal effects on many microorganisms. However, the shape and size of the gold nanoparticles are influential factors to the bactericidal effects. The surface of the bacterial cell membrane with the attached gold nanoparticles will cause disruption of the membrane and eventually leads to cell death. Gold nanoparticles combined with another antibacterial agent such as ciprofloxacin will enhance the antibacterial activity which greater than that of gold nanoparticles alone (Katas *et al.*, 2018).

#### **2.6.5 Drug delivery**

Gold nanoparticles are currently under intense exploration to use as gene and drug delivery agents especially for antitumor preparations and antibiotics due to their high capacity of surface loading. Gold nanoparticles can be transported into the cells through active or passive targeting mechanisms. For passive targeting process, gold nanoparticles accumulate within the tumour through its irregular vasculature and allow large-sized particles to penetrate through the endothelium. On the other hand, active targeting depends on the binding of gold nanoparticles to a surface ligand which increases the selectivity and specificity to the target analytes (Yeh, Creran and Rotello, 2012).

#### **2.6.6 Memory device**

Significantly, the use of gold nanoparticles in the fabrication and characterization of nano-floating gate memory devices has been extensively studied. Gold nanoparticles have been popularly used as the charge trapping element in nanoparticle-based non-volatile memory devices due to their characteristics of chemically stable and have a

high work function. Besides, many tactics have been performed to synthesise gold nanoparticles for improving the programmable memory characteristics and reliability of devices. Nowadays, gold nanoparticle based non-volatile memory devices are fabricated from conventional silicon substrates to flexible substrates (Lee, 2010).

### **2.6.7 Cosmeceutical**

Gold nanoparticles have been studied in cosmeceutical industries because of their strong antifungal and antibacterial properties. They are widely used in variety of cosmeceuticals products like foundation, lotion, face powder, moisturizer, deodorant, anti-wrinkle cream. *L'Oreal* and *L'Core Paris* are the cosmetic company that using gold nanoparticles for manufacturing more effective creams and lotions. The main properties of gold nanoparticles in beauty care are anti-inflammatory, acceleration of blood circulation, antiseptic, improvising firmness and elasticity of skin, delaying aging process and vitalizing skin metabolism (Verma *et al.*, 2018).

## CHAPTER 3

### METHODOLOGY

#### 3.1 Preparation of leaves extract

Fresh *Vernonia Amygdalina*, *Pandanus Amaryllifolius*, and *Citrus Maxima* leaves were collected from rural areas of Ipoh, Malaysia. Leaves broth used for the reduction were prepared by taking 50 g of thoroughly washed and finely cut leaves in a 500 mL Erlenmeyer flask with 200 mL sterile distilled water and then boiling the mixture for 2 minutes before finally decanting it. The process of boiling the leaves leads to rupture of the walls of leaf cells and, thus, release of intra-cellular material into solution. The prepared extract of leaves used as bioreducing agent was stored in the dark at 4 °C to be used within one week.

#### 3.2 Biosynthesis of gold nanoparticles

To study the effect of metal ion concentration, typically 5 mL of *Vernonia Amygdalina*, *Pandanus Amaryllifolius*, and *Citrus Maxima* leaves extract was added to a vigorously stirred 30 mL of chloroauric acid (HAuCl<sub>4</sub>) and stirred for 24 hours with varied concentration from 0.0025 M to 0.01 M. The same experiment was repeated by using the optimum concentration whilst varying the volume of leaves extract (4–6 mL) as shown in Figure 3.1.

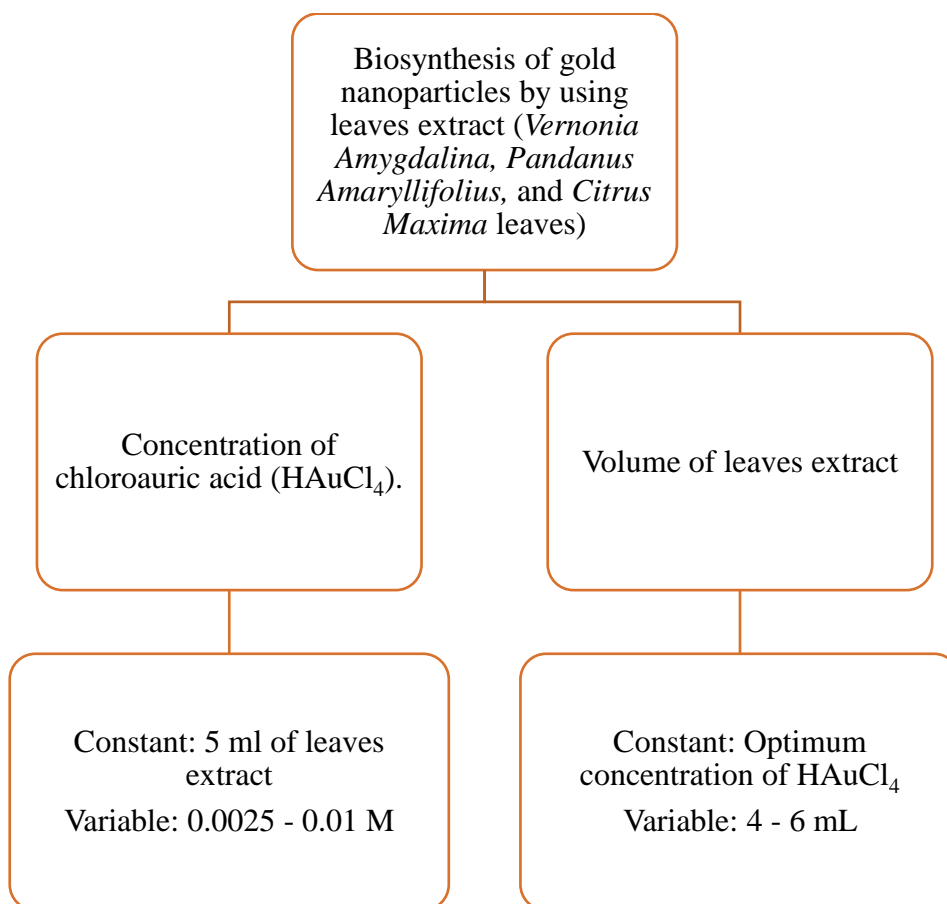


**Figure 3.1: Flow chart of research work optimization.**

### 3.3 Characterization of gold nanoparticles

Gold nanoparticles are normally characterized by their shape, size, and dispersity. The common methods of characterizing gold nanoparticles are as follows: UV–visible spectrophotometry, X-ray diffraction (XRD), field emission scanning electron microscopy (FESEM), Energy Dispersive X-Ray Spectra (EDX), Fourier transform infrared spectroscopy (FTIR), and particle size analysis.

### 3.3.1 UV-Vis Spectrophotometer analysis

UV-visible spectroscopy was used to confirm the formation of gold nanoparticles by measuring plasmon resonance and evaluating the collective oscillations of conduction band electrons in response to electromagnetic waves. Gold nanoparticles have an absorbance peak between 500 and 550 nm due to the excitation mode of the surface plasmons, which vary depending on the size of the nanoparticle. UV-vis spectra analysis was done by using Jasco V-730 UV-vis spectrophotometer as shown in Figure 3.2.



**Figure 3.2: Jasco V-730 UV-vis spectrophotometer.**

### 3.3.2 X-ray Diffraction (XRD) measurement

X-ray diffraction was used in determination of chemical composition, crystallographic structure and physical properties of gold nanoparticles. The XRD analysis was done using X-ray diffractometer XRD 6000 (Shimadzu) operating at 30 mA current and 40 kV voltages to confirm the crystalline form of gold nanoparticles.

### **3.3.3 Energy Dispersive X-Ray Spectra (EDX)**

The elemental composition of the nanoparticles can be determined by EDX analysis. The number of X-rays which are emitted to balance up the energy difference between two electrons can be detected by an EDS detector and therefore analysed qualitatively and quantitatively. In order to carry out EDX analysis, the reduced gold nanoparticles were dried and drop coated onto silicon substrate and performed on JEOL JSM-6701F FESEM instrument equipped with JEOL JED-2300 EDS system.

### **3.3.4 Field Emission Scanning Electron Microscopy (FESEM)**

FESEM was used to characterize the size and morphology of gold nanoparticles through direct visualization. For FESEM analysis, the gold nanoparticles were prepared by taking a small drop and drying it onto the silicon substrate. The FESEM observations were performed on the instrument JEOL JSM-6701F FESEM (Figure 3.3).



**Figure 3.3: JEOL JSM-6701F FESEM.**

### **3.3.5 Fourier Transform Infrared Spectrometer (FTIR)**

FTIR measurements as functional groups conformation were carried out to identify the possible biomolecules in dried biomass. FTIR spectra of dried leaves powder were recorded with Perkin Elmer Spectrum RX1 FTIR spectrometer as shown in Figure 3.4.



**Figure 3.4: Perkin Elmer Spectrum RX1 FTIR spectrometer.**

### **3.3.6 Particle Size Analysis**

Particle size analysis was used to determine the size distribution of biosynthesised gold nanoparticles. The analyser able to measure materials in the size range from 0.02 to 2000  $\mu\text{m}$ . In order to carry out particle size analysis, 30 mL of reduced gold nanoparticles were diluted with 20 mL of distilled water. The particle size analysis was performed on the instrument Malvern Mastersizer 2000 Particle Size Analyser (Figure 3.5), which operating at 2000 rpm.



**Figure 3.5: Malvern Mastersizer 2000 Particle Size Analyser.**

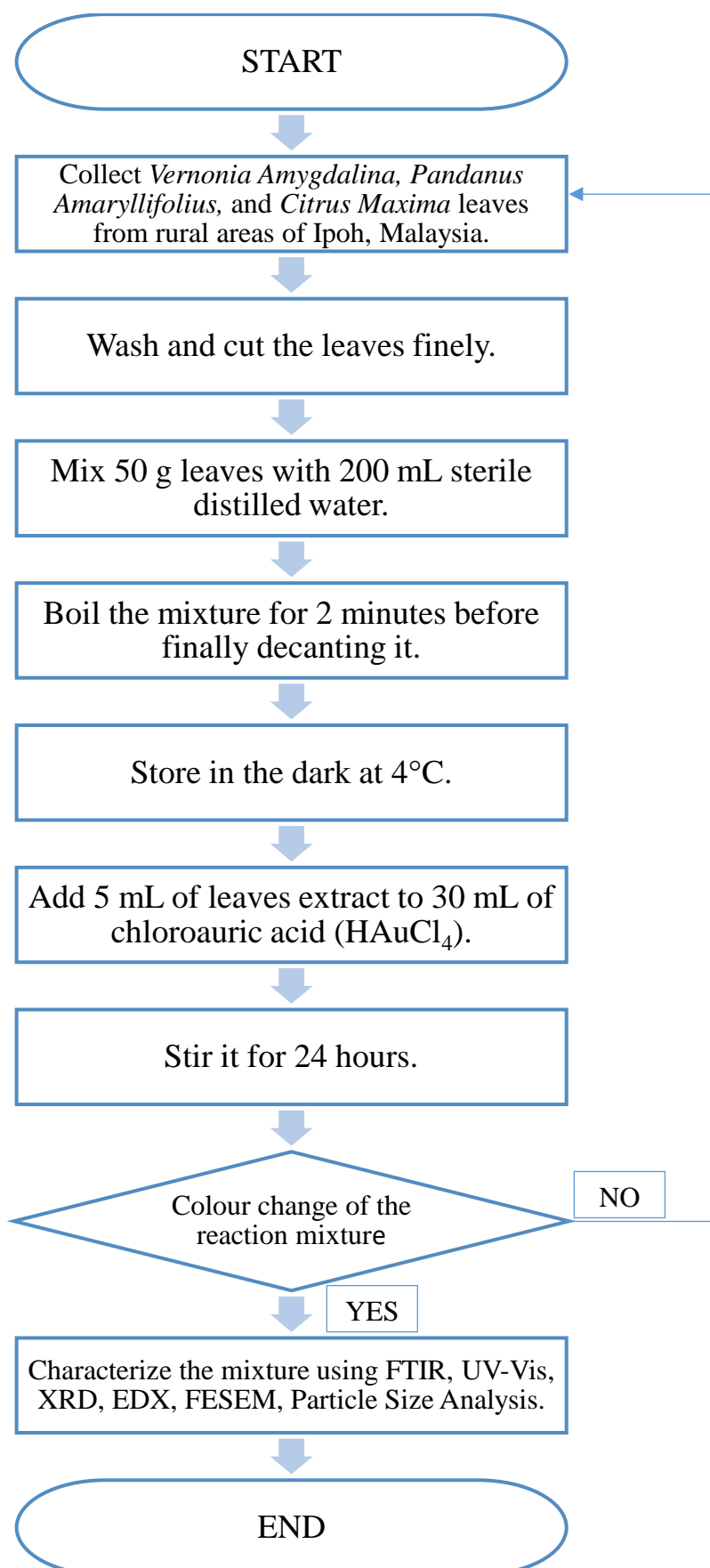


**Figure 3.6: Flowchart of the project.**

## CHAPTER 4

### RESULTS AND DISCUSSIONS

#### 4.1 Introduction

This chapter discusses the effect of tuning two different parameters in order to obtain optimum shape and size of biosynthesised gold nanoparticles by using *Vernonia Amygdalina*, *Pandanus Amaryllifolius*, and *Citrus Maxima* leaves extract. The effect of chloroauric acid ( $\text{HAuCl}_4$ ) concentration and volume of leaf broth on formation gold nanoparticles was studied to obtain the optimum parameters. The results obtained from the characterizations which are FTIR Spectroscopy, UV-Vis Spectroscopy, FESEM analysis, EDX analysis, Particle Size analysis and XRD measurement have proved that the formation of gold nanoparticles.

FTIR measurements as functional groups conformation were carried out to identify the possible biomolecules in dried biomass of *Pandanus Amaryllifolius*, *Vernonia Amygdalina* and *Citrus Maxima* leaf being responsible for the reduction, capping of and efficient stabilization of the bio-reduced gold nanoparticles. UV-visible spectroscopy was used to confirm the formation of gold nanoparticles by measuring plasmon resonance and evaluating the collective oscillations of conduction band electrons in response to electromagnetic waves. Further characterization of the size and shape of the biosynthesised gold nanoparticles was performed using FESEM through direct visualization. The elemental composition of the nanoparticles was analysed qualitatively and quantitatively by using EDX analysis. Particle Size analysis was used to determine the uniformity in size distribution of gold nanoparticles. XRD measurement was used in determination of chemical composition, crystallographic structure and physical properties of materials.

#### 4.2 Effect of *Citrus Maxima* leaf extract volume on formation of gold nanoparticles.

In order to identify the possible molecules present in leaf which are contributed for the reduction of gold nanoparticles and their stabilization, FTIR measurement were carried out. Several types of phytochemical constituents such as amino acids, flavonoids and carbohydrates are present in *Citrus Maxima* leaf. The FTIR analysis of the *Citrus Maxima* leaf (Figure 4.1) revealed the prominent bands at 618, 1064, 1636, 2345, 2375, 3448  $\text{cm}^{-1}$ . The broad bands at 3448, 2375, 2345  $\text{cm}^{-1}$  are due to the O-H stretching vibrational frequencies and strongly indicates the presence of organic molecules with alcohols and carboxylic acids functional groups. The IR band at 1636  $\text{cm}^{-1}$  is the characteristics of the C=C stretch vibrations from aromatics, while the weaker stretch at 1064  $\text{cm}^{-1}$  arises due to C-O-C vibrations of ethers. The 618  $\text{cm}^{-1}$  band is assigned to the acetylenic C-H bend present in the alkynes. The presence of functional groups in *Citrus Maxima* leaf has been summarized in Table 4.1.

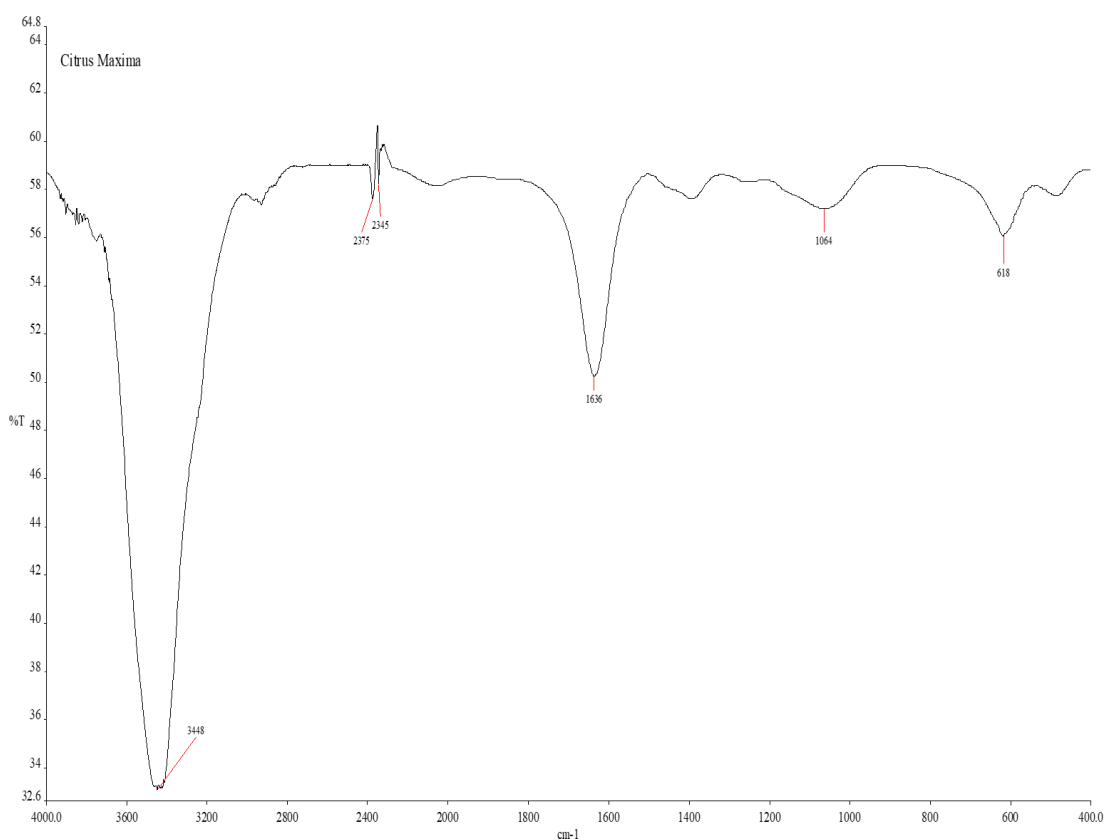


Figure 4.1: FTIR spectra of the *Citrus Maxima* leaf.

**Table 4.1: Functional groups of *Citrus Maxima* leaf.**

<b>Citrus Maxima</b>		
<b>Wavenumber (cm<sup>-1</sup>)</b>	<b>Molecular Motion</b>	<b>Functional Group</b>
3448	O-H stretch	Alcohols
2375	O-H stretch	Carboxylic Acids
2345	O-H stretch	Carboxylic Acids
1636	C=C stretch	Aromatics
1064	C-O-C stretch	Ethers
618	acetylenic C-H bend	Alkynes

The change in colour from pale yellow to violet confirmed the presence of gold nanoparticles due to gold ions reduction through the phytochemical constituents in *Citrus Maxima* leaf extract. The formation and stability of gold nanoparticles were verified by UV-Vis spectroscopy. Spectrophotometric absorption measurements in the wavelength range of 500–600 nm are used in characterizing the gold nanoparticles. Figure 4.2 shows the UV-Vis spectra of gold nanoparticles formation using constant concentration of HAuCl<sub>4</sub> (0.0025 M) with different volume of *Citrus Maxima* leaf extract from 4 to 6 mL. The spectrum showed maximum absorption band peak centered at 553 nm for gold nanoparticles with 4 mL of leaf extract which confirmed the formation of gold nanoparticles.

Addition of leaf extract from 4 to 6 mL leads to slightly increase in the absorption as shown in Figure 4.2. The spectrum of 6 mL leaf extract showed that the band peak centered at 585 nm which has the largest absorbance wavelength among three different volumes. Therefore, the broader peak using 6 mL of leaf extract which indicated the formation of larger gold nanoparticles. Red shift of the absorbance band

was observed with increasing volume of extract. As the peak absorbance wavelength increases with particle diameter, this indicates that the gold nanoparticles which synthesised by 6 mL of *Citrus Maxima* leaf extract will have larger diameter in comparison to 4 and 5 mL. The higher peaks observed for larger volume of leaves extract might be due to an increase of gold nanoparticles because of higher amount of bio-compounds present in reaction mixture (Ahmad *et al.*, 2018).

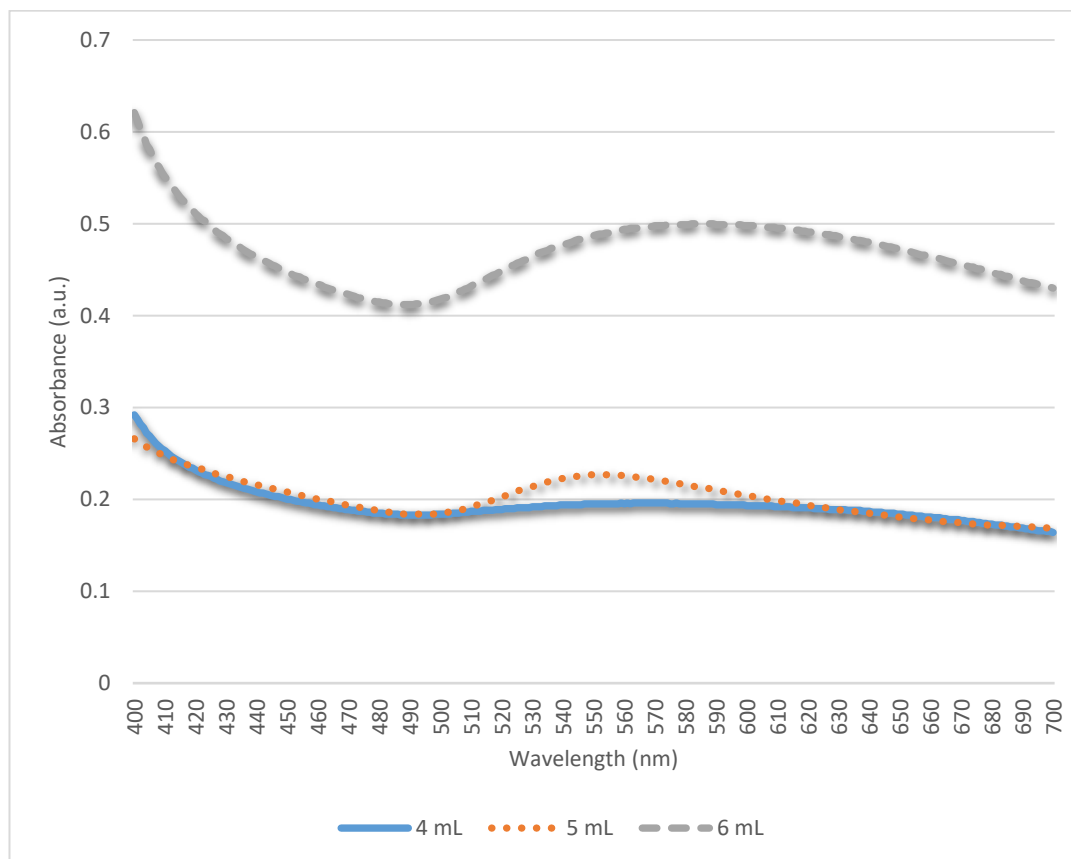
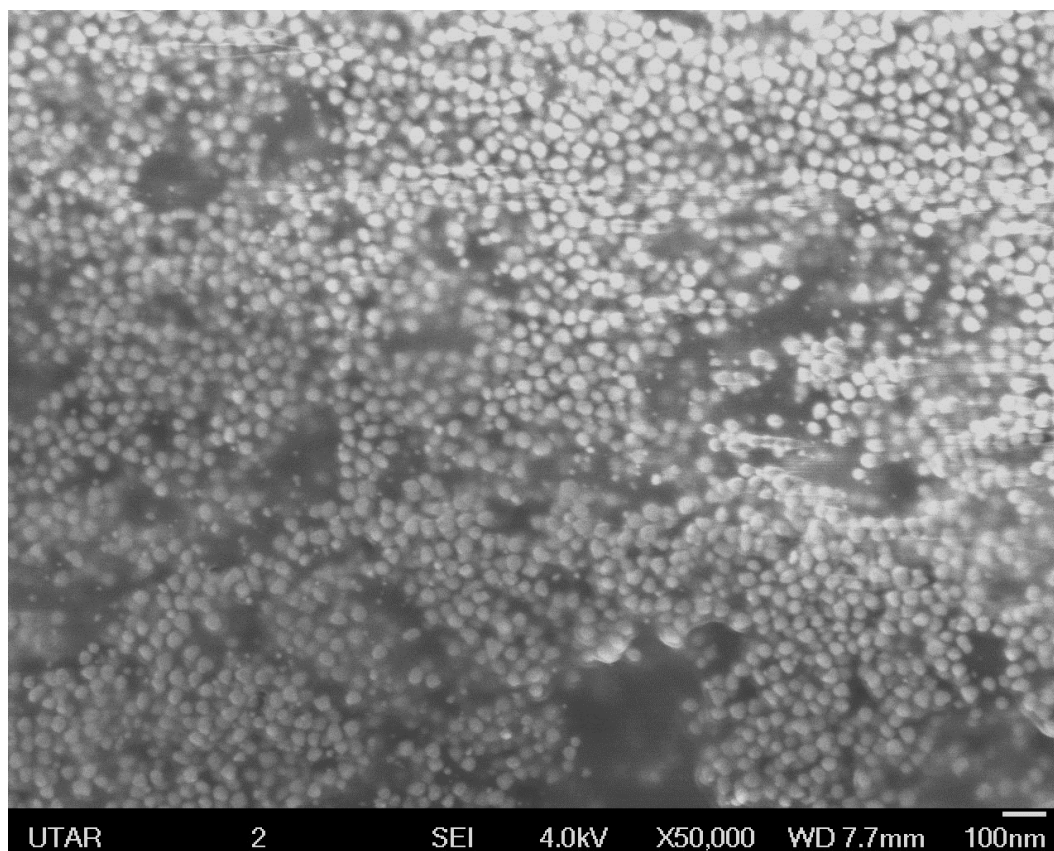


**Figure 4.2: UV-vis spectra of gold nanoparticles at different volume of *Citrus Maxima* leaf extract from 4 to 6 mL and constant concentrations of HAuCl<sub>4</sub> (0.0025 M).**

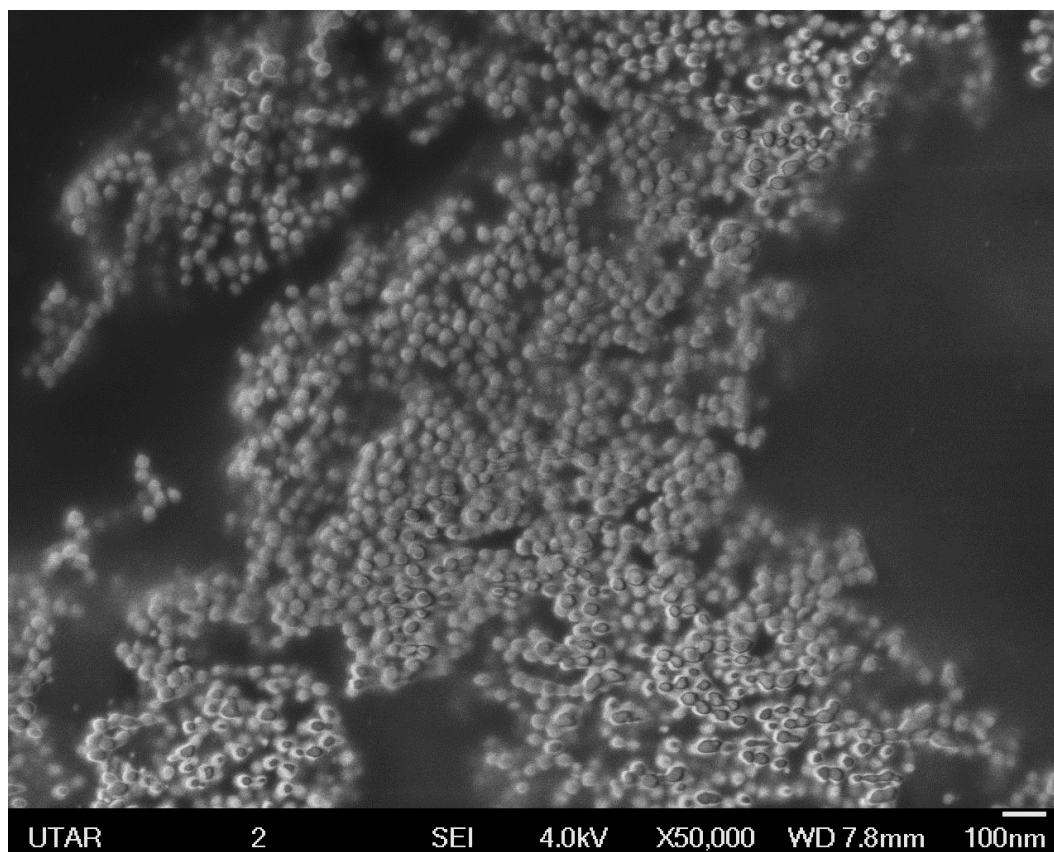
The FESEM images of gold nanoparticles show that they were mono-dispersed and spherical in nature are shown in Figure 4.3, 4.4 and 4.5. The average diameter of gold nanoparticles for each sample was measured from FESEM images by using ImageJ software. The observed morphology of gold nanoparticles was uniform with an average diameter of 29.7 nm, 25.46 nm and 35.64 nm respectively as shown in

Table 4.2. FESEM analysis revealed that the gold nanoparticles form in large numbers and almost uniform in size.

The gold nanoparticles synthesised from leaf extracts are accumulated on the surface due to the interactions such as hydrogen bond and electrostatic interaction between the biomolecules bound to the gold nanoparticles. The images clearly show that 5 mL of *Citrus Maxima* leaf extract during synthesis was capable to obtain the smaller particle size which considered as an optimum volume of extract. The particles size have been further analysed to determine the uniformity and size distribution of gold particles in three cases as shown in Figure 4.6.



**Figure 4.3: FESEM image of gold nanoparticles formed by exposing 4 mL *Citrus Maxima* leaf extract to 0.0025 M of H<sub>Au</sub>Cl<sub>4</sub>.**



**Figure 4.4: FESEM image of gold nanoparticles formed by exposing 5 mL *Citrus Maxima* leaf extract to 0.0025 M of H<sub>Au</sub>Cl<sub>4</sub>.**

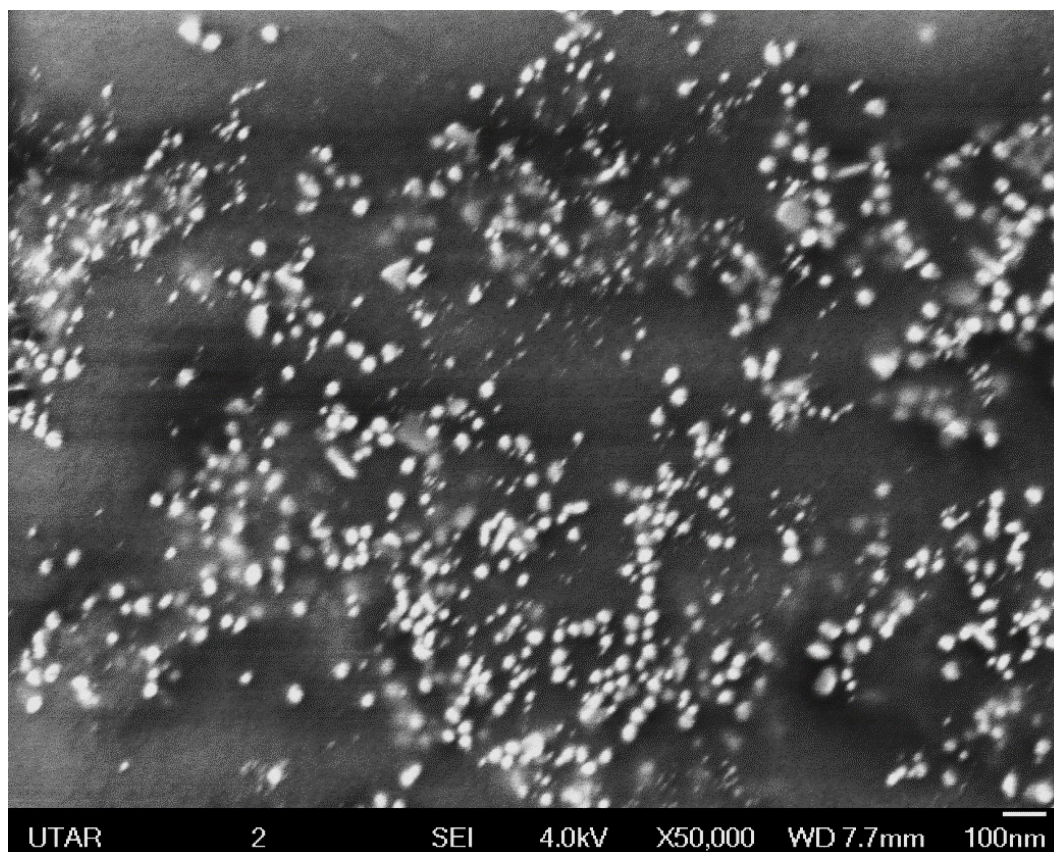


**Figure 4.5: FESEM image of gold nanoparticles formed by exposing 6 mL *Citrus Maxima* leaf extract to 0.0025 M of H<sub>AuCl<sub>4</sub></sub>.**

**Table 4.2: The average particle size synthesised by different volume of *Citrus Maxima* leaf extract with constant H<sub>AuCl<sub>4</sub></sub> concentrations.**

	4 mL	5 mL	6 mL
Mean (nm)	29.70	25.46	35.64
S.D. (nm)	6.06	5.38	8.89
Min (nm)	11.11	12.07	14.29
Max (nm)	41.98	39.51	71.43

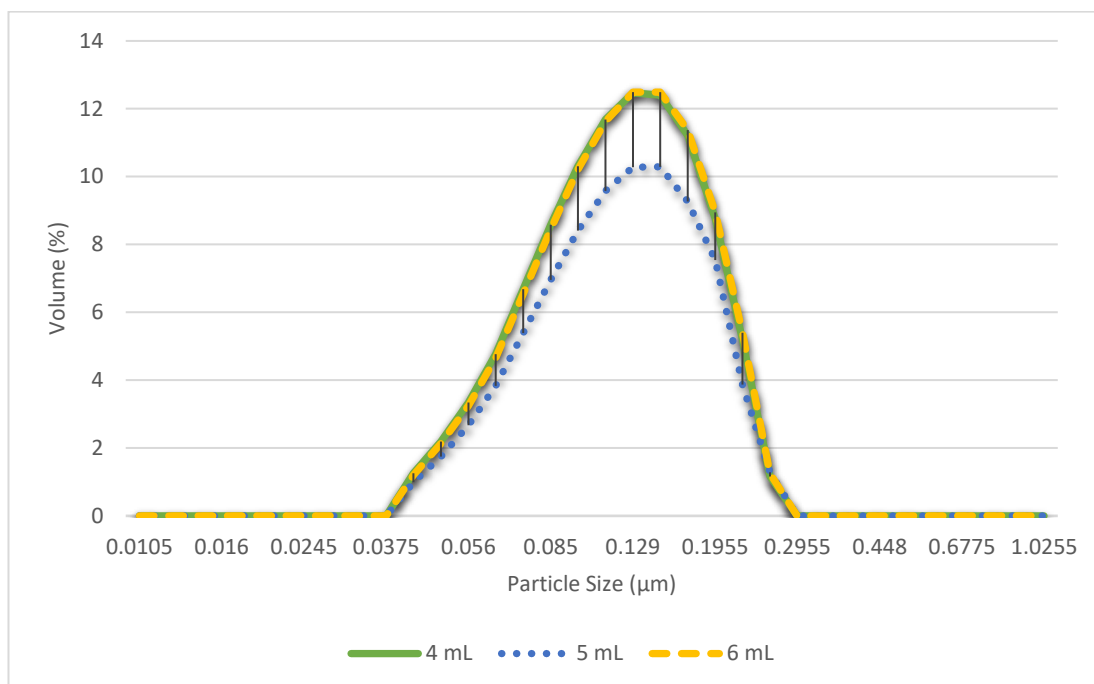


**Figure 4.6: Size distribution of gold nanoparticles formed by different volume of *Citrus Maxima* leaf extract and constant concentrations of HAuCl<sub>4</sub> (0.0025 M).**

### **4.3 Effect of chloroauric acid (HAuCl<sub>4</sub>) concentration on formation of gold nanoparticles using *Citrus Maxima* leaf broth.**

The change in colour from pale yellow to violet confirmed the presence of gold nanoparticles due to gold ions reduction through the phytochemical constituents in *Citrus Maxima* leaf extract. The formation and stability of gold nanoparticles were verified by UV-Vis spectroscopy. Spectrophotometric absorption measurements in the wavelength range of 500–600 nm are used in characterizing the gold nanoparticles. Figure 4.7 shows the UV-Vis spectra of gold nanoparticles formation using constant volume of *Citrus Maxima* leaf extract (5 mL) with different concentration of HAuCl<sub>4</sub> from 0.0025 to 0.0100 M. The spectrum showed maximum absorption band peak centered at 554 nm for gold nanoparticles with 0.0025 M of HAuCl<sub>4</sub> which confirmed the formation of gold nanoparticles.

Addition of  $\text{HAuCl}_4$  concentration from 0.0025 to 0.0100 M leads to difference in the absorption as shown in Figure 4.7. The spectrum of 0.0100 M showed that the band peak centered at 570 nm which has the largest absorbance wavelength among three different concentrations. Red shift of the absorbance band was observed with increasing concentration of  $\text{HAuCl}_4$ . As the wavelength of peak absorbance increases with diameter of particle, this indicates that the gold nanoparticles which synthesised by 0.0100 M  $\text{HAuCl}_4$  will have larger diameter in comparison to 0.0025 and 0.0050 M. The UV-Vis spectra showed a wider peak using 0.0100 M of  $\text{HAuCl}_4$  which revealed the formation of gold nanoparticles in larger size. The UV-Vis spectra peaks started to decrease with further increase in concentration of  $\text{HAuCl}_4$  from 0.0050 to 0.0100 M most likely due to insufficient amount of bio-compounds for gold ions reduction (Ahmad *et al.*, 2018).

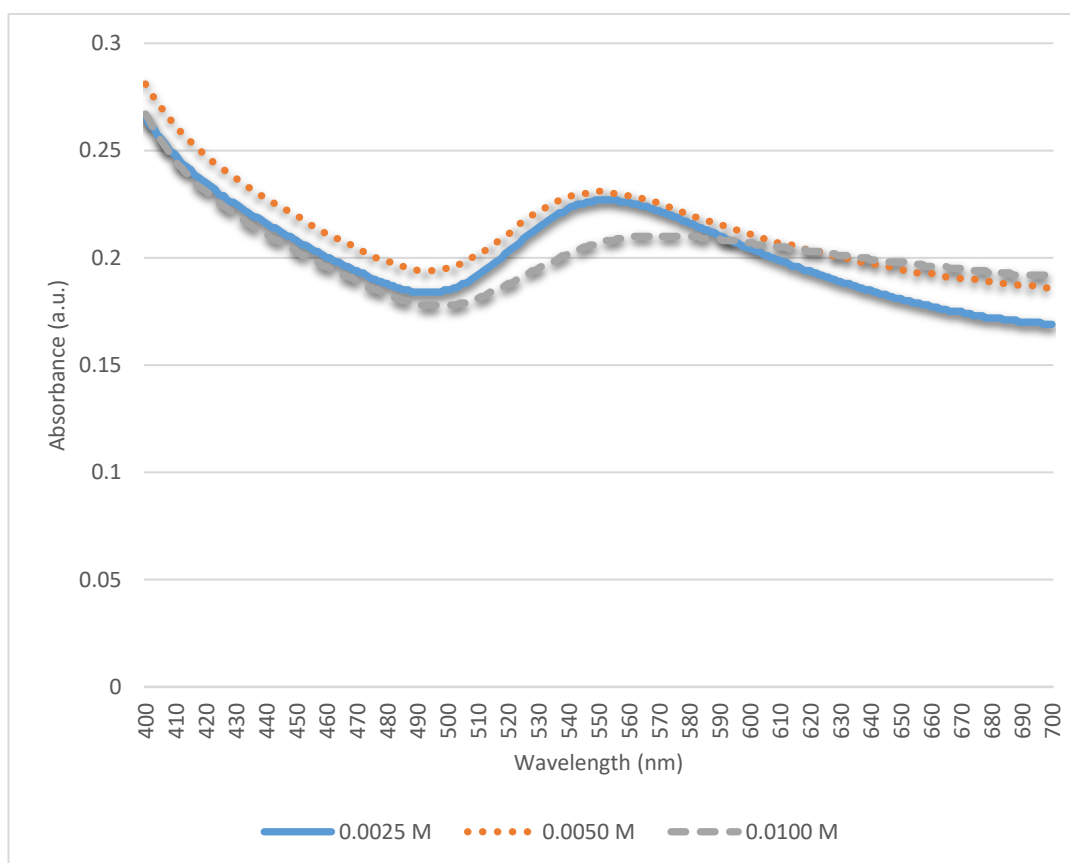


**Figure 4.7: UV-vis spectra of gold nanoparticles at different concentrations of  $\text{HAuCl}_4$  from 0.0025 to 0.0100 M and constant volume of *Citrus Maxima* leaf extract (5 mL).**

The FESEM images of gold nanoparticles show that they were mono-dispersed and spherical in nature are shown in Figure 4.8, 4.9 and 4.10. The average diameter of gold nanoparticles for each sample was measured from FESEM images by using ImageJ software. The observed morphology of gold nanoparticles was uniform with an average diameter of 25.46 nm, 30.50 nm and 45.19 nm respectively as shown in Table 4.3. This indicates that the diameter of gold nanoparticles increasing steadily with higher concentrations and it can be clearly seen on the FESEM images. FESEM analysis revealed that the gold nanoparticles form in large numbers and almost uniform in size.

The gold nanoparticles synthesised from leaf extracts are accumulated on the surface due to the interactions such as hydrogen bond and electrostatic interaction between the bio-organic capping molecules bound to the gold nanoparticles. The images clearly show that 0.0025 M of  $\text{HAuCl}_4$  during synthesis was capable to obtain the smaller particle size which considered as an optimum concentration. The particles size have been further analysed to determine the uniformity and size distribution of gold particles in three cases as shown in Figure 4.13.

Further analysis of the gold nanoparticles by EDX confirmed the presence of the signals characteristic of gold. Figure 4.11 shows the EDX spectra of biosynthesised gold nanoparticles by *Citrus Maixma* leaf extract. The remaining of weaker signals may be due to the biomolecules responsible for capping agent of the nanoparticles (Akhir, Fairuzi and Ismail, 2015).

The formation of gold nanoparticles synthesised using *Citrus Maxima* leaf extract was further supported by XRD measurements (Figure 4.12). The XRD pattern of the nanoparticle solution is an evidence for crystalline nature of gold nanoparticle. The peaks could be ascribed to FCC gold (JCPDS No.04-0784). The diffraction peaks appeared at  $2\theta = 38.26^\circ$  and  $44.50^\circ$  which corresponded to the (111) and (200) planes of the standard gold cubic respectively. Therefore, the intensity of the (200) plane was the highest among the other planes (Ng *et al.*, 2015).

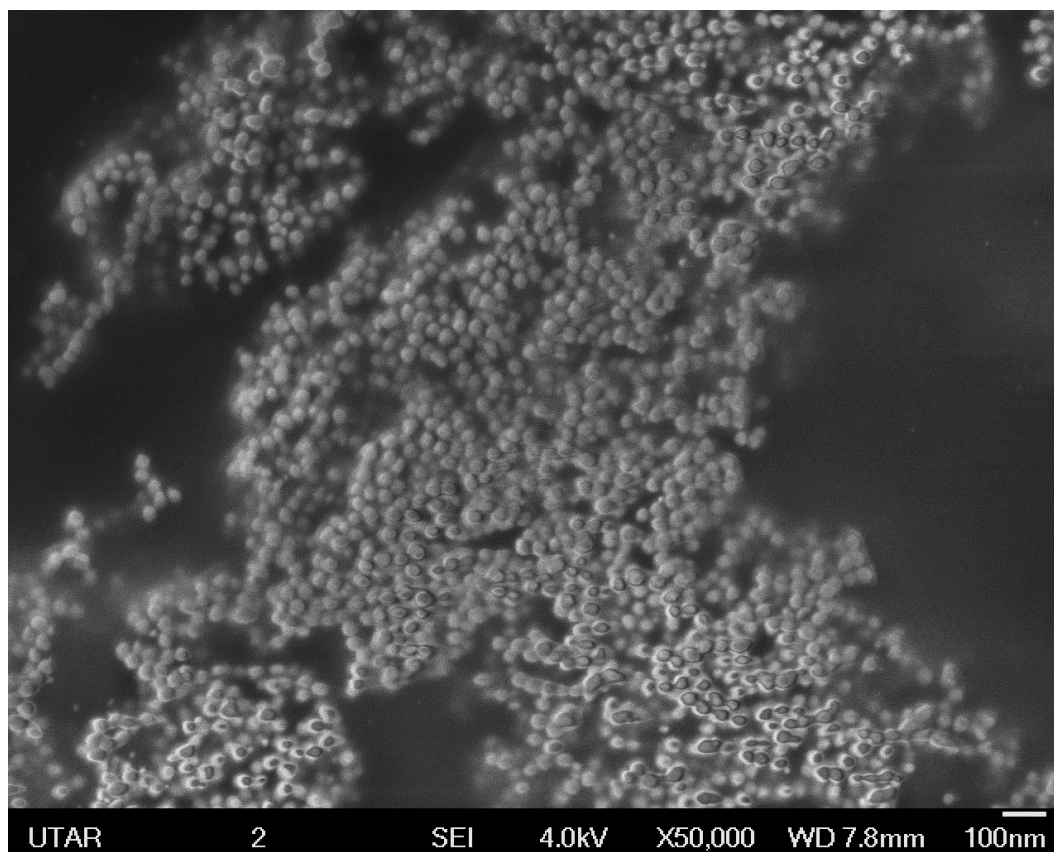


**Figure 4.8: FESEM image of gold nanoparticles formed by exposing 5 mL *Citrus Maxima* leaf extract to 0.0025 M of H<sub>Au</sub>Cl<sub>4</sub>.**

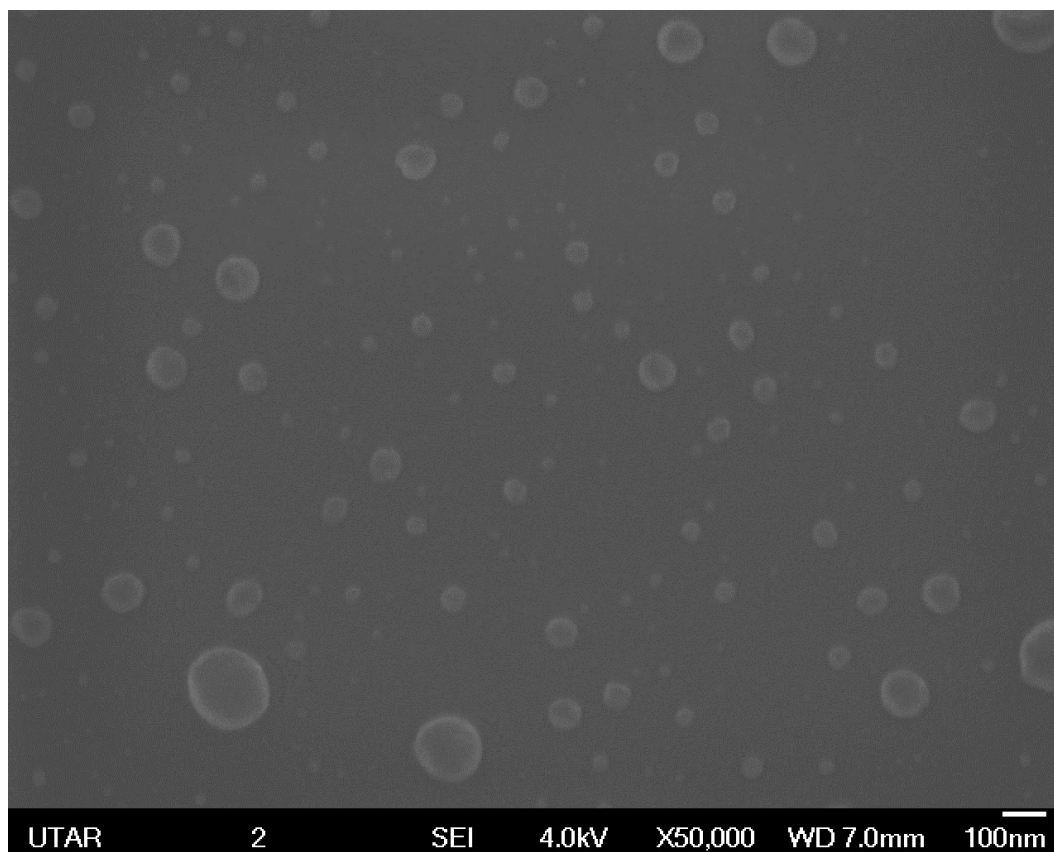


**Figure 4.9: FESEM image of gold nanoparticles formed by exposing 5 mL *Citrus Maxima* leaf extract to 0.0050 M of H<sub>Au</sub>Cl<sub>4</sub>.**

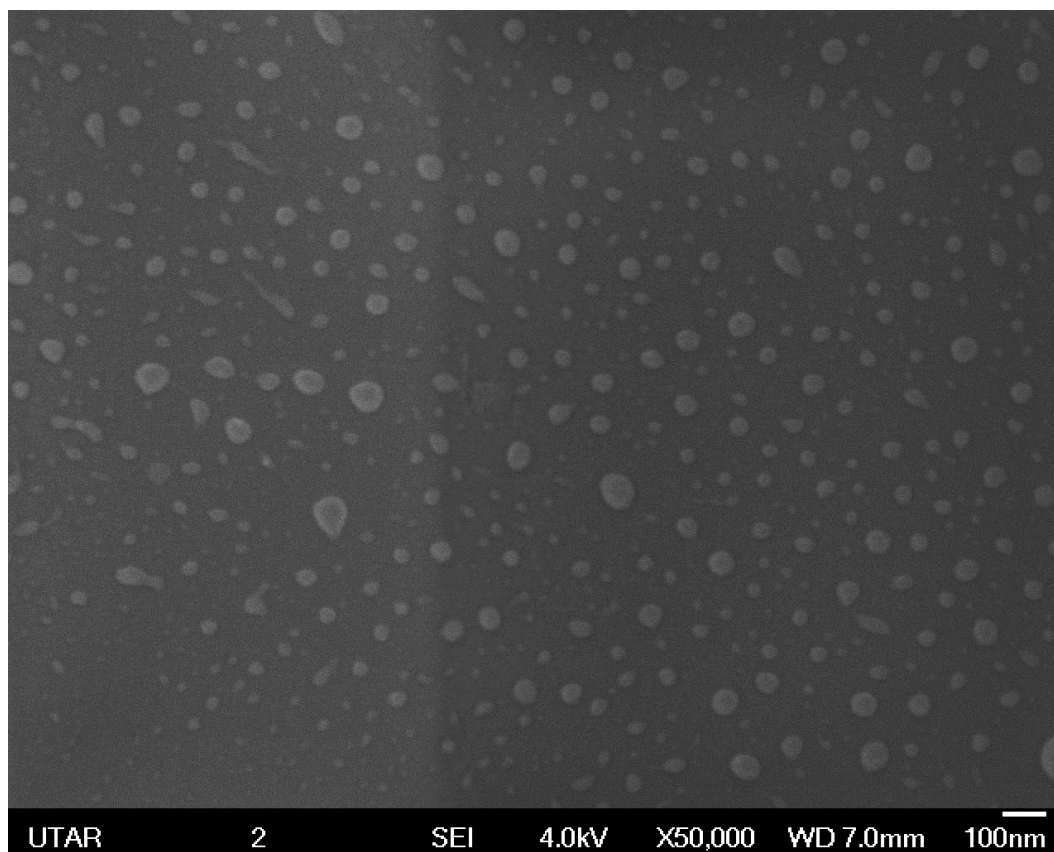


**Figure 4.10: FESEM image of gold nanoparticles formed by exposing 5 mL *Citrus Maxima* leaf extract to 0.0100 M of H<sub>Au</sub>Cl<sub>4</sub>.**

**Table 4.3: The average particle size synthesised by different concentration of HAuCl<sub>4</sub> with constant volume of *Citrus Maxima* leaf extract.**

	0.0025 M	0.0050 M	0.0100 M
Mean (nm)	25.46	30.50	45.19
S.D. (nm)	5.38	18.90	12.40
Min (nm)	12.07	7.85	10.03
Max (nm)	39.51	104.00	83.52

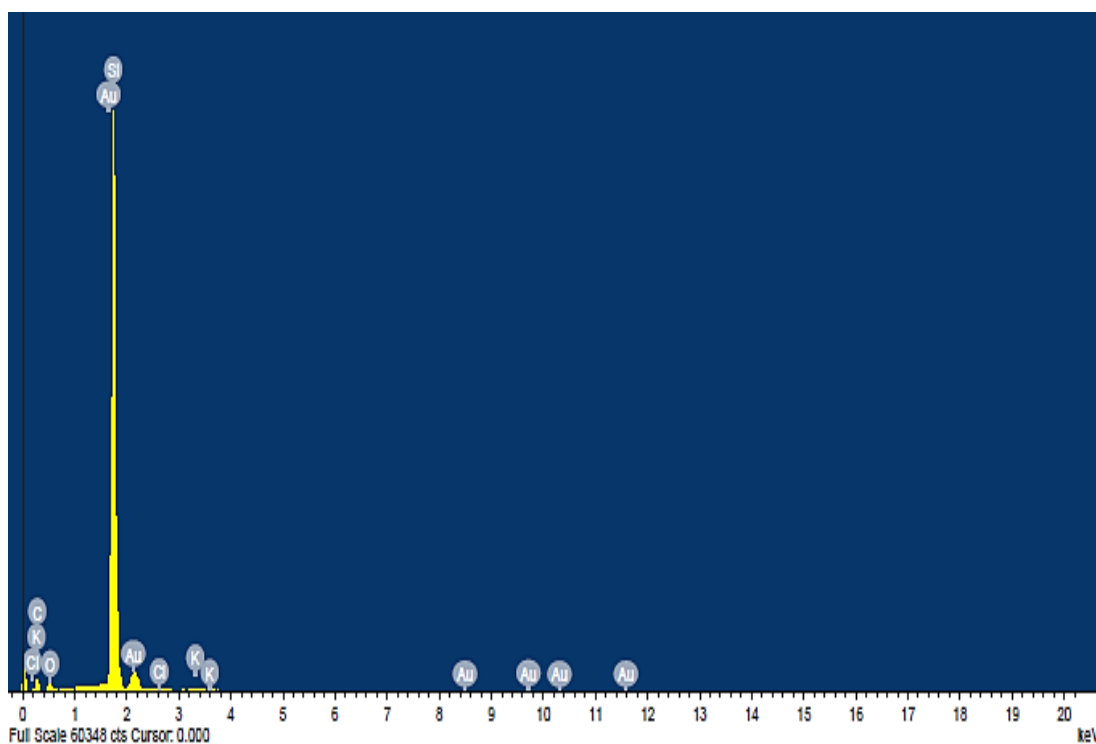


**Figure 4.11: EDX spectrum of gold nanoparticles resulting from the experiment using *Citrus Maxima* leaf.**

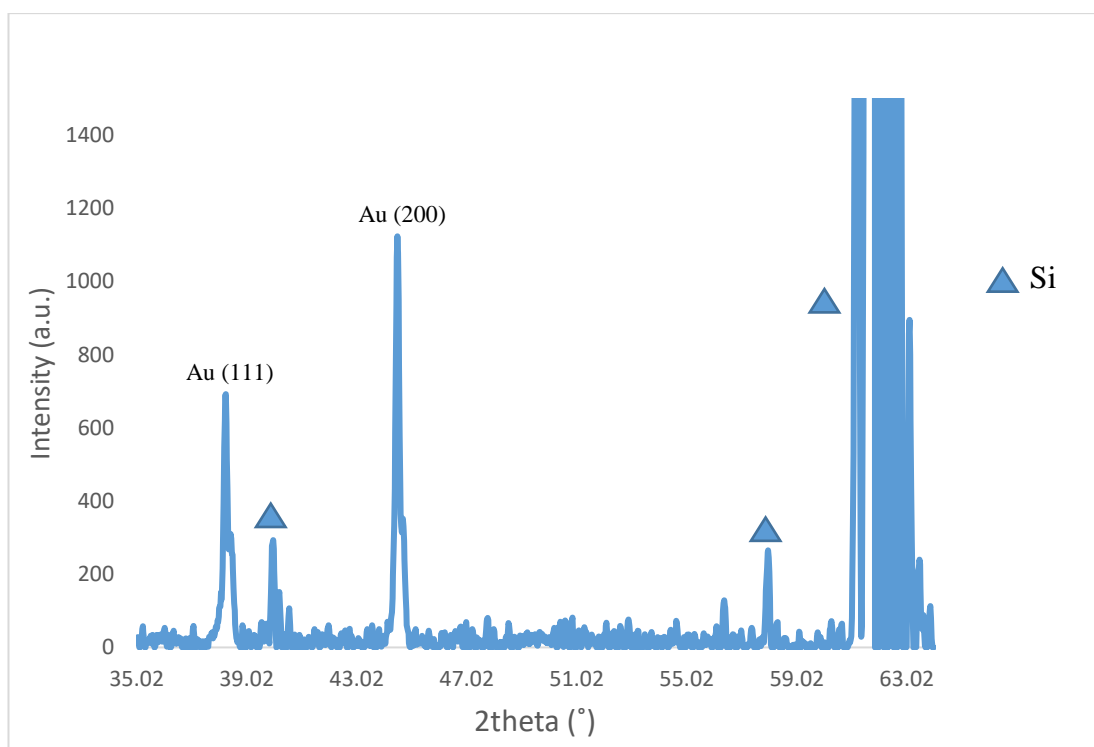


**Figure 4.12: XRD patterns for gold nanoparticles synthesised using *Citrus Maxima* leaves on silicon substrates.**

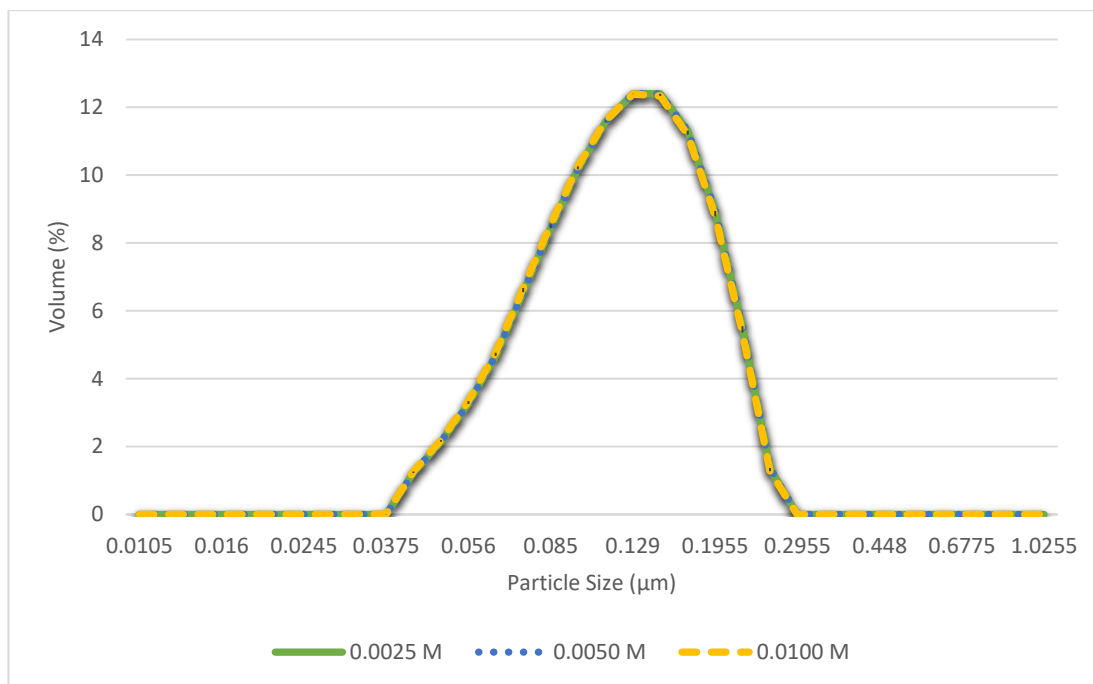


**Figure 4.13: Size distribution of gold nanoparticles formed by different concentrations of HAuCl<sub>4</sub> and constant volume of *Citrus Maxima* leaf extract (5 mL).**

#### 4.4 Effect of *Pandanus Amaryllifolius* leaf extract volume on formation of gold nanoparticles.

A variety of secondary metabolites such as alkaloids, tannins, saponins, flavonoids and polyphenol are present in *Pandanus Amaryllifolius*. The FTIR spectrum of the pandan leaf (Figure 4.14) showed the absorption bands at 617, 1063, 1400, 1636, 2345, 2364, 2928, 3422 cm<sup>-1</sup>. The intense broad absorbance at 3422, 2364 and 2345 cm<sup>-1</sup> are the characteristics of the hydroxyl functional group in alcohols and carboxylic acids. The IR bands observed at 2928, 1636 and 1400 cm<sup>-1</sup> are the characteristics of the C-H and C=H stretching vibrations, respectively of the aromatics group. The band at 1063 cm<sup>-1</sup> arises from the C-O-C vibrations of ethers. The IR band at 617 cm<sup>-1</sup> corresponds to acetylenic C-H bend of alkynes released by the leaves. The presence of functional groups in *Pandanus Amaryllifolius* leaf has been summarized in Table 4.4.

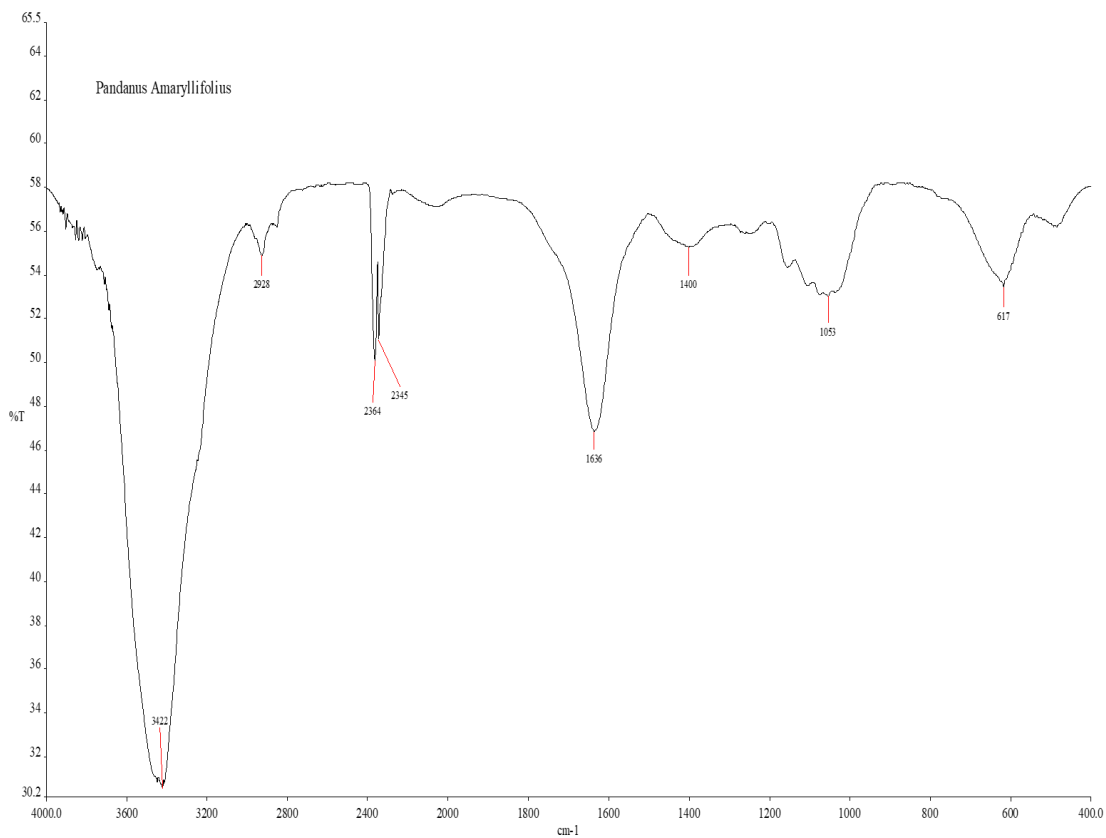


**Figure 4.14:** FTIR spectra of the *Pandanus Amaryllifolius*.

**Table 4.4: Functional groups of *Pandanus Amaryllifolius* leaf.**

<b>Pandanus Amaryllifolius</b>		
<b>Wavenumber (cm<sup>-1</sup>)</b>	<b>Molecular Motion</b>	<b>Functional Group</b>
3422	O-H stretch	Alcohols
2928	C-H stretch	Aromatics
2364	O-H stretch	Carboxylic Acids
2345	O-H stretch	Carboxylic Acids
1636	C=C stretch	Aromatics
1400	C=C stretch	Aromatics
1063	C-O-C stretch	Ethers
617	acetylenic C-H bend	Alkynes

The change in colour from pale yellow to violet confirmed the presence of gold nanoparticles due to gold ions reduction through the phytochemical constituents in *Pandanus Amaryllifolius* leaf extract. The formation and stability of gold nanoparticles were verified by UV-Vis spectroscopy. Spectrophotometric absorption measurements in the wavelength range of 500–600 nm are used in characterizing the gold nanoparticles. Figure 4.15 shows the UV-Vis spectra of gold nanoparticles formation using constant concentration of HAuCl<sub>4</sub> (0.0025 M) with different volume of *Pandanus Amaryllifolius* leaf extract from 4 to 6 mL. The spectrum showed maximum absorption band peak centered at 542 nm for gold nanoparticles with 4 mL of leaf extract which confirmed the formation of gold nanoparticles.

Addition of leaf extract from 4 to 6 mL leads to difference in the absorption as shown in Figure 4.15. The spectrum of 6 mL leaf extract showed that the band peak

centered at 546 nm. Therefore, the gold nanoparticles synthesised by three different volumes have similar absorption band peak indicated that they are in average diameter. Red shift of the absorbance band was observed with increasing volume of extract. As the peak absorbance wavelength increases with particle diameter, this indicates that the gold nanoparticles will have larger diameter. The higher peaks observed for 5 mL of leaves extract might be due to an increase of gold nanoparticles because of higher amount of biomolecules present in reaction mixture. The UV-Vis spectra peaks started to decrease with further increase in volume of extract from 5 to 6 mL most likely due to insufficient amount of gold ions to be reduced by bio-compounds. It could be considered as the excess amount of reducing, capping and stabilizing agent left in reaction mixture to synthesise gold nanoparticles (Ahmad *et al.*, 2018).

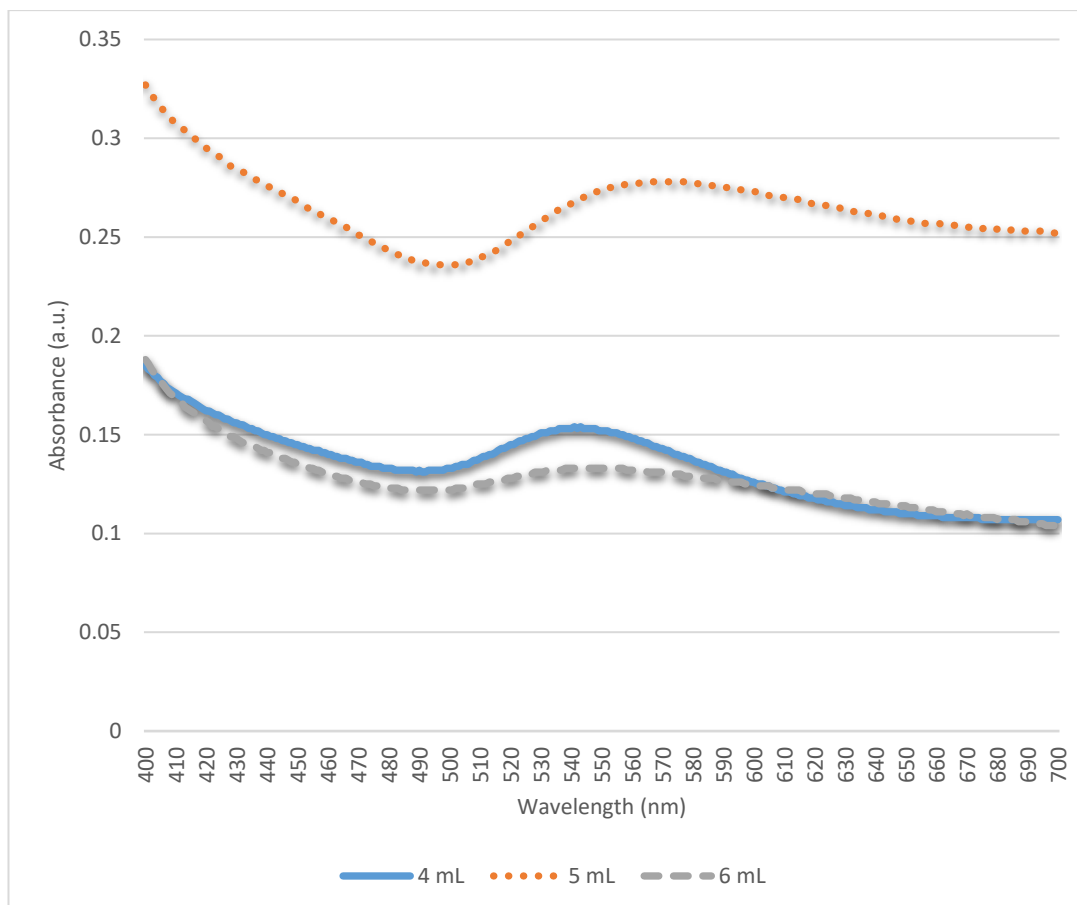


**Figure 4.15: UV-vis spectra of gold nanoparticles at different volume of *Pandanus Amaryllifolius* leaf extract from 4 to 6 mL and constant concentrations of H<sub>Au</sub>Cl<sub>4</sub> (0.0025 M).**

The average diameter of gold nanoparticles for each sample was measured from FESEM images by using ImageJ software. The FESEM image of gold nanoparticles show that they were spherical in nature with 4 mL of leaf extract are shown in Figure 4.16. However, agglomeration of gold nanoparticles was spotted when the synthesis dealing with 4 mL of leaf extract. On the other hand, the FESEM revealed that the gold nanoparticles synthesised by 5 and 6 mL were spherical and a very few of them showed hollow morphology (Figure 4.17, 4.18). The evolution from such hollow structure from spherical gold nanoparticles can be assumed to be some of the particles indicated favoured reaction along certain directions lead to hollow cores opening up completely (Selvakannan and Sastry, 2005). The hollow gold nanoparticles

also can be known as silica-core gold nanoshells which might be due to the reaction between gold nanoparticles with silicon substrate (Edgar *et al.*, 2008). This is because gold nanoparticles colloid was dried on silicon substrate before FESEM characterization.

The observed spherical morphology of gold nanoparticles was uniform with an average diameter of 31.64 nm, 28.88 nm and 28.21 nm respectively as shown in Table 4.5. FESEM analysis revealed that the gold nanoparticles form in large numbers and almost uniform in size. The gold nanoparticles synthesised from leaf extracts are mounted up on the surface due to the interactions such as hydrogen bond and electrostatic interaction between the biomolecules as capping agent that bound to the gold nanoparticles. Although 6 mL of *Pandanus Amaryllifolius* leaf extract during synthesis was capable to obtain particles with smaller size, but the particles in Figure 4.18 are less mono-dispersed in comparison to those in Figure 4.16. The images clearly show that 4 mL of *Pandanus Amaryllifolius* leaf extract during synthesis was capable to obtain more mono-dispersed gold nanoparticles which considered as an optimum volume of extract. The particles size have been further analysed to determine the uniformity and size distribution of gold particles in three cases as shown in Figure 4.19.

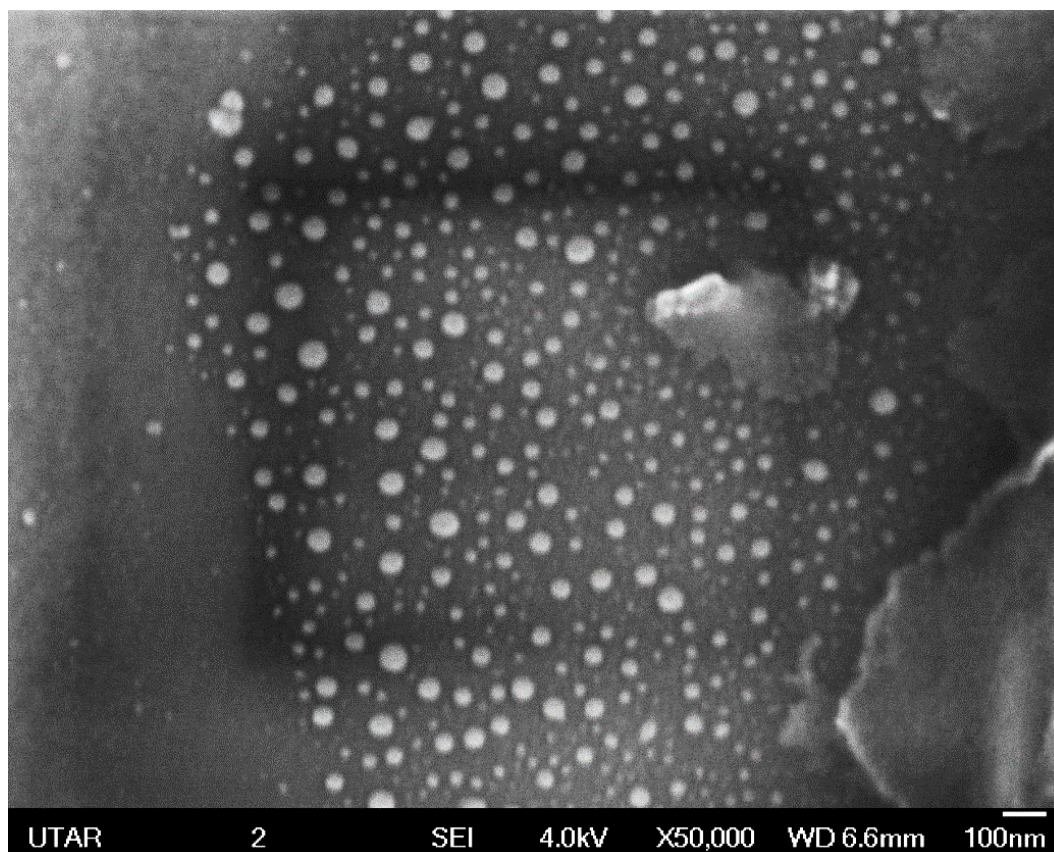


**Figure 4.16:** FESEM image of gold nanoparticles formed by exposing 4 mL *Pandanus Amaryllifolius* leaf extract to 0.0025 M of HAuCl<sub>4</sub>.

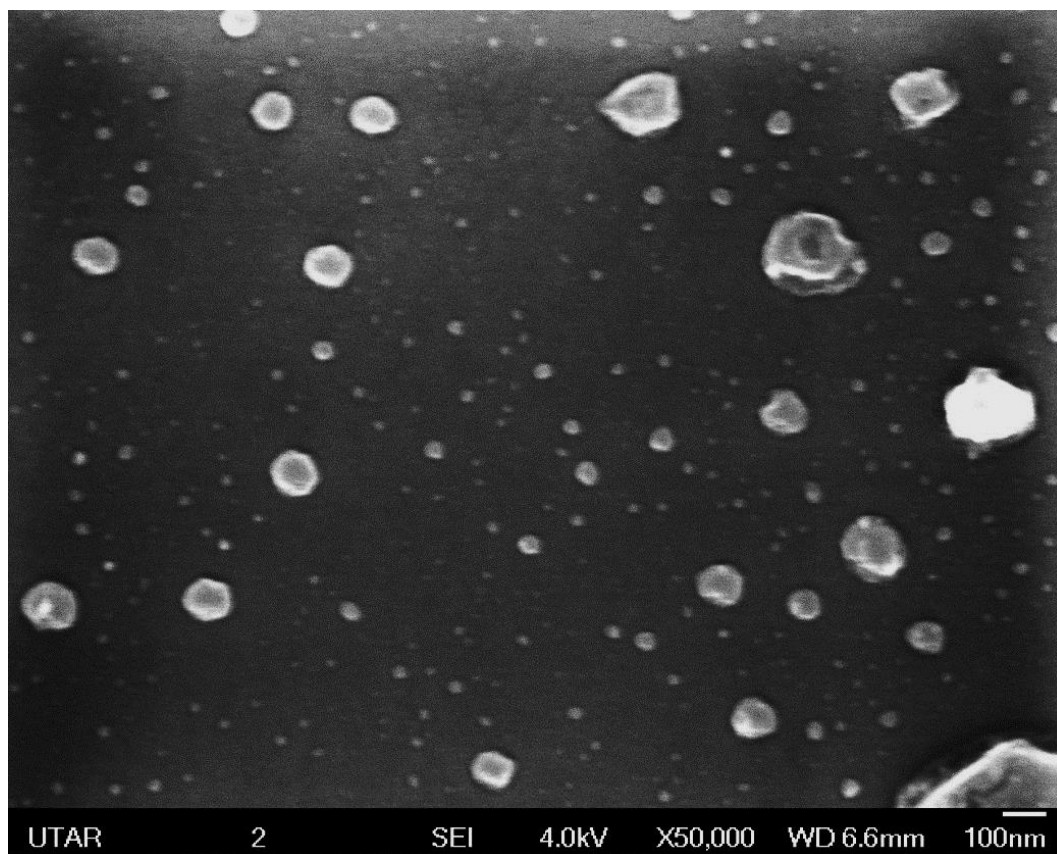


**Figure 4.17:** FESEM image of gold nanoparticles formed by exposing 5 mL *Pandanus Amaryllifolius* leaf extract to 0.0025 M of H<sub>Au</sub>Cl<sub>4</sub>.

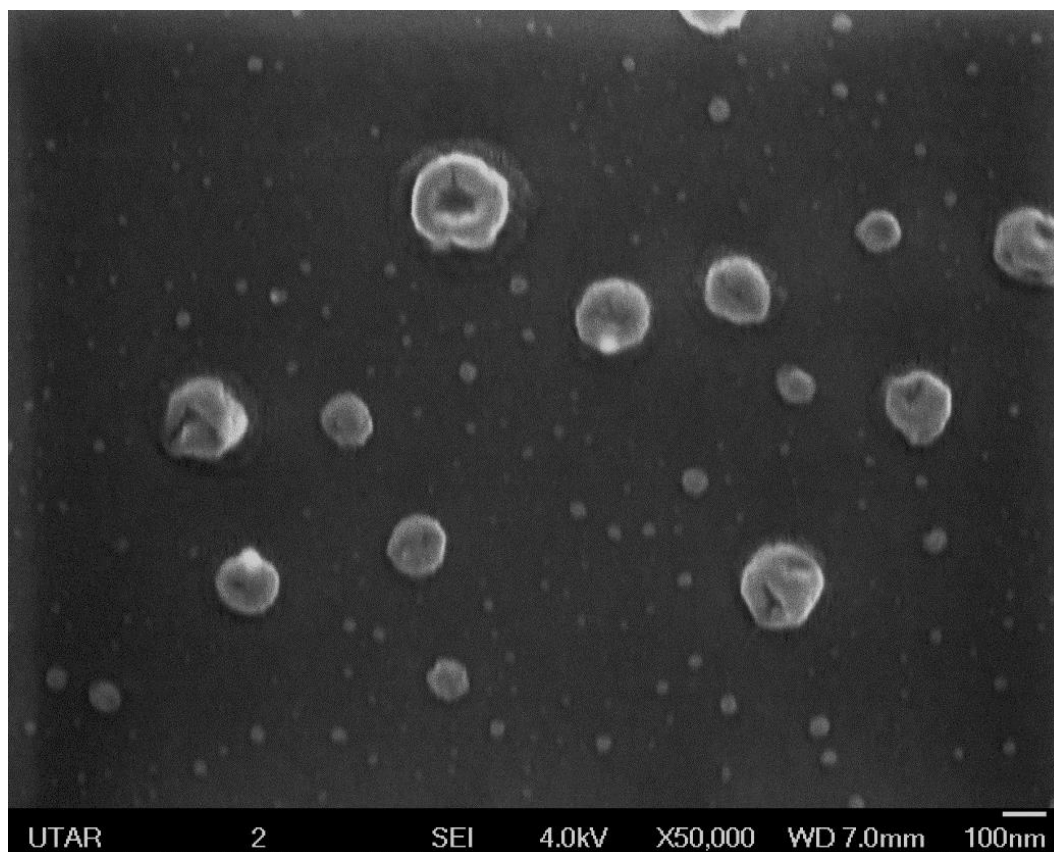


**Figure 4.18:** FESEM image of gold nanoparticles formed by exposing 6 mL *Pandanus Amaryllifolius* leaf extract to 0.0025 M of H<sub>Au</sub>Cl<sub>4</sub>.

**Table 4.5: The average particle size synthesised by different volume of *Pandanus Amaryllifolius* leaf extract with constant H<sub>Au</sub>Cl<sub>4</sub> concentrations.**

	4 mL	5 mL	6 mL
Mean (nm)	31.64	28.88	28.21
S.D. (nm)	10.35	19.10	26.05
Min (nm)	9.29	12.82	8.53
Max (nm)	70.59	121.06	179.18

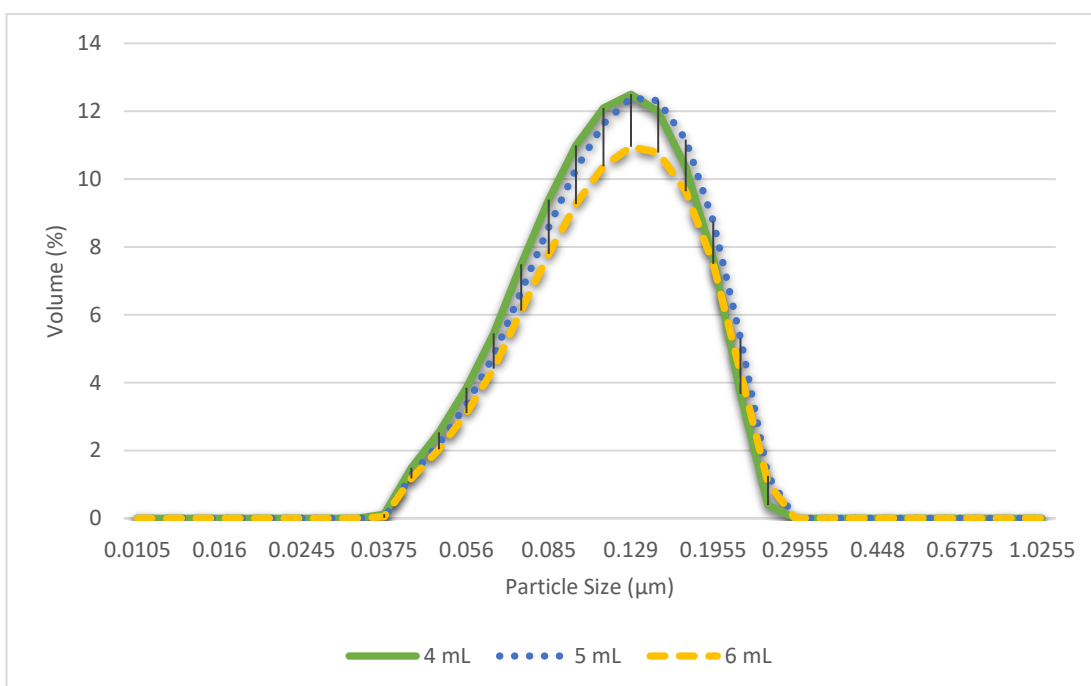


**Figure 4.19: Size distribution of gold nanoparticles formed by different volume of *Pandanus Amaryllifolius* leaf extract and constant concentrations of H<sub>Au</sub>Cl<sub>4</sub> (0.0025 M).**

#### **4.5 Effect of chloroauric acid (HAuCl<sub>4</sub>) concentration on formation of gold nanoparticles using *Pandanus Amaryllifolius* leaf broth.**

The change in colour from pale yellow to violet confirmed the presence of gold nanoparticles due to gold ions reduction through the phytochemical constituents in *Pandanus Amaryllifolius* leaf extract. The formation and stability of gold nanoparticles were verified by UV-Vis spectroscopy. Spectrophotometric absorption measurements in the wavelength range of 500–600 nm are used in characterizing the gold nanoparticles. Figure 4.20 shows the UV-Vis spectra of gold nanoparticles formation using constant volume of *Pandanus Amaryllifolius* leaf extract (5 mL) with different concentration of HAuCl<sub>4</sub> from 0.0025 to 0.0100 M. The spectrum showed maximum absorption band peak centered at 568 nm for gold nanoparticles with 0.0025M of HAuCl<sub>4</sub> which confirmed the formation of gold nanoparticles.

Addition of HAuCl<sub>4</sub> concentration from 0.0025 to 0.0100 M leads to difference in the absorption as shown in Figure 4.20. The spectrum of 0.0100 M showed that the band peak centered at 595 nm which has the largest absorbance wavelength among three different concentrations. Red shift of the absorbance band was observed with increasing concentration of HAuCl<sub>4</sub>. As the wavelength of peak absorbance increases with diameter of particle, this indicates that the gold nanoparticles which synthesised by 0.0100 M HAuCl<sub>4</sub> will have larger diameter in comparison to 0.0025 and 0.0050 M. The UV-Vis spectra showed a wider peak using 0.0100 M of HAuCl<sub>4</sub> which revealed the formation of gold nanoparticles in larger size. The UV-Vis spectra peaks started to decrease with further increase in concentration of HAuCl<sub>4</sub> from 0.0050 to 0.0100 M most likely due to insufficient amount of biomolecules for gold ions reduction (Ahmad *et al.*, 2018).

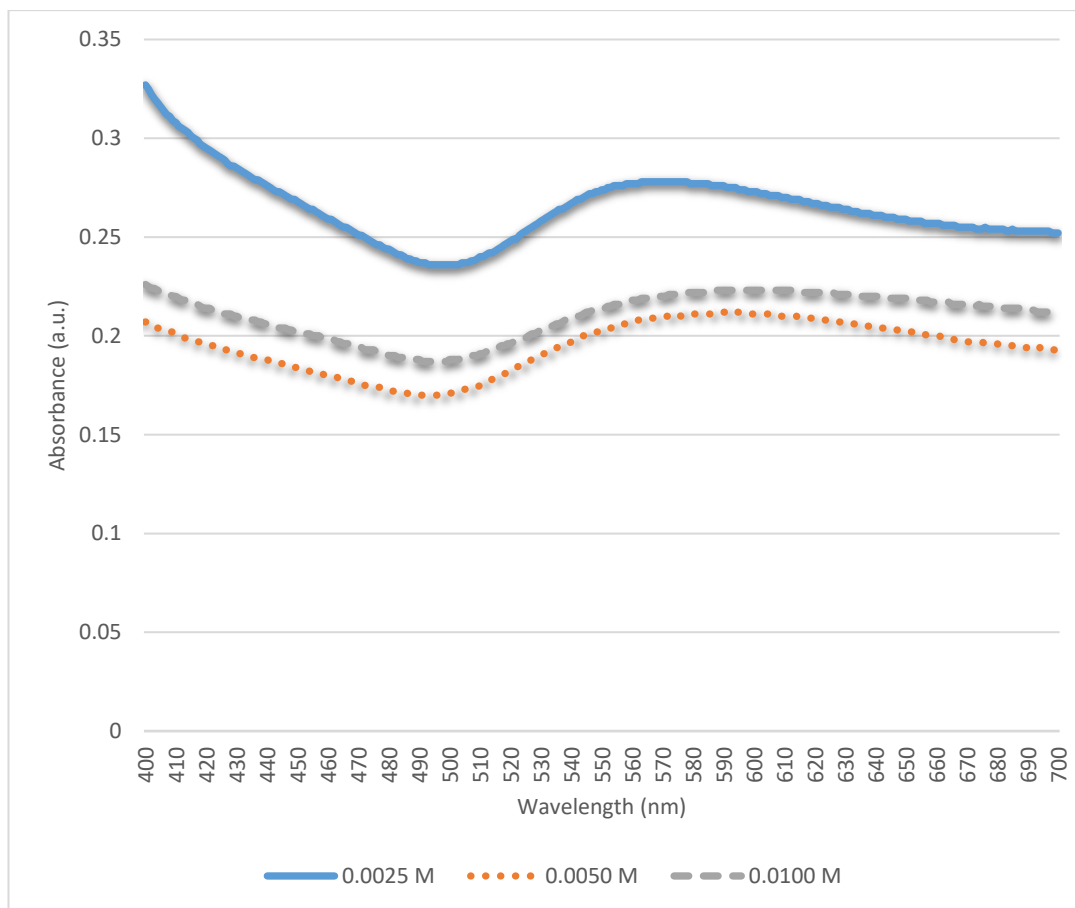


**Figure 4.20: UV-vis spectra of gold nanoparticles at different concentrations of HAuCl<sub>4</sub> from 0.0025 to 0.0100 M and constant volume of *Pandanus Amaryllifolius* leaf extract (5 mL).**

The average diameter of gold nanoparticles for each sample was measured from FESEM images by using ImageJ software. The FESEM image of gold nanoparticles show that they were spherical in nature with 0.0050 M HAuCl<sub>4</sub> are shown in Figure 4.22. However, some of the aggregation grains was observed when the synthesis dealing with 0.0050 M of HAuCl<sub>4</sub>. Moreover, the FESEM revealed that the gold nanoparticles synthesised by 0.0025 and 0.0100 M were spherical and a very few of them showed hollow morphology (Figure 4.21, 4.23). The evolution from such hollow structure from spherical gold nanoparticles can be assumed to be some of the particles indicated favoured reaction along certain directions lead to hollow cores opening up completely (Selvakannan and Sastry, 2005). The hollow gold nanoparticles also can be known as silica-core gold nanoshells which might be due to the reaction

between gold nanoparticles with silicon substrate (Edgar *et al.*, 2008). This is because gold nanoparticles colloid was dried on silicon substrate before FESEM characterization.

The observed spherical morphology of gold nanoparticles was uniform with an average diameter of 28.88 nm, 30.75 nm and 47.65 nm respectively as shown in Table 4.6. This showed the diameter of gold nanoparticles increasing steadily with higher concentrations. FESEM analysis revealed that the gold nanoparticles form in large numbers and almost uniform in size. The gold nanoparticles synthesised from leaf extracts are mounted up on the surface due to the interactions such as hydrogen bond and electrostatic interaction between the biomolecules as capping agent that bound to the gold nanoparticles.

Although 0.0025 M of HAuCl<sub>4</sub> during synthesis was capable to obtain particles with smaller size, but the particles in Figure 4.22 are less mono-dispersed in comparison to those in Figure 4.21. The images clearly show that 0.0050 M of HAuCl<sub>4</sub> during synthesis was capable to obtain more mono-dispersed gold nanoparticles which considered as an optimum concentration. The particles size have been further analysed to determine the uniformity and size distribution of gold particles in three cases as shown in Figure 4.26.

Further analysis of the gold nanoparticles by EDX confirmed the presence of the signals characteristic of gold. Figure 4.24 shows the EDX spectra of biosynthesised gold nanoparticles by *Pandanus Amaryllifolius* leaf extract. The remaining of weaker signals may be due to the biomolecules responsible for capping agent of the nanoparticles (Akhir, Fairuzi and Ismail, 2015).

The formation of gold nanoparticles synthesised using *Pandanus Amaryllifolius* leaf extract was further supported by XRD measurements (Figure 4.25). The XRD pattern of the nanoparticle solution is an evidence for crystalline nature of gold nanoparticle. The peaks could be ascribed to FCC gold (JCPDS No.04-0784). The diffraction peaks appeared at  $2\theta = 38.24^\circ$  and  $44.48^\circ$  which corresponded to the (111) and (200) planes of the standard gold cubic respectively. Therefore, the intensity of the (200) plane was the highest among the other planes (Ng *et al.*, 2015).

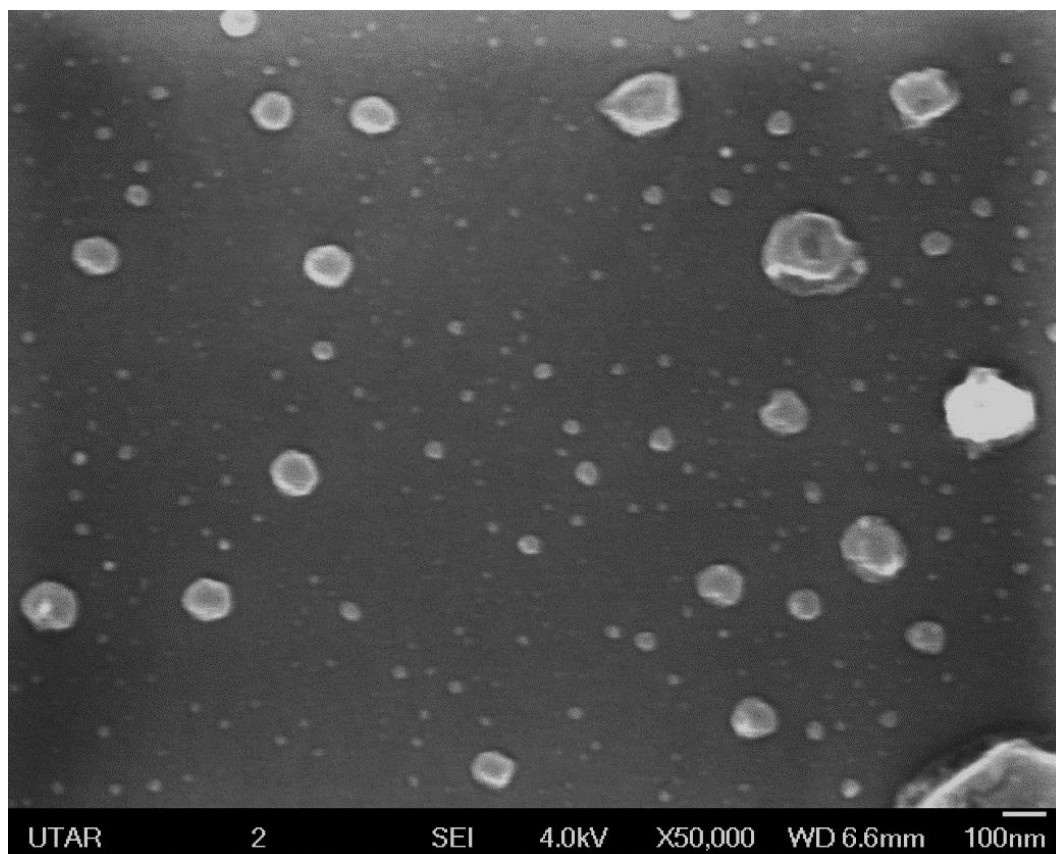


**Figure 4.21:** FESEM image of gold nanoparticles formed by exposing 5 mL *Pandanus Amaryllifolius* leaf extract to 0.0025 M of HAuCl<sub>4</sub>.

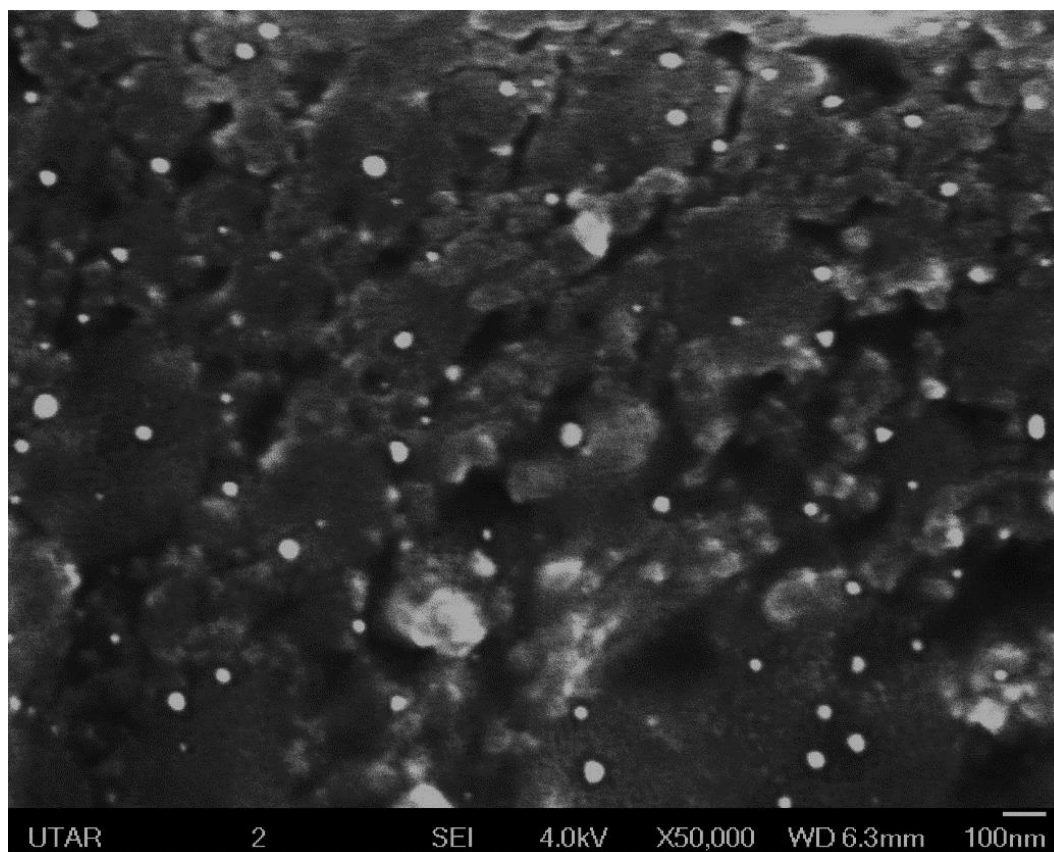


**Figure 4.22:** FESEM image of gold nanoparticles formed by exposing 5 mL *Pandanus Amaryllifolius* leaf extract to 0.0050 M of HAuCl<sub>4</sub>.

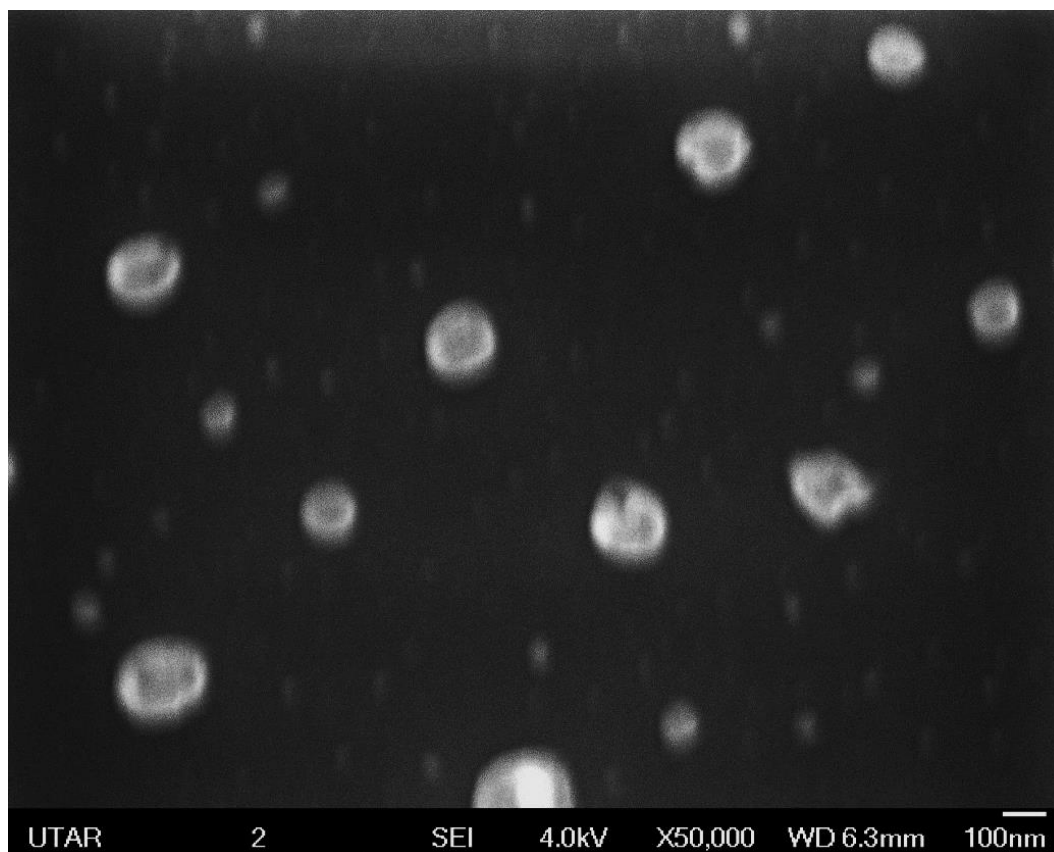


**Figure 4.23:** FESEM image of gold nanoparticles formed by exposing 5 mL *Pandanus Amaryllifolius* leaf extract to 0.0100 M of HAuCl<sub>4</sub>.

**Table 4.6: The average particle size synthesised by different concentration of HAuCl<sub>4</sub> with constant volume of *Pandanus Amaryllifolius* leaf extract.**

	0.0025 M	0.0050 M	0.0100 M
Mean (nm)	28.88	30.75	47.65
S.D. (nm)	19.10	10.38	51.01
Min (nm)	12.82	11.22	6.44
Max (nm)	121.06	67.29	213.97

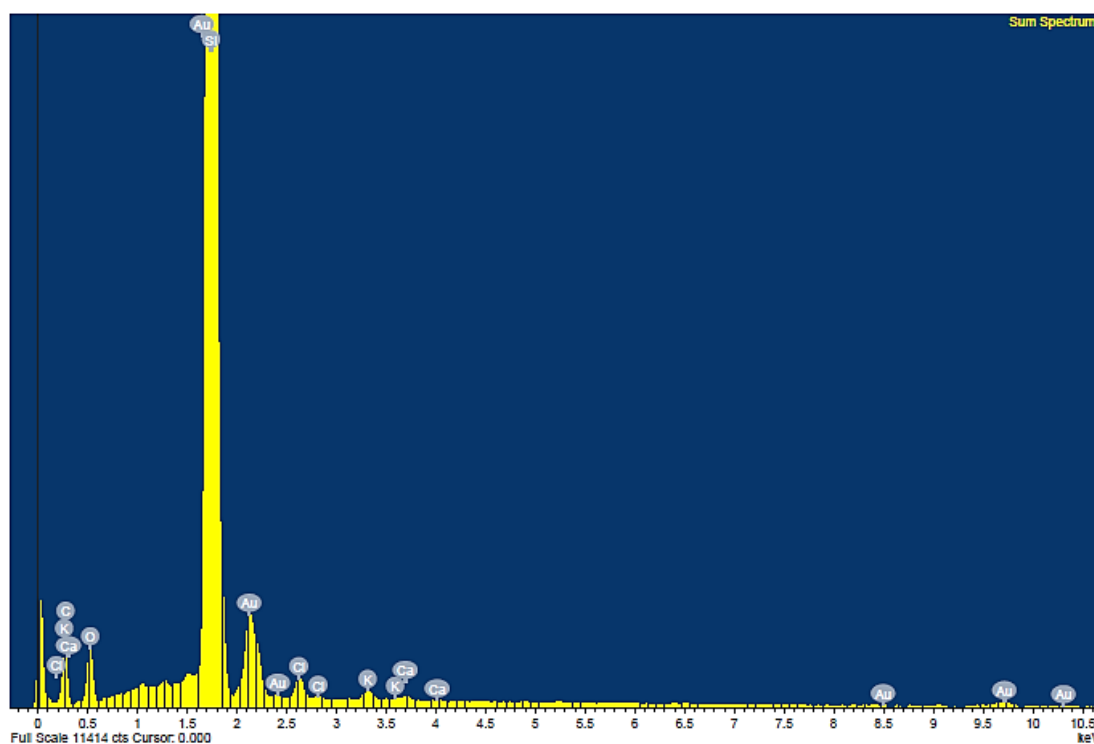


**Figure 4.24: EDX spectrum of gold nanoparticles resulting from the experiment using *Pandanus Amaryllifolius* leaf.**

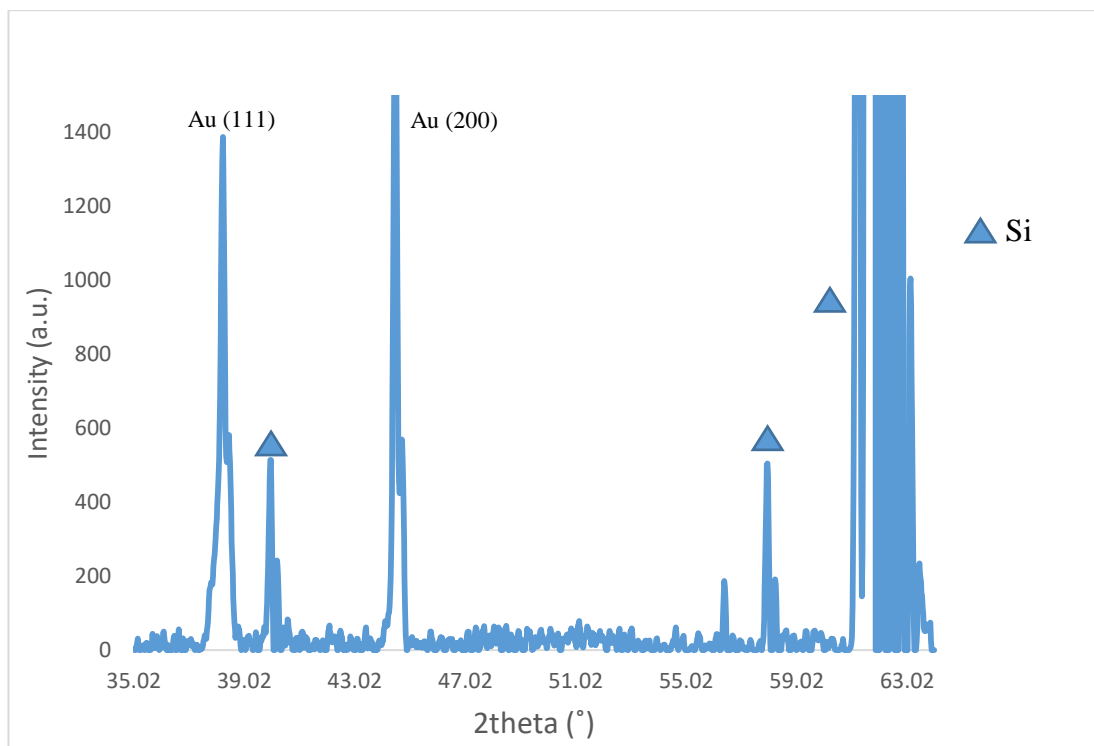


**Figure 4.25: XRD patterns for gold nanoparticles synthesised using *Pandanus Amaryllifolius* leaves on silicon substrates.**

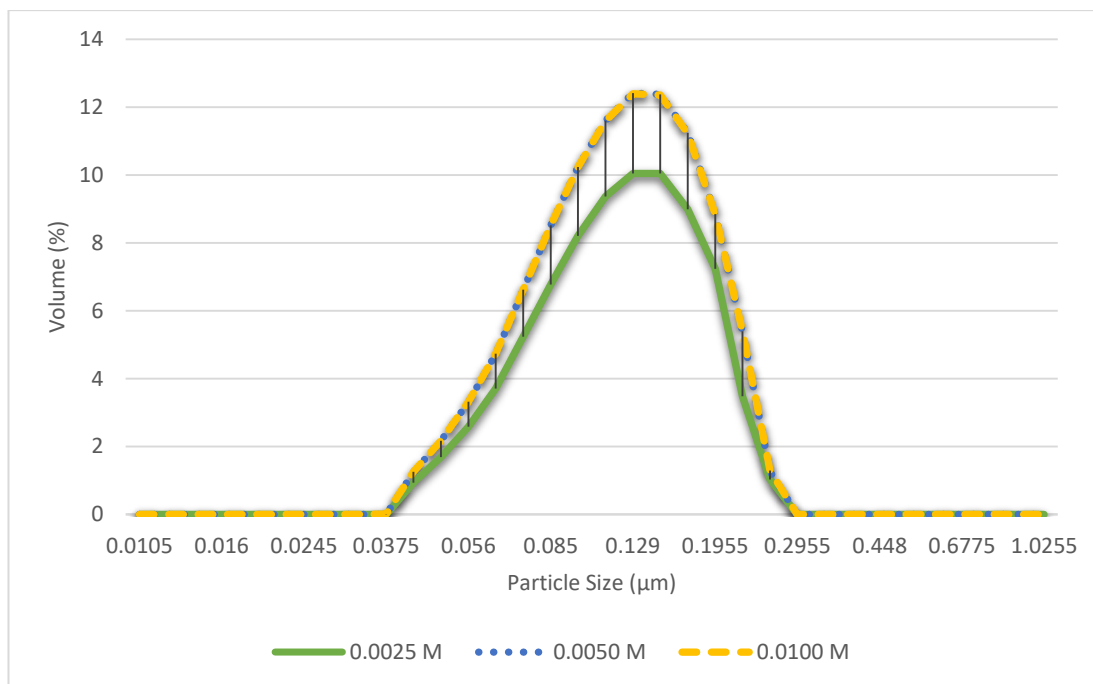


**Figure 4.26: Size distribution of gold nanoparticles formed by different concentrations of HAuCl<sub>4</sub> and constant volume of *Pandanus Amaryllifolius* leaf extract (5 mL).**

#### **4.6 Effect of *Vernonia Amygdalina* leaf extract volume on formation of gold nanoparticles.**

Some previous studies on extraction of pharmaceutical components from the *Vernonia Amygdalina* showed that oxalate, phytate, tannins, saponins, flavonoid, alkaloids, cyanogenic glycoside, anthraquinone, steroid and phenols exist in such a leaf. The FTIR absorption spectra of the *Vernonia Amygdalina* (Figure 4.27) showed the absorbance bands at 618, 1074, 1637, 2345, 2365, 2928, 3422 cm<sup>-1</sup>. The strong IR bands observed at 3422, 2365, 2345 cm<sup>-1</sup> in dried *Vernonia Amygdalina* are the characteristics of the O-H stretching modes of alcohols and carboxylic acids. The IR bands at 2928 and 1637 cm<sup>-1</sup> were associated with the stretch vibration of C-H and C=H respectively of the aromatics group. The band at 1074 cm<sup>-1</sup> might be contributed by the C-O-C vibrations of ethers while the stretch at 618 cm<sup>-1</sup> arises due to the

acetylenic C-H bend present in the alkynes. The presence of functional groups in *Vernonia Amygdalina* leaf has been summarized in Table 4.7.

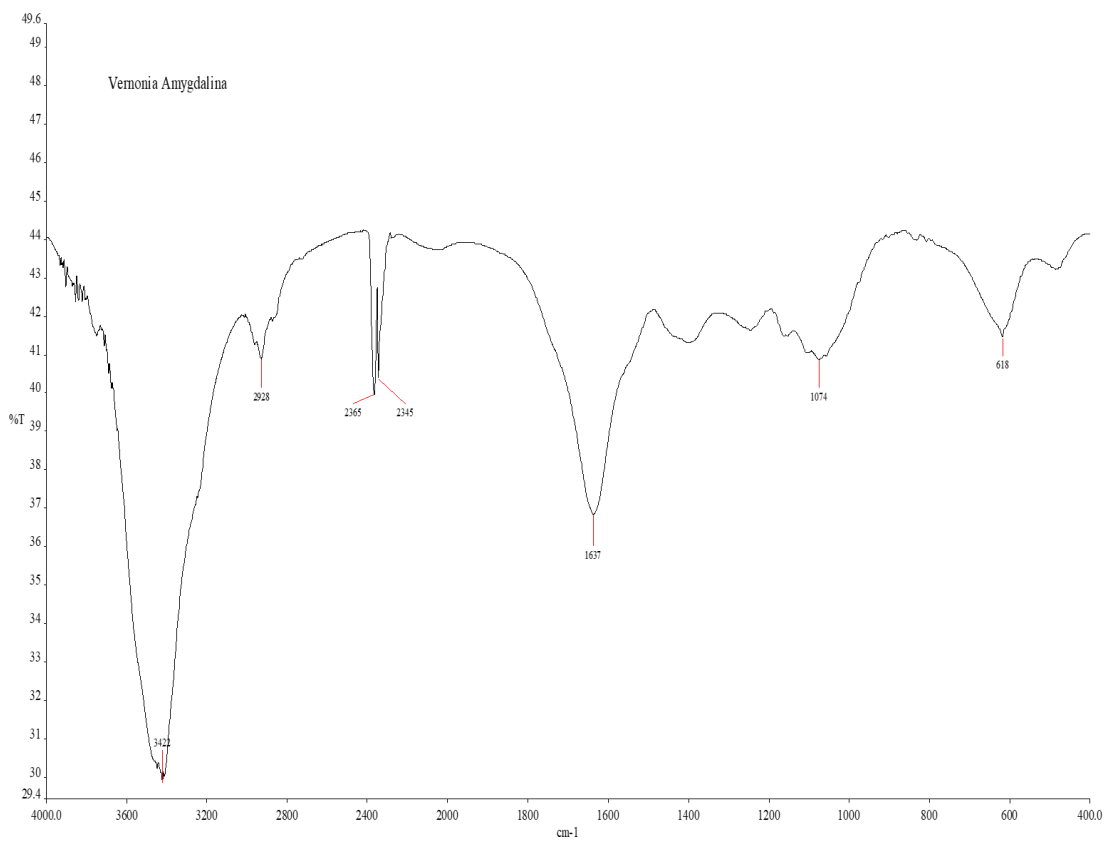


**Figure 4.27: FTIR spectra of the *Vernonia Amygdalina*.**

**Table 4.7: Functional groups of *Vernonia Amygdalina* leaf.**

<b>Vernonia Amygdalina</b>		
<b>Wavenumber (cm<sup>-1</sup>)</b>	<b>Molecular Motion</b>	<b>Functional Group</b>
3422	O-H stretch	Alcohols
2928	C-H stretch	Aromatics
2365	O-H stretch	Carboxylic Acids
2345	O-H stretch	Carboxylic Acids
1637	C=C stretch	Aromatics
1074	C-O-C stretch	Ethers
618	acetylenic C-H bend	Alkynes

The change in colour from pale yellow to violet confirmed the presence of gold nanoparticles due to gold ions reduction through the phytochemical constituents in *Vernonia Amygdalina* leaf extract. The formation and stability of gold nanoparticles were verified by UV-Vis spectroscopy. Spectrophotometric absorption measurements in the wavelength range of 500–600 nm are used in characterizing the gold nanoparticles. Figure 4.28 shows the UV-Vis spectra of gold nanoparticles formation using constant concentration of H<sub>Au</sub>Cl<sub>4</sub> (0.0025 M) with different volume of *Vernonia Amygdalina* leaf extract from 4 to 6 mL. The spectrum showed maximum absorption band peak centered at 542 nm for gold nanoparticles with 4 mL of leaf extract which confirmed the formation of gold nanoparticles.

Addition of leaf extract from 4 to 6 mL leads to difference in the absorption as shown in Figure 4.28. The spectrum of 6 mL leaf extract showed that the band peak centered at 560 nm which has the largest absorbance wavelength among three different

concentrations. As the wavelength of peak absorbance increases with diameter of particle, this indicates that the gold nanoparticles which synthesised by 6 mL of leaf extract will have larger diameter in comparison to 4 and 5 mL. Red shift of the absorbance band was observed with increasing volume of extract. As the peak absorbance wavelength increases with particle diameter, this indicates that the gold nanoparticles will have larger diameter. The higher peaks observed for 5 mL of leaves extract might be due to an increase of gold nanoparticles because of higher amount of bio-compounds present in reaction mixture. The UV-Vis spectra peaks started to decrease with further increase in volume of extract from 5 to 6 mL most likely due to insufficient amount of gold ions to be reduced by bio-compounds. It could be considered as the excess amount of reducing, capping and stabilizing agent left in reaction mixture to synthesise gold nanoparticles (Ahmad *et al.*, 2018).

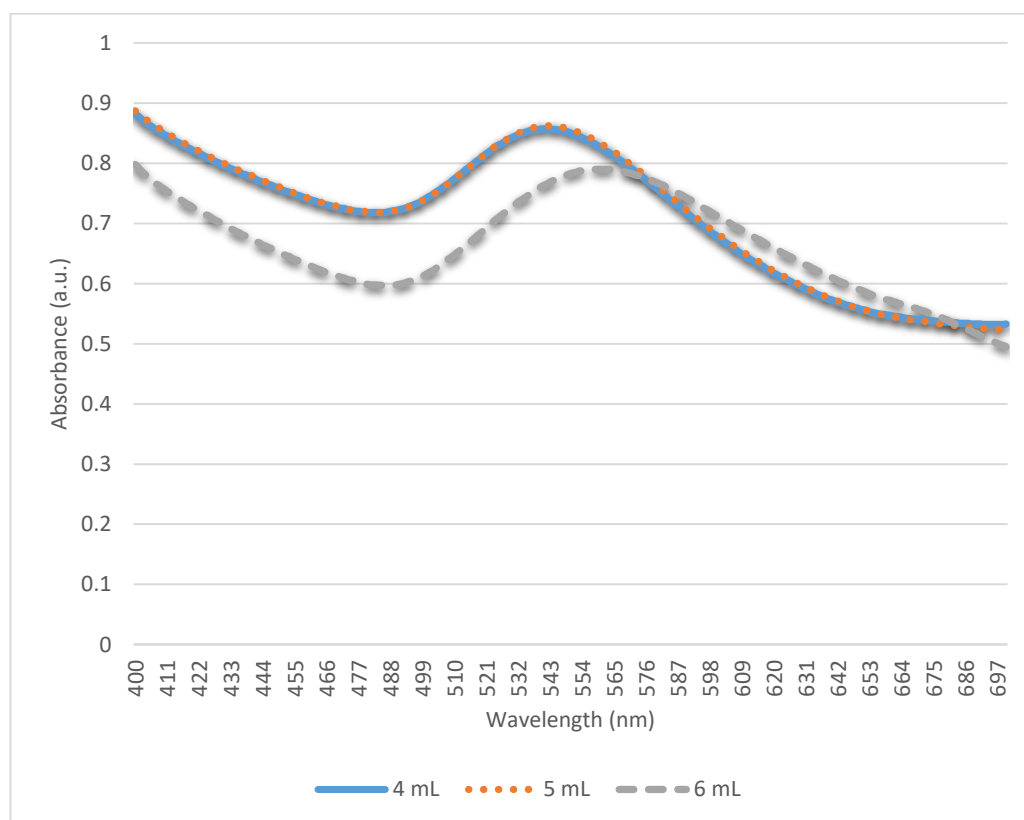


**Figure 4.28: UV-vis spectra of gold nanoparticles at different volume of *Vernonia Amygdalina* leaf extract from 4 to 6 mL and constant concentrations of HAuCl<sub>4</sub> (0.0025 M).**

The average diameter of gold nanoparticles for each sample was measured from FESEM images by using ImageJ software. The FESEM image of gold nanoparticles show that they were spherical in nature with 5 and 6 mL of leaf extract are shown in Figure 4.30 and Figure 4.31. However, agglomeration of gold nanoparticles was spotted when the synthesis dealing with 5 mL of leaf extract. On the other hand, the FESEM revealed that a variety of shapes of gold nanostructures was seen, including spherical and hexagonal gold nanoparticles synthesised by 4 mL of leaf extract (Figure 4.29). Thus, it might the effect of lower concentration of these potential reducing, capping and stabilizing agents contributed to the shape differences (Dzimitrowicz *et al.*, 2018). The observed spherical morphology of gold nanoparticles was uniform with an average diameter of 22.22 nm, 52.68 nm and 148.37 nm respectively as shown in Table 4.8. FESEM analysis revealed that the gold nanoparticles form in large numbers and almost uniform in size. The gold nanoparticles synthesised from leaf extracts are mounted up on the surface due to the interactions such as hydrogen bond and electrostatic interaction between the biomolecules as capping agent that bound to the gold nanoparticles.

Although 4 mL of *Vernonia Amygdalina* leaf extract during synthesis was capable to obtain particles with smaller size, but the particles in Figure 4.29 are less mono-dispersed in comparison to those in Figure 4.30. The images clearly show that 5 mL of *Vernonia Amygdalina* leaf extract during synthesis was capable to obtain more mono-dispersed gold nanoparticles which considered as an optimum volume of extract. The particles size have been further analysed to determine the uniformity and size distribution of gold particles in three cases as shown in Figure 4.32.

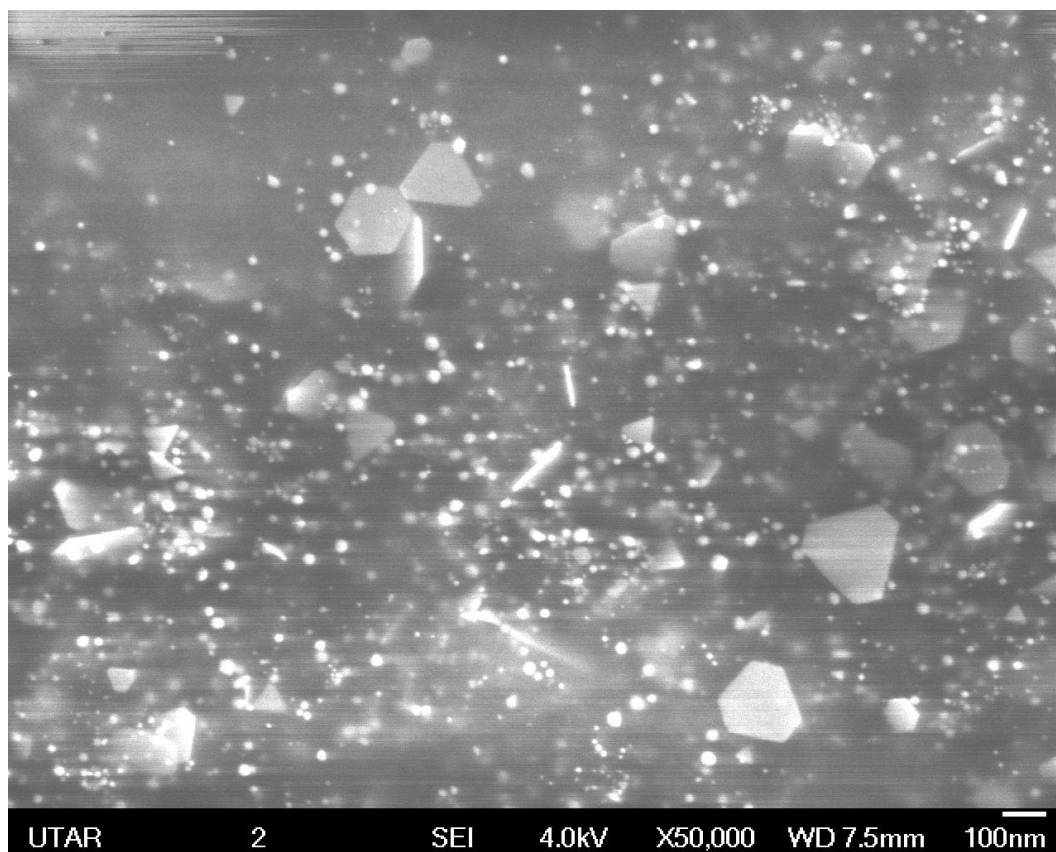


**Figure 4.29:** FESEM image of gold nanoparticles formed by exposing 4 mL *Vernonia Amygdalina* leaf extract to 0.0025 M of H<sub>Au</sub>Cl<sub>4</sub>.

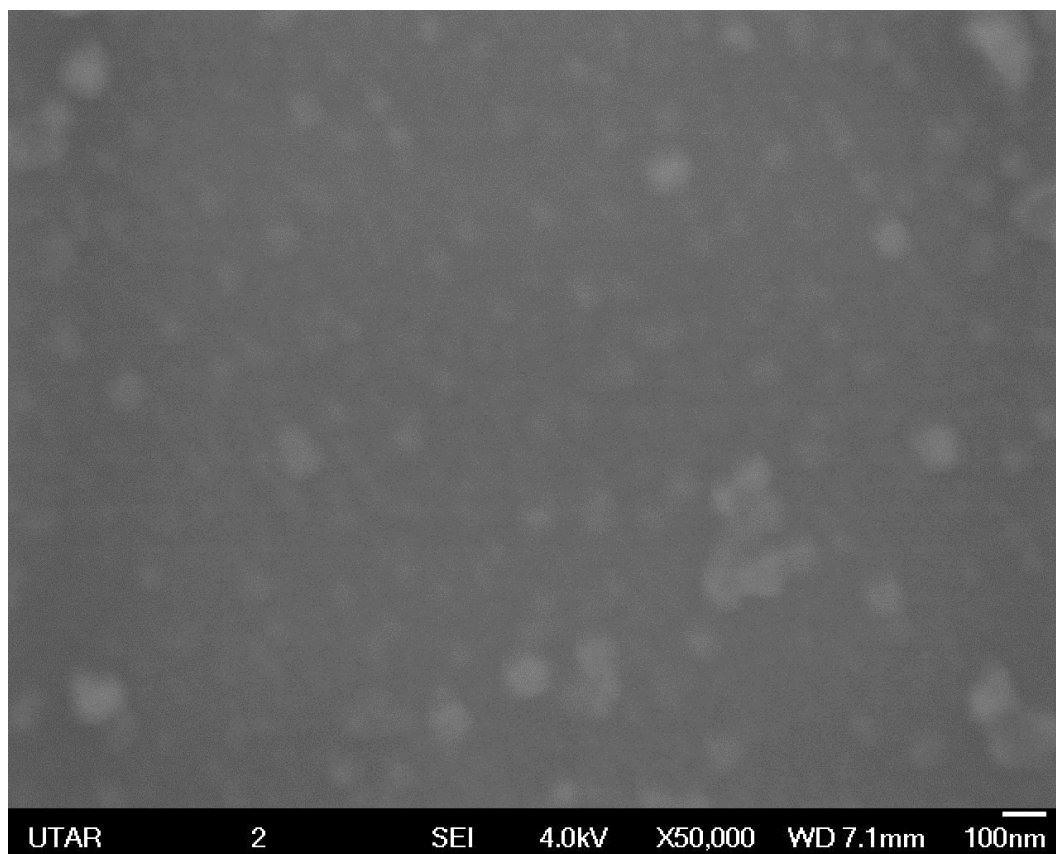


**Figure 4.30:** FESEM image of gold nanoparticles formed by exposing 5 mL *Vernonia Amygdalina* leaf extract to 0.0025 M of H<sub>AuCl</sub><sub>4</sub>.

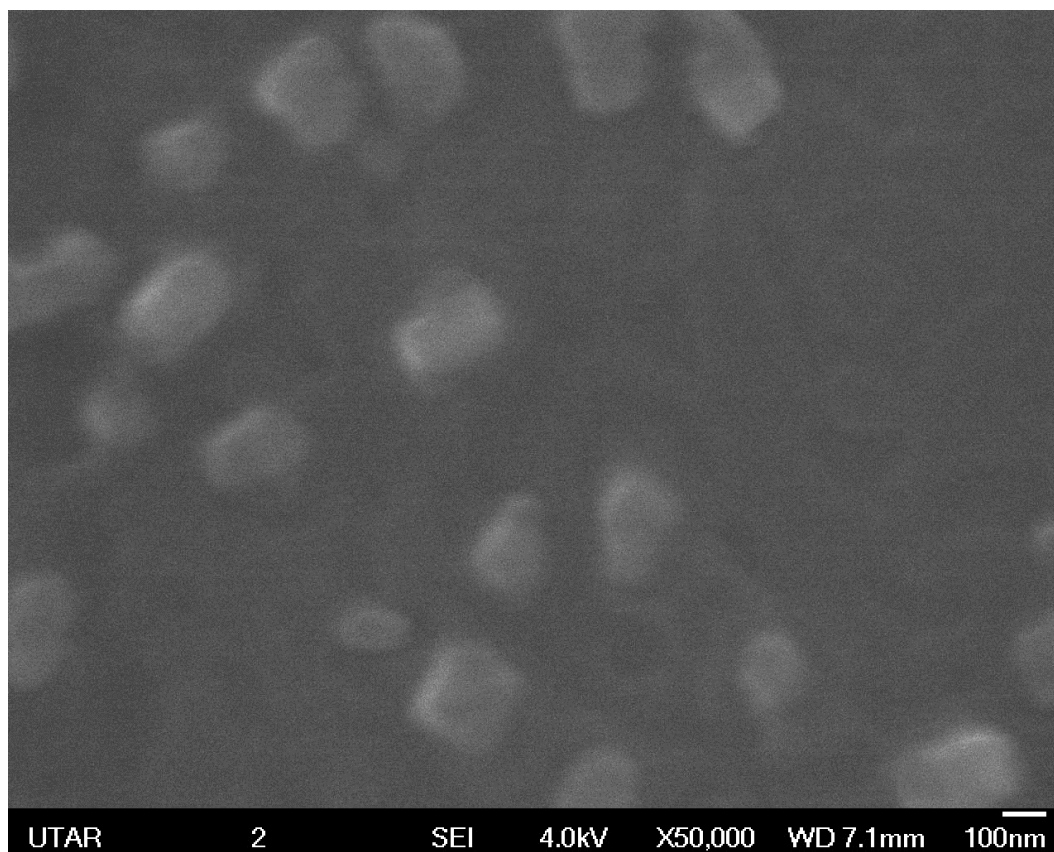


**Figure 4.31: FESEM image of gold nanoparticles formed by exposing 6 mL *Vernonia Amygdalina* leaf extract to 0.0025 M of H<sub>Au</sub>Cl<sub>4</sub>.**

**Table 4.8: The average particle size synthesised by different volume of *Vernonia Amygdalina* leaf extract with constant H<sub>AuCl<sub>4</sub></sub> concentrations.**

	4 mL	5 mL	6 mL
Mean (nm)	22.22	52.67	148.37
S.D. (nm)	6.84	26.47	56.38
Min (nm)	11.22	25.00	56.60
Max (nm)	45.51	177.44	286.79

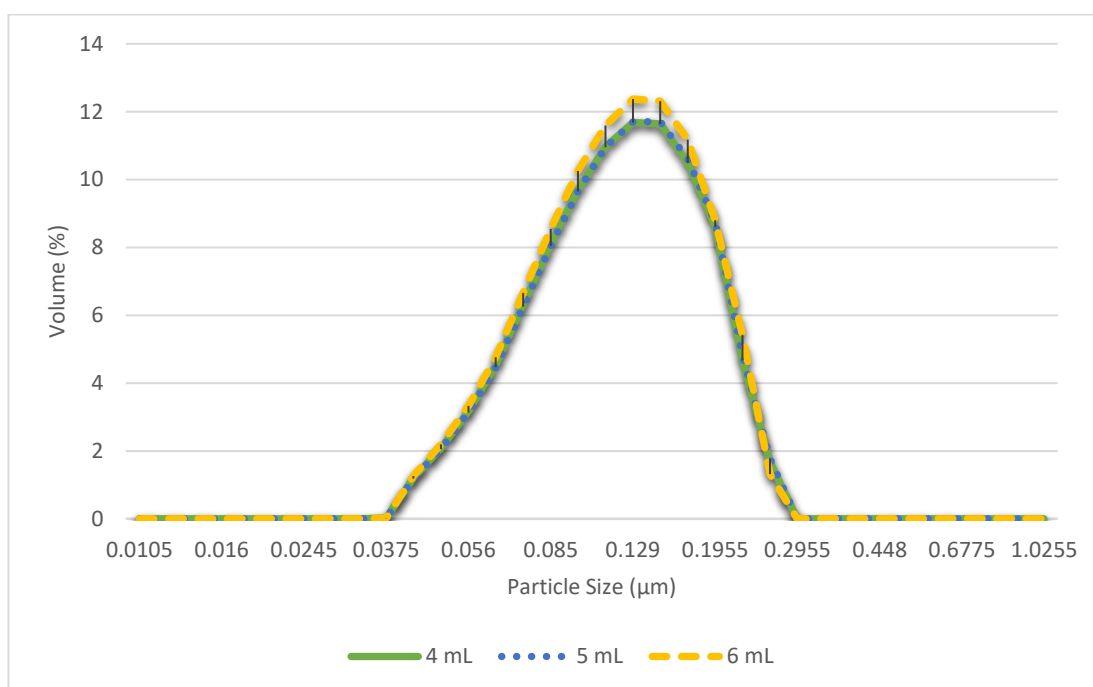


**Figure 4.32: Size distribution of gold nanoparticles formed by different volume of *Vernonia Amygdalina* leaf extract and constant concentrations of H<sub>AuCl<sub>4</sub></sub> (0.0025 M).**

#### **4.7 Effect of chloroauric acid (HAuCl<sub>4</sub>) concentration on formation of gold nanoparticles using *Vernonia Amygdalina* leaf broth.**

The change in colour from pale yellow to violet confirmed the presence of gold nanoparticles due to gold ions reduction through the phytochemical constituents in *Vernonia Amygdalina* leaf extract. The formation and stability of gold nanoparticles was verified by UV-Vis spectroscopy. Spectrophotometric absorption measurements in the wavelength range of 500–600 nm are used in characterizing the gold nanoparticles. Figure 4.33 shows the UV-Vis spectra of gold nanoparticles formation using constant volume of *Vernonia Amygdalina* leaf extract (5 mL) with different HAuCl<sub>4</sub> concentration from 0.0025 to 0.01 M. The spectrum showed maximum absorption band peak centered at 541 nm for gold nanoparticles with 0.0025 M of HAuCl<sub>4</sub> which confirmed the formation of gold nanoparticles.

Addition of HAuCl<sub>4</sub> concentration from 0.0025 to 0.01 M leads to slightly increase in the absorption as shown in Figure 4.33. It can be noticed that the gradual increase of the absorbance spectra which clearly indicates the increase of HAuCl<sub>4</sub> concentration. As the peak absorbance wavelength increases with particle diameter, this indicates that the gold nanoparticles which synthesised by 0.0100 M HAuCl<sub>4</sub> will have larger diameter in comparison to 0.0025 and 0.0050 M. The higher peak observed for higher concentration of HAuCl<sub>4</sub> might be due to an increase in formation of gold nanoparticles which means the higher amount of gold ions present in reaction mixture (Ahmad *et al.*, 2018).

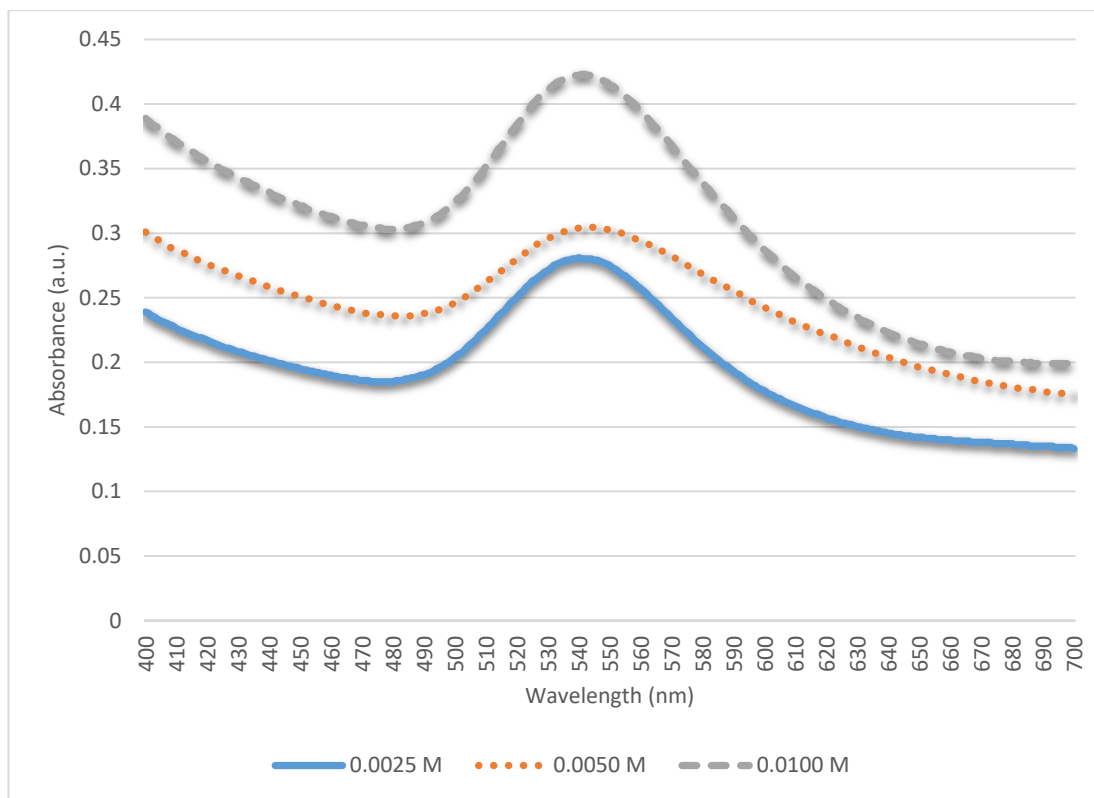


**Figure 4.33: UV-vis spectra of gold nanoparticles at different concentrations of HAuCl<sub>4</sub> from 0.0025 to 0.0100 M and constant volume of *Vernonia Amygdalina* leaf extract (5 mL).**

The FESEM images of gold nanoparticles show that they were mono-dispersed and spherical in nature are shown in Figure 4.34, 4.35 and 4.36. The observed morphology of gold nanoparticles was uniform with an average diameter of 52.76 nm, 64.34 nm and 84.73 nm respectively as shown in Table 4.9. This showed the diameter of gold nanoparticles increasing steadily with higher concentrations. The images clearly showed that higher concentration during synthesis leads to larger particle size. FESEM analysis revealed that the gold nanoparticles form in large numbers and almost uniform in size.

The gold nanoparticles synthesised from leaf extracts are accumulated on the surface due to the interactions such as hydrogen bond and electrostatic interaction between the bio-organic capping molecules bound to the gold nanoparticles. The images clearly show that 0.0025 M of HAuCl<sub>4</sub> during synthesis was capable to obtain

the smaller particle size which considered as an optimum concentration. The particles size have been further analysed to determine the uniformity and size distribution of gold particles in three cases as shown in Figure 4.39.

Further analysis of the gold nanoparticles by EDX confirmed the presence of the signals characteristic of gold. Figure 4.37 shows the EDX spectra of biosynthesised gold nanoparticles by *Citrus Maixma* leaf extract. The remaining of weaker signals may be due to the biomolecules responsible for capping agent of the nanoparticles (Akhir, Fairuzi and Ismail, 2015).

The formation of gold nanoparticles synthesised using *Citrus Maxima* leaf extract was further supported by XRD measurements (Figure 4.38). The XRD pattern of the nanoparticle solution is an evidence for crystalline nature of gold nanoparticle. The peaks could be ascribed to FCC gold (JCPDS No.04-0784). The diffraction peaks appeared at  $2\theta = 38.52^\circ$  and  $44.76^\circ$  which corresponded to the (111) and (200) planes of the standard gold cubic respectively. Therefore, the intensity of the (200) plane was the highest among the other planes (Ng *et al.*, 2015).

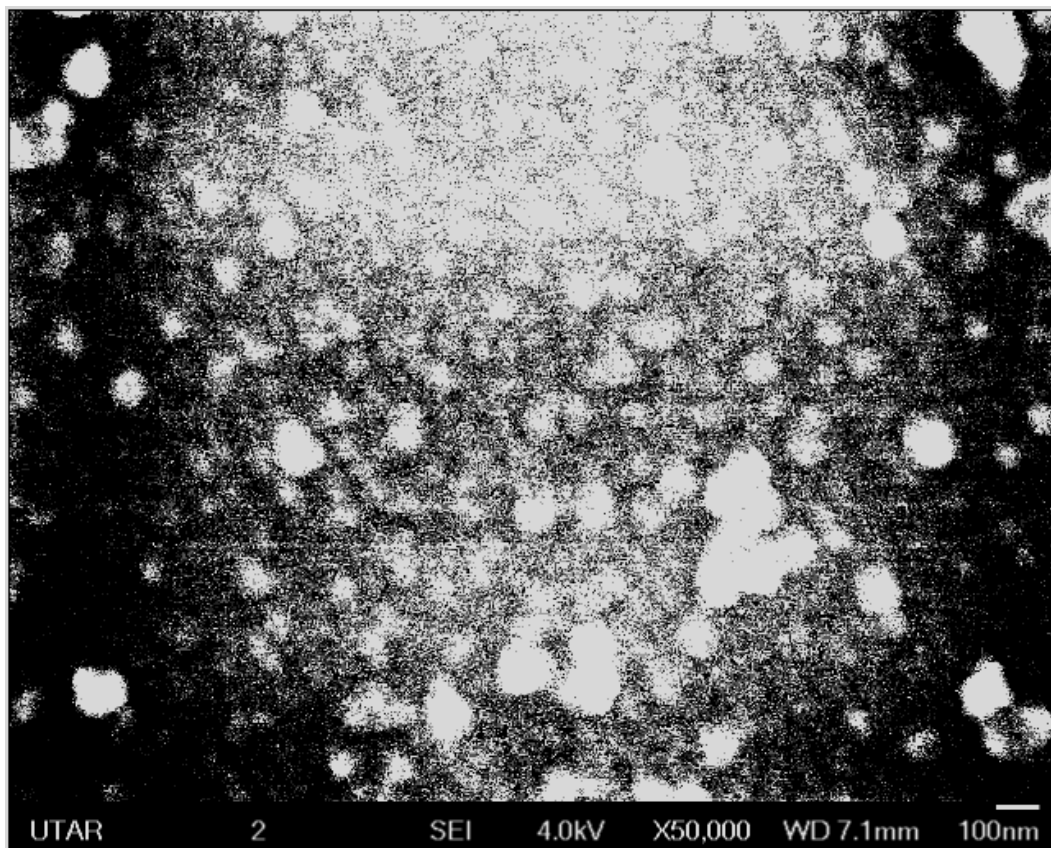


**Figure 4.34:** FESEM image of gold nanoparticles formed by exposing 5 mL *Vernonia Amygdalina* leaf extract to 0.0025 M of H<sub>Au</sub>Cl<sub>4</sub>.

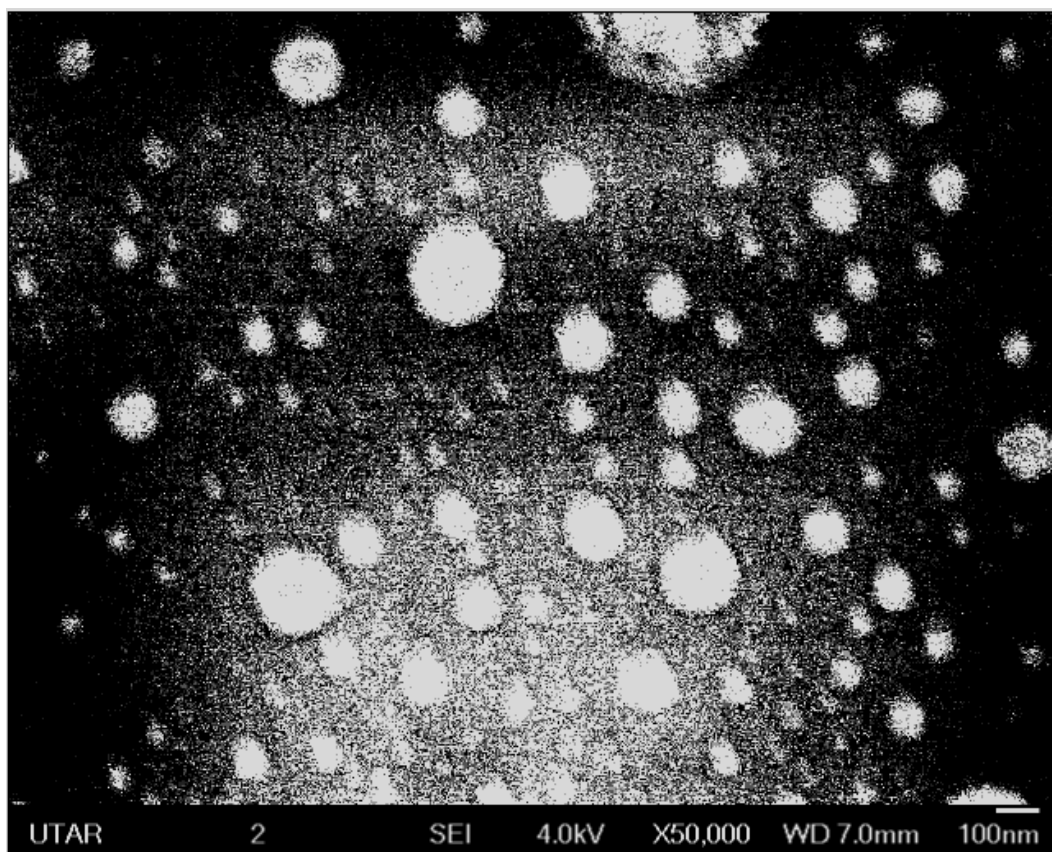


**Figure 4.35:** FESEM image of gold nanoparticles formed by exposing 5 mL *Vernonia Amygdalina* leaf extract to 0.0050 M of  $\text{HAuCl}_4$ .

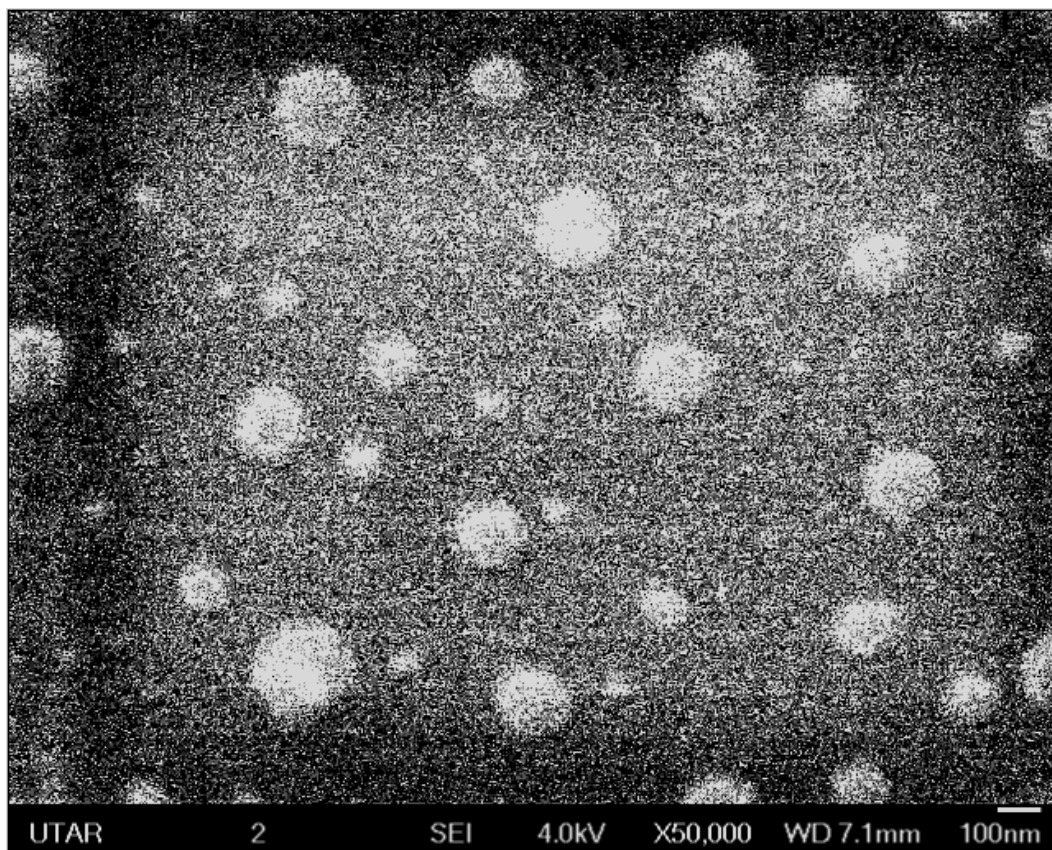


**Figure 4.36: FESEM image of gold nanoparticles formed by exposing 5 mL *Vernonia Amygdalina* leaf extract to 0.0100 M of H<sub>Au</sub>Cl<sub>4</sub>.**

**Table 4.9: The average particle size synthesised by different concentration of HAuCl<sub>4</sub> with constant volume of *Vernonia Amygdalina* leaf extract.**

	0.0025 M	0.0050 M	0.0100 M
Mean (nm)	52.67	64.34	84.73
S.D. (nm)	26.47	26.40	44.48
Min (nm)	25.00	22.90	25.88
Max (nm)	177.44	153.27	250.15

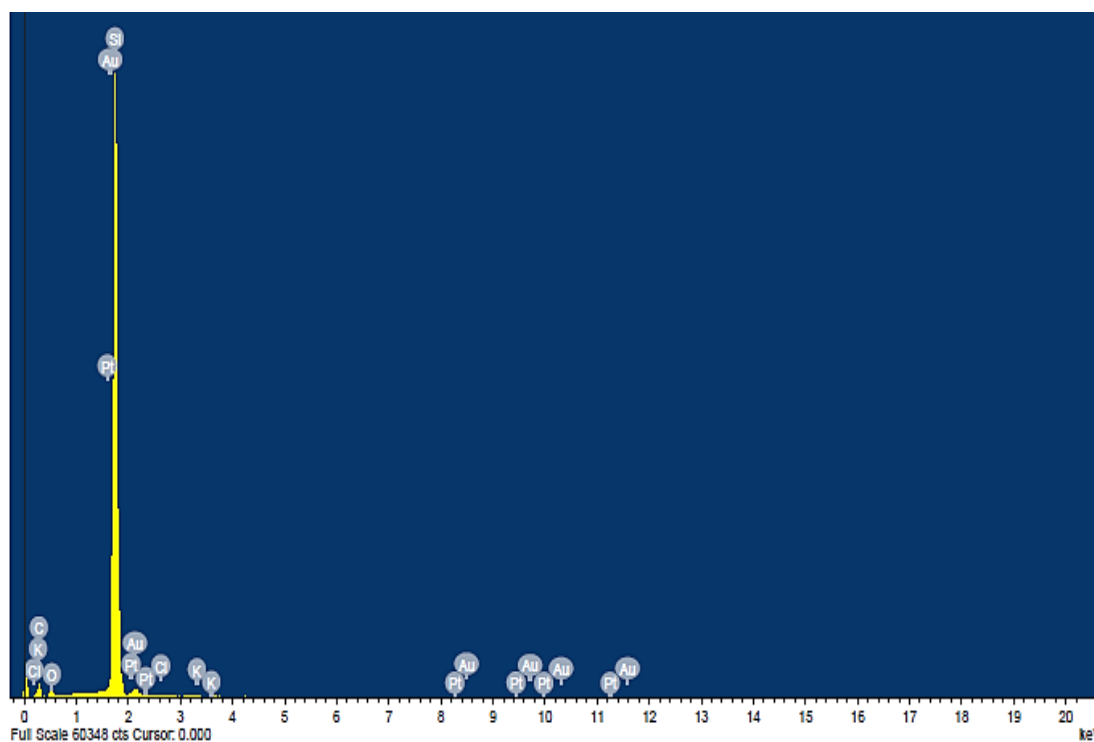


**Figure 4.37: EDX spectrum of biosynthesised gold nanoparticles resulting from the experiment using *Vernonia Amygdalina* leaf.**

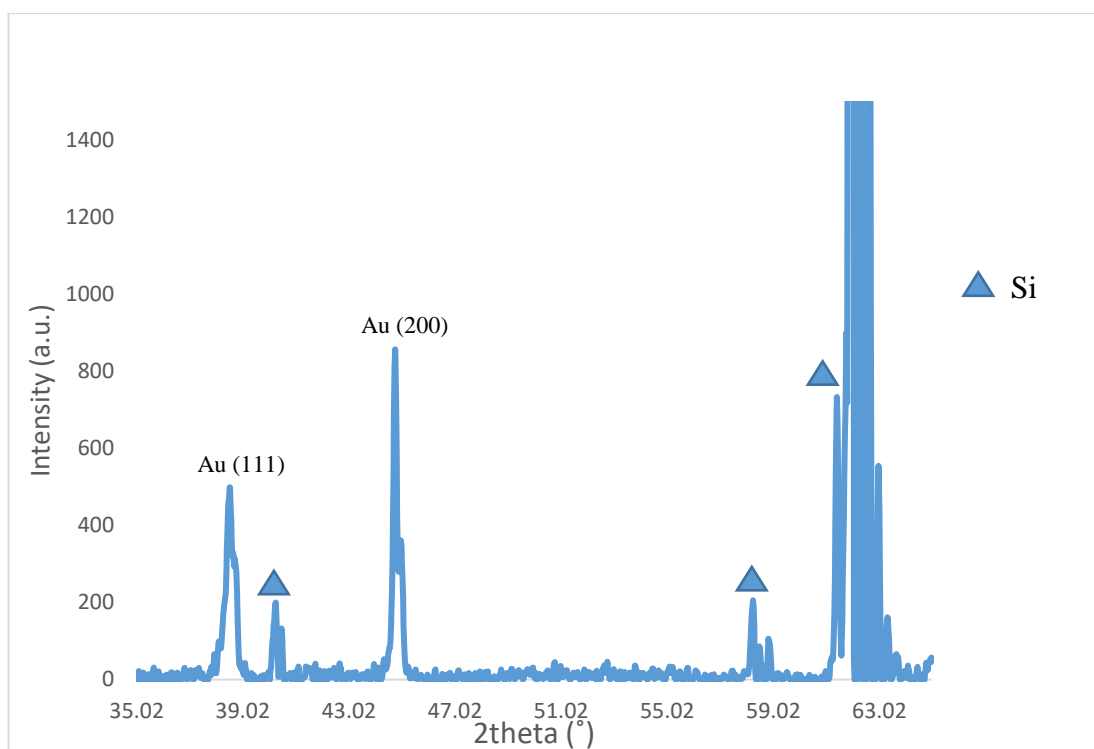


**Figure 4.38:** XRD patterns for gold nanoparticles synthesised using *Vernonia Amygdalina* leaves on silicon substrates.

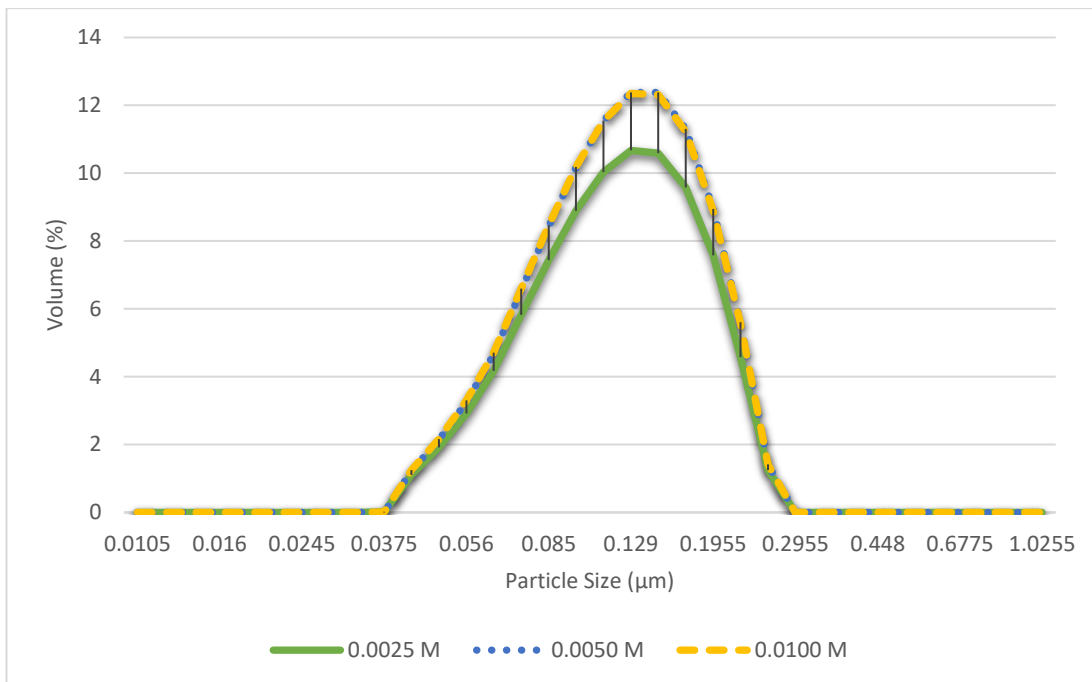


**Figure 4.39: Size distribution of gold nanoparticles formed by different concentrations of HAuCl<sub>4</sub> and constant volume of *Vernonia Amygdalina* leaf extract (5 mL).**

## CHAPTER 5

### CONCLUSION AND RECOMMENDATIONS

In this study, gold nanoparticles were successfully synthesised by using aqueous *Vernonia Amygdalina*, *Pandanus Amaryllifolius*, and *Citrus Maxima* leaves extracts. Volume of leaves extract and concentrations of gold chloroauric acid (HAuCl<sub>4</sub>) have significant impact on size and shape of gold nanoparticles. Gold nanoparticles were synthesised by using the present method having average diameter of 22.22-148.37 nm with spherical shaped. A small amount of hexagonal and hollow gold nanoparticles also can be spotted during the characterization. Energy needed to synthesise gold nanoparticles has been reduced as the synthesis was carried out at room temperature and under aqueous conditions. The use of toxic free solvent is the factor of leaves extract that minimizes environmental impact.

Gold nanoparticles synthesised by the green chemistry approach reported in this study using *Vernonia Amygdalina*, *Pandanus Amaryllifolius*, and *Citrus Maxima* leaves extract could have potent applications in non-linear optics, biomedical and biotechnological applications. This simple procedure for the biosynthesis of gold nanoparticles has several advantages such as cost-effectiveness, compatibility for biomedical and pharmaceutical applications as well as for large-scale commercial production.

Leaf broth from boiling fresh plant leaves was used to synthesise gold nanoparticles for present study. However, some fresh leaves are seasonal so they would not be ready all the time. Therefore, dried biomass was recommended as it has the advantageous over broth because of the difficulties on controlling some parameters precisely such as the optimum boiling time while dealing with the broth.

There are some recommendations suggested for future research works:

- Study on the effect of dried biomass.
- Study on the effect of leaf extract concentration.
- Study on the effect of pH.
- Study on the effect of temperature.
- Study on the effect of time.

## REFERENCES

- Adesuji, E. T. *et al.* (2014) 'Green synthesis and growth kinetics of nanosilver under bio-diversified plant extracts influence', *Journal of Nanostructure in Chemistry*, 5(1), pp. 85–94. doi: 10.1007/s40097-014-0139-5.
- Agroforestry Database (2009) 'Citrus maxima Merr .', 0, pp. 1–5.
- Ahmad, T. *et al.* (2018) 'Effect of volume of gold chloroauric acid on size, shape and stability of biosynthesized AuNPs using aqueous *Elaeis guineensis* (oil palm) leaves extract', *International Journal of Automotive and Mechanical Engineering*, 15(1), pp. 5135–5145. doi: 10.15282/ijame.15.1.2018.18.0397.
- Ahmed, S. *et al.* (2016) 'Biosynthesis of gold nanoparticles: A green approach', *Journal of Photochemistry and Photobiology B: Biology*. Elsevier B.V., 161, pp. 141–153. doi: 10.1016/j.jphotobiol.2016.04.034.
- Aini, R. and Mardiyarningsih, A. (2016) 'Pandan leaves extract (*Pandanus amaryllifolius* Roxb) as a food preservative', *Jurnal Kedokteran dan Kesehatan Indonesia*, 7(4), pp. 166–173. doi: 10.20885/jkki.vol7.iss4.art8.
- Akhir, R. M., Fairuzi, A. A. and Ismail, N. H. (2015) 'Plant-mediated synthesis of biosilver nanoparticles using *Pandanus amaryllifolius* extract and its bactericidal activity', *AIP Conference Proceedings*, 1674. doi: 10.1063/1.4928836.
- Al-Batayneh, K. *et al.* (2018) 'Synthesis of Gold Nanoparticles Using Leaf Extract of *Ziziphus zizyphus* and their Antimicrobial Activity', *Nanomaterials*, 8(3), p. 174. doi: 10.3390/nano8030174.
- Ankamwar, B. (2010) 'Biosynthesis of Gold Nanoparticles (Green-Gold) Using Leaf Extract of *Terminalia Catappa* BALAPRASAD ANKAMWAR ', 7(4), pp. 1334–1339. Available at: file:///C:/Documents and Settings/Akshat/My Documents/Downloads/745120.pdf.
- Arole, V. M. and Munde, S. V (2014) 'Faabrication of nanomaterials by top-down and bottom-up approaches- an overview', *journal of Advances in applied*, 1(2), pp. 2–89. Available at: <https://pdfs.semanticscholar.org/34f8/921434fb256c9c8cca886722b5c920a1e4d2.pdf>.
- Bangal, M. *et al.* (2005) 'Semiconductor nanoparticles', *Hyperfine Interactions*, 160(1–4), pp. 81–94. doi: 10.1007/s10751-005-9151-y.

- Caruso, F. *et al.* (2012) 'Nanomedicine themed issue', *Chemical Society Reviews*, (7). doi: 10.1039/c1cs15240h.
- Cha, C. *et al.* (2013) 'Carbon-Based Nanomaterials : Multifunctional Materials for', *ACS Nano*, 7(4), pp. 2891–2897. doi: 10.1021/nn401196a.
- Correa-Duarte, M. A., Giersig, M. and Liz-Marzán, L. M. (1998) 'Stabilization of CdS NCs against Photodegradation by a Silica Coating Procedure', *Chemical Physics Letters*, (April), pp. 497–501.
- Coulie, B. *et al.* (2006) 'System in a Pharmaceutical Drug Discovery Environment', *Drug Development Research*, 67(2), pp. 107–118. doi: 10.1002/ddr.
- Das, S. K., Das, A. R. and Guha, A. K. (2009) 'Gold nanoparticles: Microbial synthesis and application in water hygiene management', *Langmuir*, 25(14), pp. 8192–8199. doi: 10.1021/la900585p.
- Dikshit, A. *et al.* (2018) 'Advances in Biogenic Nanoparticles and the Mechanisms of antimicrobial Effects', *Indian Journal of Pharmaceutical Sciences*, 80(4). doi: 10.4172/pharmaceutical-sciences.1000398.
- Dizaj, S. M. *et al.* (2015) 'Antimicrobial activity of carbon-based nanoparticles', *Advanced Pharmaceutical Bulletin*, 5(1), pp. 19–23. doi: 10.5681/apb.2015.003.
- Dzimitrowicz, A. *et al.* (2018) 'Fermented juices as reducing and capping agents for the biosynthesis of size-defined spherical gold nanoparticles', *Journal of Saudi Chemical Society*. King Saud University, 22(7), pp. 767–776. doi: 10.1016/j.jscs.2017.12.008.
- Edgar, J. A. *et al.* (2008) 'Synthesis of hollow gold nanoparticles and rings using silver templates', *Proceedings of the 2008 International Conference on Nanoscience and Nanotechnology, ICONN 2008*, pp. 36–39. doi: 10.1109/ICONN.2008.4639239.
- El-kholy, S., Aboushousha, T. and Ageez, A. (2017) 'Research Article EXPRESSION PATTERN OF CYCLIN D1 IN MAJOR TYPES OF BLADDER', 8, pp. 17475–17480. doi: 10.24327/IJRSR.
- Farombi, E. O. and Owoeye, O. (2011) 'Antioxidative and chemopreventive properties of Vernonia amygdalina and Garcinia biflavonoid', *International Journal of Environmental Research and Public Health*, 8(6), pp. 2533–2555. doi: 10.3390/ijerph8062533.
- Food, A. *et al.* (2016) 'Pandan leaves : " Vanilla of the East " as Pandan leaves : " Vanilla of the East " as potential natural food ingredient', 25(May 2014), pp. 10–14. doi: 10.1097/BRS.0000000000000195.
- Galoppini, E. (2004) 'Linkers for anchoring sensitizers to semiconductor nanoparticles', *Coordination Chemistry Reviews*, 248(13–14), pp. 1283–1297. doi: 10.1016/j.ccr.2004.03.016.

- Gobbi, M. *et al.* (2010) 'Lipid-based nanoparticles with high binding affinity for amyloid- $\beta$ 1-42peptide', *Biomaterials*. Elsevier Ltd, 31(25), pp. 6519–6529. doi: 10.1016/j.biomaterials.2010.04.044.
- Habiba, K. *et al.* (2014) *Fabrication of Nanomaterials by Pulsed Laser Synthesis, Manufacturing Nanostructures (OCN)*. doi: 10.13140/RG.2.2.16446.28483.
- Habtamu, A. and Melaku, Y. (2018) 'Antibacterial and Antioxidant Compounds from the Flower Extracts of *Vernonia amygdalina*', *Advances in Pharmacological Sciences*, 2018, pp. 1–6. doi: 10.1155/2018/4083736.
- Hall, J. B. *et al.* (2008) 'Interaction of colloidal gold nanoparticles with human blood: effects on particle size and analysis of plasma protein binding profiles', *Nanomedicine: Nanotechnology, Biology and Medicine*. Elsevier Inc., 5(2), pp. 106–117. doi: 10.1016/j.nano.2008.08.001.
- Hasan, S. (2014) 'A Review on Nanoparticles : Their Synthesis and Types', *Research Journal of Recent Sciences Res . J. Recent . Sci . Uttar Pradesh ( Lucknow Campus )*, 4, pp. 1–3. doi: 10.3233/978-1-61499-057-4-57.
- He, N. *et al.* (2007) 'Biosynthesis of silver and gold nanoparticles by novel sundried *Cinnamomum camphora* leaf ', *Nanotechnology*, 18(10), p. 105104. doi: 10.1088/0957-4484/18/10/105104.
- Hong, Z., Reis, R. L. and Mano, J. F. (2009) 'Preparation and in vitro characterization of novel bioactive glass ceramic nanoparticles', *Journal of Biomedical Materials Research - Part A*, 88(2), pp. 304–313. doi: 10.1002/jbm.a.31848.
- Ismail, E. H. *et al.* (2014) 'Biosynthesis of gold nanoparticles using extract of grape (*Vitis vinifera*) leaves and seeds', *Progress in Nanotechnology and Nanomaterials*, 3(1), pp. 1–12.
- Kadiri, O. and Olawoye, B. (2017) 'Vernonia amygdalina: An Underutilized Vegetable with Nutraceutical Potentials – A Review', *Turkish Journal of Agriculture - Food Science and Technology*, 4(9), p. 763. doi: 10.24925/turjaf.v4i9.763-768.570.
- Kane, S. N., Mishra, A. and Dutta, A. K. (2016) 'Preface: International Conference on Recent Trends in Physics (ICRTP 2016)', *Journal of Physics: Conference Series*, 755(1). doi: 10.1088/1742-6596/755/1/011001.
- Katas, H. *et al.* (2018) 'Biosynthesis and Potential Applications of Silver and Gold Nanoparticles and Their Chitosan-Based Nanocomposites in Nanomedicine', *Journal of Nanotechnology*, 2018. doi: 10.1155/2018/4290705.
- Khalil, M. M. H., Ismail, E. H. and El-Magdoub, F. (2010) 'Biosynthesis of Au nanoparticles using olive leaf extract', *Arabian Journal of Chemistry*. King Saud University, 5(4), pp. 431–437. doi: 10.1016/j.arabjc.2010.11.011.

- Khan, Ibrahim, Saeed, K. and Khan, Idrees (2017) 'Nanoparticles: Properties, applications and toxicities', *Arabian Journal of Chemistry*. The Authors. doi: 10.1016/j.arabjc.2017.05.011.
- 'Kharjul et al. ', (2012), 3(12), pp. 4913–4918.
- Kumari, A., Yadav, S. K. and Yadav, S. C. (2010) 'Biodegradable polymeric nanoparticles based drug delivery systems', *Colloids and Surfaces B: Biointerfaces*, 75(1), pp. 1–18. doi: 10.1016/j.colsurfb.2009.09.001.
- Lee, J. (2010) 'Recent progress in gold nanoparticle-based no volatile.pdf', 43(3), pp. 189–199.
- Miller, A. D. (2013) 'Lipid-Based Nanoparticles in Cancer Diagnosis and Therapy', *Journal of Drug Delivery*, 2013(Figure 1), pp. 1–9. doi: 10.1155/2013/165981.
- Mody, V. et al. (2010) 'Introduction to metallic nanoparticles', *Journal of Pharmacy and Bioallied Sciences*, 2(4), p. 282. doi: 10.4103/0975-7406.72127.
- Nagavarma, B. V. N. et al. (2012) 'Different techniques for preparation of polymeric nanoparticles- A review', *Asian Journal of Pharmaceutical and Clinical Research*, 5(SUPPL. 3), pp. 16–23. doi: 10.1186/s13104-016-1898-5.
- Nanotechnology, I. (2004) 'Introduction 1.', p. 2004. doi: 10.1016/B978-0-08-051557-1.50005-6.
- Narayanan, K. B. and Sakthivel, N. (2008) 'Coriander leaf mediated biosynthesis of gold nanoparticles', *Materials Letters*, 62(30), pp. 4588–4590. doi: 10.1016/j.matlet.2008.08.044.
- Ng, S. A. et al. (2015) 'Growth of gold nanoparticles using aluminum template via low-temperature hydrothermal method for memory applications', *Journal of Materials Science: Materials in Electronics*, 26(9), pp. 6484–6494. doi: 10.1007/s10854-015-3240-8.
- Nor, F. M. et al. (2008) 'Antioxidative properties of Pandanus amaryllifolius leaf extracts in accelerated oxidation and deep frying studies', *Food Chemistry*, 110(2), pp. 319–327. doi: 10.1016/j.foodchem.2008.02.004.
- Noruzi, M. (2015) 'Biosynthesis of gold nanoparticles using plant extracts', *Bioprocess and biosystems engineering*, 38(1), pp. 1–14. doi: 10.1007/s00449-014-1251-0.
- Nouailhat, A. (2008) *An Introduction to Nanoscience and Nanotechnology Loew\_et\_al-1976-Journal\_of\_Heterocyclic\_Chemistry.pdf*. doi: 10.1002/9780470610954.
- Pandey, G., Rawtani, D. and Agrawal, Y. K. (2016) 'Aspects of Nanoelectronics in Materials Development', *Nanoelectronics and Materials Development*. doi: 10.5772/64414.

- Patra, J. K. and Baek, K.-H. (2014) 'Green Nanobiotechnology: Factors Affecting Synthesis and Characterization Techniques', *Journal of Nanomaterials*, 2014, pp. 1–12. doi: 10.1155/2014/417305.
- Sajti, C. L. *et al.* (2010) 'Gram scale synthesis of pure ceramic nanoparticles by laser ablation in liquid', *Journal of Physical Chemistry C*, 114(6), pp. 2421–2427. doi: 10.1021/jp906960g.
- Selvakannan, P. R. and Sastry, M. (2005) 'Hollow gold and platinum nanoparticles by a transmetallation reaction in an organic solution', *Chemical Communications*, (13), pp. 1684–1686. doi: 10.1039/b418566h.
- Shah, M. (2014) 'Gold nanoparticles: various methods of synthesis and antibacterial applications', *Frontiers in Bioscience*, 19(8), p. 1320. doi: 10.2741/4284.
- Singh, A. K. (2016) 'Introduction to Nanoparticles and Nanotoxicology', *Engineered Nanoparticles*, pp. 1–18. doi: 10.1016/b978-0-12-801406-6.00001-7.
- Singh, H. *et al.* (2018) 'Ecofriendly synthesis of silver and gold nanoparticles by Euphrasia officinalis leaf extract and its biomedical applications', *Artificial Cells, Nanomedicine and Biotechnology*. Informa UK Limited, trading as Taylor & Francis Group, 46(6), pp. 1163–1170. doi: 10.1080/21691401.2017.1362417.
- Smith, B. *et al.* (2012) 'Lipid-Based Nanoparticles as Pharmaceutical Drug Carriers: From Concepts to Clinic', *Critical Reviews™ in Therapeutic Drug Carrier Systems*, 26(6), pp. 523–580. doi: 10.1615/critrevtherdrugcarriersyst.v26.i6.10.
- Song, J. Y., Jang, H. K. and Kim, B. S. (2009) 'Biological synthesis of gold nanoparticles using Magnolia kobus and Diopyros kaki leaf extracts', *Process Biochemistry*, 44(10), pp. 1133–1138. doi: 10.1016/j.procbio.2009.06.005.
- Sutherland, D. (2010) 'Chapter 1 – Introduction to Nanoscience and Nanotechnologies', *Training*, (September), pp. 1–29.
- Swiss Reinsurance Company (2004) 'Nanotechnology: Small Matter, Many Unknowns', *Chemical Engineering News*, (August), p. 56.
- Taha, A. and Shamsuddin, M. (2013) 'Malaysian Journal of Fundamental and Applied Sciences Biosynthesis of Gold Nanoparticles Using Psidium Guajava Leaf Extract', pp. 119–122.
- Thomas, S. *et al.* (2015) 'Ceramic Nanoparticles: Fabrication Methods and Applications in Drug Delivery', *Current Pharmaceutical Design*, 21(42), pp. 6165–6188. doi: 10.2174/1381612821666151027153246.
- Thompson, D. T. (2007) 'Using gold nanoparticles for catalysis', *Nano Today*, 2(4), pp. 40–43. doi: 10.1016/S1748-0132(07)70116-0.

- Tikariha, S. *et al.* (2012) 'Biosynthesis of Gold Nanoparticles, Scope and Application: a Review', *International Journal of Pharmaceutical Sciences and Research*, 3(06), pp. 1603–1615. Available at: <http://ijpsr.com/V3I6/8> Vol. 3, Issue 6, June 2012, IJPSR-524, Paper 8.pdf.
- Tiwari, J. N., Tiwari, R. N. and Kim, K. S. (2012) 'Progress in Materials Science three-dimensional nanostructured materials for advanced electrochemical energy devices', *Progress in Materials Science*. Elsevier Ltd, 57(4), pp. 724–803. doi: 10.1016/j.pmatsci.2011.08.003.
- Udochukwu, U. *et al.* (2015) 'Phytochemical analysis of Vernonia amygdalina and Ocimum gratissimum extracts and their antibacterial activity on some drug resistant bacteria', *American Journal o Research Communication*, 3(5), pp. 225–235.
- Venkatesh, N. (2018) 'Metallic Nanoparticle: A Review', *Biomedical Journal of Scientific & Technical Research*, 4(2), pp. 1–11. doi: 10.26717/bjstr.2018.04.0001011.
- Verma, D. *et al.* (2018) 'Role of Nanotechnology in Cosmeceuticals: A Review of Recent Advances', *Journal of Pharmaceutics*, 2018, pp. 1–19. doi: 10.1155/2018/3420204.
- Vijaylakshmi, P. and Radha, R. (2015) 'An overview : Citrus maxima', *The Journal of Phytopharmacology*, 4(5), pp. 263–267.
- Wakte, K. V. *et al.* (2009) 'Pandanus amaryllifolius Roxb. cultivated as a spice in coastal regions of India', *Genetic Resources and Crop Evolution*, 56(5), pp. 735–740. doi: 10.1007/s10722-009-9431-5.
- Yeh, Y. C., Creran, B. and Rotello, V. M. (2012) 'Gold nanoparticles: Preparation, properties, and applications in bionanotechnology', *Nanoscale*, 4(6), pp. 1871–1880. doi: 10.1039/c1nr11188d.